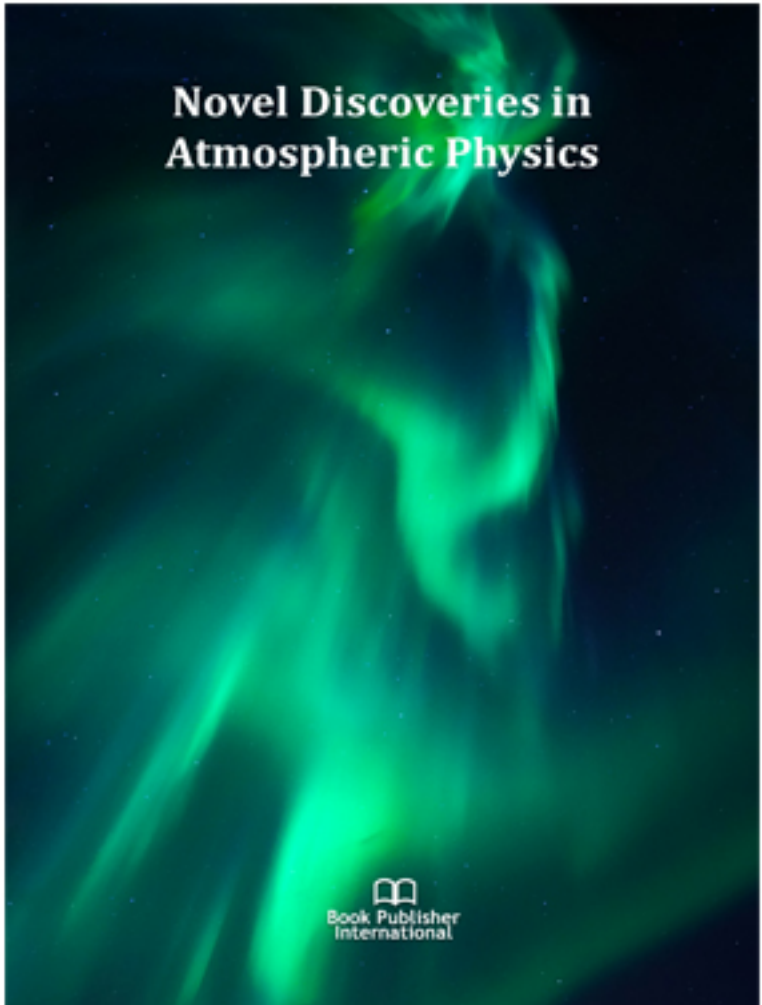
Novel Discoveries in
Atmospheric Physics
Book Publisher
International

Novel Discoveries in Atmospheric Physics

Novel Discoveries in Atmospheric Physics

India ▪ United Kingdom

Book Publisher International

Author(s)

Thomas Allmendinger[1*]

[1]Independent Scholar, ETH (Swiss Federal Institute of Technology), Zurich, Switzerland.
*Corresponding author: E-mail: inventor@sunrise.ch;

FIRST EDITION 2020

ISBN 978-93-89816-94-5 (Print)
ISBN 978-93-89816-95-2 (eBook)
DOI: 10.9734/bpi/mono/978-93-89816-94-5

Contents

Preface

This book deals with novel discoveries in atmospheric physics. The book also covers key areas in albedo, heat-emission, Stefan-Boltzmann law, climate-modelling, solar-tube, gas-temperature, radiation-absorption, kinetic-gas-theory, solar adsorption coefficient, radiation equilibrium etc. This book contains various materials suitable for students, researchers and academicians of this area.

Print ISBN: 978-93-89816-94-5, eBook ISBN: 978-93-89816-95-2

Novel Discoveries in Atmospheric Physics

Thomas Allmendinger[1*]

DOI: 10.9734/bpi/mono/978-93-89816-94-5

ABSTRACT

Climate change is currently an eminent theme in politics. Thereby, so-called greenhouse gases such as CO_2 are considered as the real cause for the temperature rise of the global atmosphere. This theory traces back to measurements of *Tyndall* at the end of the 19th century which revealed that CO_2 absorbs thermal radiation, in contrast to N_2 and O_2, the main components of the air, which do not absorb. Subsequently, *Arrhenius* tried to theoretically implement the *Stefan-Boltzmann law,* which meanwhile became known, assuming that the atmosphere is warmed up by the black-body radiation of the Earth surface, but solely due to the CO_2 and to similar IR (infrared) absorbing greenhouse gases such as CH_4. This means: The atmosphere would not be warmed up if no CO_2 or other greenhouse gases were there. Thus the temperature of the atmosphere would be identical with the temperature of the absolute zero. After the Second World War, this approach was continued by *Plass* and others, based on IR- spectroscopic, and regarding an extra-terrestrial *albedo* or *solar reflection coefficient*.

However, such an extra-terrestrial reflection coefficient for solar light, which implicates a viewpoint outside of the atmosphere, cannot be exactly defined since various effects are occurring within the atmosphere, for instance turbulences by winds. They cannot be expressed by a simple coefficient given by the ratio between emitted light and incident light. Moreover, by means of the usual determination methods, applying radiative field measurements, no reliable values for the *terrestrial* albedo were available, since the incident sunlight is independent of the distance to the surface, whereas the emitted light depends on the distance.

In contrast, the method developed by the author and described in the first enclosed article entitled »**The solar-reflective characterization of solid opaque materials«** enables the *direct determination of the – colour dependent – solar absorption coefficient*, thus of the complement of the solar reflection coefficient. This determination is feasible with a lab-like method by measuring the temperature increases of well-characterized plates, preferably from aluminium, during a permanent solar irradiation period. Since any solid plate emits thermal radiation when its temperature is increasing, a constant limiting temperature is reached when the intensity of the emitted radiation is identically equal to the intensity of the emitted radiation. Since this limiting temperature could not be achieved within the measuring period of 30 minutes when 20 mm thick aluminium plates were used, due to their high heat capacity, separate *cooling down measurements* were made in a darkened room, which enabled a mathematical modelling of the whole process and a determination of the – colour dependent - limiting temperatures. Besides the evaluation of the colour-specific solar absorption coefficients, this method also enables studying the influence of other factors affecting the warming up process, such as the heat capacity of the plates or the convection of the air.

A second, even graver flaw in conventional atmospheric physics arises from the fact that, with regard to the interactions between infrared light and gases, solely the *light absorption* was measured, but never the *warming-up* that is the temperature rise of irradiated gases. For the usual IR-spectroscopic application, whereby specific bonds in organic molecules can be identified, those features are not relevant. However, in this case where the temperature represents the relevant parameter, it should have been a peculiar requirement to gather empirical facts in order to ascertain the theoretical assumptions. But incredibly enough, this has never been done so far. Hence it was the subject of the author's further work, described in the second enclosed article entitled **»The thermal behaviour of**

[1]*Independent Scholar, ETH (Swiss Federal Institute of Technology), Zurich, Switzerland.*
**Corresponding author: E-mail: inventor@sunrise.ch;*

gases under the influence of infrared-radiation«, and delivering surprising results which entirely contradicted the former conventional perception.

The particular difficulty at this measuring problem arises from the very low heat capacity of gases, which runs the risk that the measurement results are interfered by the measuring vessel ore tube. Moreover, the walls of the vessel or tube may directly be warmed up by the (IR) light, which has to be used for the irradiation of the gas, indirectly influencing the gas temperature. This problem could be widely solved by using quadratic (25 cm x 25 cm) 1 m long tubes from Styrofoam which were mirrored with thin aluminium foils and covered by thin transparent plastic foils on both ends. The temperatures were measured at three different positions with mirrored Hg-thermometers. Besides sunlight, mainly IR-spots were used as radiation sources. However, in the latter case an inherent intensity loss along the tube could not be eliminated but solely minimized.

Such a simple apparatus may appear unprofessional and not suited for modern research work. However, it is indeed adequate to the problem, although it necessitates only simple materials which are partly available in do-it-yourself shops. But these materials were not available at the time when the pioneer work was done, whereas the professional IR-spectrometers are not suited for this measuring problem since they were constructed for another, analytical purpose. Besides, one should be aware that many trials were needed in order to optimize the apparatus and to obtain reliable results, and that the measurements required considerable skill.

Surprisingly, these results revealed that *all* gases absorb infrared radiation, even noble gases. Thereby they are warmed up to a limiting temperature where the intensity of the absorbed radiation was identically equal to the intensity of the emitted radiation by the gas. Moreover, air (or a 4:1 N_2/O_2 mixture) and pure carbon-dioxide were warmed up to a nearly equal extent. Solely in the line Argon – Neon – Helium significant differences appeared. Applying the kinetic gas theory, the radiation intensity of the emitted light turned out to be proportional to the *collision frequency of the particles* (atoms or molecules). When the particle size of different gases is unchanged, the collision frequency is *proportional to the gas pressure and to the square root of its absolute temperature*. Comparing the results obtained under sunlight with those obtained with artificial light, and applying Planck's temperature-dependent radiative distribution law, the effective wave length was roughly estimated at 1,9 µm.

This behaviour can be explained by the occurrence of an *internal energy* of the molecules or atoms, which is due to vibrations of the atom nuclei or of the electron shells, and which is induced by the applied IR-radiation. That kind of energy is not identical with the *apparent heat* of the gas which is measurable with a thermometer, and which is due to the kinetic translation energy of the entire atoms or molecules. Thus, when the particles are in an excited vibrational state, induced by thermal radiation, solely a part of this internal energy is transformed into apparent heat, induced via collisions, whereas another part is emitted as radiation, without having achieved a change of apparent heat. Contrariwise, warming up of a gas leads to acceleration of the particles, and via collisions to enhanced internal vibrations enabling thermal radiation.

Obviously, in this case the amount of absorbed IR-radiation is so low that it cannot be detected with a conventional IR-spectrometer. However, it is high enough to induce a measurable temperature increase. On the other hand, the absorption values obtained with IR-spectroscopic methods appear to be irrelevant for a temperature enhancement, since that kind of adsorption may possibly lead to internal vibrations which cannot be readily converted to apparent heat but rather to a radiation emission.

As a consequence of the theoretical finding that the thermal radiation of a gas was proportional to the pressure, one could assume that the atmosphere emits thermal radiation in both directions, namely towards Space as well towards the Earth surface, and that the intensity of the atmosphere radiation at the Earth surface was proportional to the atmospheric pressure and to the square root of the absolute temperature of the atmosphere at the Earth surface. Thus in the case of a steady equilibrium state the intensity of the black-body radiation of the Earth surface – or of a particular section of it – must be equal to the intensity of the thermal atmospheric radiation which may be called *counter-radiation*. This approach is similar to the approach of the Stefan-Boltzmann relation. However, it is more expressive since it comprises the pressure as a predominant parameter, whereas in the Stefan-Boltzmann

relation solely the absolute temperature appears (in the fourth power). Thereby no information is given as to how this temperature is achieved.

Thus, in the third enclosed article entitled **»The Thermal Radiation of the Atmosphere and its Role in the so-called Greenhouse Effect«** it stood to reason to validate this approach by empirical evidence, (1) by using the method described in the first article where coloured aluminium plates were exposed to sunlight, and (2) by varying the atmospheric pressure by means of varying the sea level of the measurement station. Thereby, the steady states at the limiting temperatures were needed where the intensity of the emitted thermal radiation of the plates is equal to the intensity of the counter-radiation of the atmosphere. In order to get the real limiting temperatures (and not the computed ones), thinner aluminium plates were used (8 mm thick, instead of the original 20 mm ones) which entailed shorter measurement periods.

In order to get optimal results, it would be necessary to solely vary the atmospheric pressure whereas the other parameters (atmospheric temperature and intensity of the sunlight) should be invariant. However, in reality this condition can inherently not be fulfilled since the variation of the sea level of the measuring station implicates a variation of the temperature of the ambient atmosphere as well of the intensity and the character of the sunlight. Thereby, at higher sea levels the atmospheric temperature decreases whereas the intensity of the sunlight increases. Nevertheless, acceptable results were obtained with four differently coloured plates (white, blue, green and black) at the two measuring stations in Switzerland *Glattbrugg* (430 m above sea level, approx. 0.948 bar atmospheric pressure) and *Furka-Pass* (2430 m above sea level, approx. 0.738 bar atmospheric pressure), yielding a so-called *atmospheric emission constant A* of approx. 22 $Wm^{-2}bar^{-1}K^{-0.5}$.

As a consequence, it can be stated that the counter radiation of the atmosphere indeed contributes to the climate, but as a whole and insofar as the atmospheric temperature decreases at higher sea levels. Thereby the trace gas is insignificant. Furthermore, it can be supposed that the mean temperature of the Earth surface would decrease when, as a result of a reduced assimilation of plants, the oxygen-content of the atmosphere and therefore the atmospheric pressure would generally decrease since the nitrogen-content can be assumed to be constant. This may possibly explain – or at least partly – climate changes during earlier palaeontology aeons. But in particular, it reveals the important role of nitrogen in the atmosphere, which does not only reduce the chemical aggressiveness of oxygen, but, due to the thereby enhanced atmospheric pressure, it also enables an overall convenient climate, which is prerequisite for life on this earth.

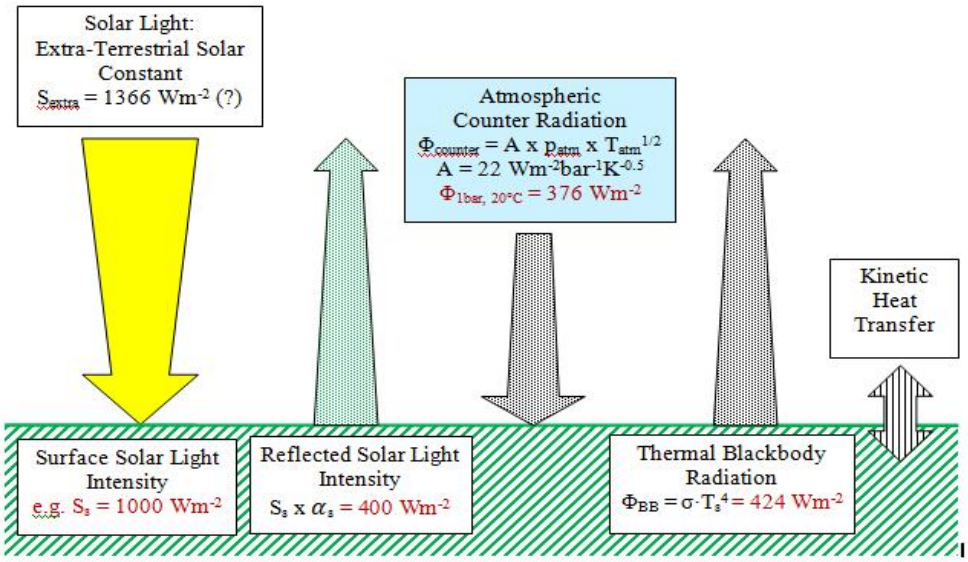

Scheme: Radiation- and Heat-Exchange at the Earth Surface (red figures: arbitrary values)

Keywords: Albedo; heat-emission; Stefan-Boltzmann law; climate-modelling; solar-tube; gas-temperature; radiation-absorption; kinetic-gas-theory; solar adsorption coefficient; radiation equilibrium.

1. THE SOLAR-REFLECTIVE CHARACTERIZATION OF SOLID OPAQUE MATERIALS

1.1 Summary

With respect to the reflective behaviour of solar radiation on solid surfaces being relevant for (micro)-climate modelling, particularly at pavements, buildings and roofs, it is proposed making a difference between the colour dependent terms *albedo* a_s and *solar reflection coefficient* α_s, the former being related to a white surface, and the latter being related to the total incident solar radiation. As a complement to the solar reflection coefficient, the *solar absorption coefficient* $\beta_s = 1 - \alpha_s$ is defined. For conceiving the thermal behaviour of solid materials in the presence of sunlight, a novel method is described for directly determining the solar absorption coefficient, instead of the usual but delicate methods where the incident and the reflected radiation are measured delivering the solar reflection coefficient. Thereto, the heat absorbance rate of coloured solid plates is determined by measuring their temperatures, and regarding their heat capacities. Since the warming-up process is interfered by a heat emission, the *cooling down behaviour* has to be known. Thereto, separate measurements were made with preheated plates in a darkened room, the obtained results differing from the forecast by the widely used Stefan-Boltzmann law. For both processes, mathematic modelling was derived enabling an arithmetic combination of the warming-up and the cooling-down process yielding limiting temperatures being solely dependent on the surface colour. Finally, some comparing albedo-measurements were made using a normal *light-meter* being directed towards wooden boards which have been coloured the same as the original plates, yielding a remarkably good accordance of the two methods.

1.2 Introduction

For climate modelling, the so called »albedo« plays an important part. In particular, it explains the so called urban heat island effect. The term is derived from Latin meaning »whiteness«, and was introduced by Johann Heinrich Lambert in his 1760 work »Photometria«, being commonly assumed as the colour-dependent *solar reflection coefficient*, normally indicated by α, concerning solar light and expressing the intensity-ratio of light being reflected by a surface compared to the incident light. A bright surface exhibits a high albedo that which is tantamount to a high portion of reflected light. Logically, the highest possible value of the albedo is 1.

But already with the definition of the term »albedo« some ambiguities arise, for, strictly speaking and regarding its true meaning, the albedo value should not be an absolute one but a relative one, namely being related to a white surface. However, in the literature such a distinction is not made. Rather, the terms »albedo« and »solar reflection coefficient« are used as synonyms. Moreover, according to the citations in the publication of Coulson and Reynolds (1971), one finds the apparent synonyms »spectral reflectance«, »optical reflection«, »reflection of direct radiation« and »reflectivity«.

A further intricacy is given by the fact that actually not the *reflection* of the light is relevant for thermal changes of the solid Earth surface – or of their artificial modifications such as buildings – but the *absorption*, hence in climate modelling indeed the solar absorption coefficient (here named β_s) is used, and not the solar reflection coefficient (here named α_s). Arithmetically, the two terms are complementary: $\beta_s = 1 - \alpha_s$. However, physically there is a principal difference insofar as the absorbed energy is of another type than the reflected one: the first one affects partly heat, while the second one affects only radiation power. Moreover, as a result of this reflection the radiation is transformed and scattered, changing its character and its colour, since this kind of reflection is not the same as a reflection of light on a mirror surface. And furthermore, both energies may engender subsequent implications, in particular warming-up the adjacent atmosphere. Therefore, the above equation is not such trivial as it appears prima facie.

This fact is insofar relevant as normally the reflection coefficient is determined, and not the absorption coefficient. That's because for the field measurements being originally made, concerning landscapes or cities, the former method is easier to carry out but still exhibiting several difficulties. For example, field-measurements of the optical reflection characteristics of various natural sands and soils at different wavelengths by Coulson et al. (1965) showed that there is a strong dependency of the intensity and degree of polarization of the reflected radiation on the angle of the incident radiation, particularly at longer wavelengths. Similar dependencies were also found for various other surfaces, soils and types of vegetation (Coulson and Reynolds, 1971; Nkemdirim, 1972).

Normally, the solar reflection coefficient is determined by »*albedometers*« where the intensities of incident solar light, on the one hand, and of reflected light, on the other hand, are compared. A principal description is given in the *ASTM Standard E1918-06*. Therein, the light intensity is simultaneously measured by two diametrically opposed »*pyranometers*«, being approx. adapted to the electromagnetic spectrum of solar light extending from wavelength 300 to 3500 nm, where the range <380 nm matches UV (ultraviolet) radiation, and the range >760 nm matches IR (infrared) radiation. In the above standard specification, a pyranometer operating in the range 280-2800 nm is recommended. Thereby, it is worth knowing that the *entire* infrared range extends up to much longer wavelengths, also comprising the thermal radiation of solids describable by *Planck's law* (according to which the intensity peak e.g. at 300 K is in the region of 10'000 nm = 10 µm), while here only the *short wavelength range of IR* (also called NIR = near IR) is involved. However, the above mentioned special character of the reflected light leads to several inherent measuring problems being originally described by Coulson (1975) and later by Zerlaut (1989). The state of the art, comprising subsequent improvements, is outlined by Levinson et al. (2010).

An alternative, more sophisticated approach for describing the reflection behaviour of pigments is based on spectroscopic measurements on *transparent films*, focussing the near-infrared range of the irradiance. Thereby, the reflectance and the transmittance of a freely suspended transparent film, being coated with a pigment, are detected. A comprehensive description of this method, being established by several authors, as well as some specific results, is given by Levinson, Berdahl and Akbari (2005). It starts from the feature of the North-American solar irradiance spectrum (300-2500 nm) that visible light (400-700 nm) accounts for only 43% of the energy in the air-mass, while the remainder arrives as near-infrared (700-2500 nm, 52%) or ultraviolet (300-400 nm, 5%) radiation. The intention of the relating philosophy is to improve preferentially the reflection-power in the NIR-range of radiation, and not the one in the visible range, thus creating dark pigments with a high albedo. This wondrous inversion is aptly expressed by the title of a publication of Brady et al. (1992) in a commercial magazine: "When black is white." However, with respect to the practical relevance of its results, this method has to be queried since a direct coherence to coloured solid opaque materials is not given, and a calculation of the heat absorbance degree is not possible. Moreover, the assessment of the empirical results affords a quite complicated theory exhibiting a variety of parameters, while comparing measurements on base of a different method are missing.

In reality, the circumstances are even more complex since the surface material overtime grows warm giving off heat to the atmosphere, be it by radiative emission, or be it by conductive heat transfer. Hence, the transformative reflection of solar light is superimposed by an emission of heat.

For theoretically describing the temperature dependent *radiative emission* of a solid surface, usually the formula of Stefan (1879) and Boltzmann (1884) is applied, expanded by the "spectral emissivity" ε (cf. Visconti, 2001, p.8), and delivering a value for the limiting surface temperature $T_{\lim}$ in the presence of vertically incident solar radiation:

$$S^* \cdot \beta_s = \varepsilon \cdot \sigma (T_{\lim}^4 - T_{air}^4) \tag{1.1}$$

S^* = solar-constant at the Earth surface (= terrestrial solar-constant)

β_s = solar absorption-coefficient = $1 - \alpha_s$

ε = spectral emissivity

σ = currently assumed Stefan-Boltzmann-constant = $5.67 \cdot 10^{-8}$ $Wm^{-2}K^{-4}$

The forth power of the absolute temperatures at ordinary temperature conditions near the Earth surface may be substituted by the simple first power expression

$$T_1^4 - T_2^4 \cong 4T_2^3(T_1 - T_2) \tag{1.2}$$

where the factor $4\sigma \cdot T_2^3$ becomes theoretically approx. 6 $Wm^{-2}K^{-1}$ when T_2 = 300 K (cf. Meschede, 2002, p.236).

Actually, Stefan's approach – being deduced from ancient measurements of Dulong and Petit (1817) - supposes a radiation and a back-radiation. However, apart from the peculiar spectral emissivity term, this formula exhibits a raw point by assuming that the two radiation sources are of similar type, namely black bodies. But it seems quite unlikely assuming the atmosphere as a black body. Moreover, the formula comprehends *no distance term* for the two sources. Therefore, it appears advisable empirically checking the validity of that formula, comparing it with the *Newton law* (1.3), resembling to equation (1.2) but exhibiting another factor *B* named *heat transfer coefficient [$Wm^{-2}K^{-1}$]*:

$$S^* \cdot \beta_s = B(T_{\lim} - T_{air}) \tag{1.3}$$

One of the first *practical material specific information* is 1963 given by J. F. Black regarding asphalt pavements. More than 30 years later, but referring to a previous paper of Johnson and Watson (1984), Asaeda et al. (1996) observed and analysed the *heat flux* at the air/ground interface for various pavement materials on summer days. The surface temperature, heat storage and its subsequent emission to the atmosphere were significantly greater for asphalt than for concrete or bare soil. At the maximum, asphalt pavement emitted an additional 150 Wm^{-2} in infrared radiation and 200 Wm^{-2} in sensible transport compared to bare soil surface. Analyses of the atmosphere indicated that most of the infrared long wave radiation from the ground was absorbed within 200 m of the lower atmosphere affecting air temperature near the ground. With large difference between air and ground surface temperature at noon, the rate of infrared absorption by the lower atmosphere over asphalt pavement was greater by 60 Wm^{-2} than that over the soil surface or concrete pavement.

With the objective of reducing the demand of air-conditioning costs in warm places by reducing the interior temperature of buildings, Pomerantz et al. (1999) made temperature measurements with twelve 10 cm square pavement-samples in an array being attached to an insulating foam board which had been covered with an unpainted cotton artist's canvas. Underneath each sample, a thermocouple was placed. The sample board was placed on a wooden roof platform only 10 cm above the roof surface and tilted up to face the midday sun (zenith angle, 55°). The wind conditions were "breezy enough to move papers around but less than a stiff wind", hence quite undefined. No on-site wind *measurements* were performed though it was conceded that the effect of convection were quite evident. The temperature rise was measured relative to the local air temperature. Each sample attained its maximum - or stagnation - temperature after a few minutes in the sun. Thereafter, the sample temperatures fluctuated erratically, by several degrees, as gusts of wind come and go. The relevant heat emission of the samples was not measured but solely calculated, using the Stefan-Boltzmann relation. Possible distortions, particularly of the wind, have not been quantitatively incorporated or minimized, thus an analytical consideration delivering material specific values is not feasible.

Doulos et al. (2004) and Synnefa et al. (2006, 2007) studied different building materials recording the mean hourly ambient temperature during the day as well as during the night, and using sampling tiles with a normal size of 40 cm x 40 cm. The sampling tiles were placed on an especially modulated platform covering a surface of 40 m^2, but being not embedded within a heat-isolating material such as Styrofoam, and being not orientated in a well-defined direction. The selected sample materials consisted of several different construction materials, of different surface colour materials, and of different surface texture materials. The basic experimental equipment used for the implementation of

the measurements consisted of an infrared camera to measure surface temperatures. Measurements were also performed by using contact thermometers in order to take into account minor errors associated with reflected infrared radiation and the non-complete knowledge of the material emissivity. The optical and thermal criteria were both regarded but not separated, so the classification »cold materials« were vaguely characterized by a high reflectivity factor to the short-wave radiation and a high emissivity factor to the long-wave radiations. Within the study published in 2006, an infrared camera was used in order to observe the temperature distribution on the surface of the samples as well as to depict the temperature differences between the samples, whilst within the study published in 2007, the infrared emittance of the samples was also measured with the use of an »emissometer«, while the spectral reflectance of the samples was measured using a UV/VIS/NIR spectro-photometer. Yet again, the reported results do not deliver definite material specific information but solely comparisons.

Hagishima and Tanimoto (2003) made field measurements for estimating the convective heat transfer coefficient at building surfaces, being defined as the quotient of the convection heat flux [Wm^{-2}] and the temperature difference between air and surface. The material specificity was not studied, but mainly the dependence on wind velocity. Generally, the variation of the results was quite large.

In view of these uncertainties, it appeared appropriate, instead of delicately measuring the reflected radiation, applying a *thermal method with respect to the substrate* directly delivering the *absorbance coefficient*, while the complementary reflectance coefficient could be calculated, according to the relation $\alpha_s = 1 - \beta_s$. As a consequence, the *heat capacity of the substrate* (or the appropriate areal-specific *thermal admittance* [$Jm^{-2}K^{-1}$]), will be relevant. Moreover, a simultaneous *heat-transfer* between the substrate and the adjacent atmosphere-layer is to be expected insofar the sample gets warmer, reaching a limiting temperature where the warming-up rate is equal to the heat-emission rate. For fulfilling the empirical requirement of the investigation and thus excluding the hereof hypothetical relation of Stefan-Boltzmann, the cooling-down process should have to be studied empirically within separate experiments. Astonishingly, such a laboratory-like method with well-defined boundary conditions has not been presented, yet. The only known being roughly relevant seems that one described by Schwerdtfeger (1976), using a simple apparatus consisting of aluminium disks being set into insulating Styrofoam-blocks and laterally equipped with Hg-thermometers. Since they are cooled by an electric blower during the solar insolation, the influence of air convection is maximized instead of minimized. Moreover, this method affects only limiting, i.e. stagnation conditions.

Summarizing it may be stated, firstly, that commonly no distinction is made between the notation »albedo« as a relative term, and the notation »solar reflection coefficient« as an absolute term, although it would be meaningful. Secondly, the indirect determination of the solar absorption coefficient β_s by determining the solar reflection coefficient α_s is delicate suggesting its direct determination. Thirdly, any hitherto applied thermic measuring methods implicated solely limiting temperatures without delivering the basis for a mathematical description of the temporal course of the heating-up and the cooling-down process. Moreover, they mostly were disturbed by uncontrollable influences of the surroundings, exhibiting rather field-like than laboratory-like conditions. All in all, in spite of the great amount of investigations and of the great efforts which have been expended yet, there is still no method available which yields more than relative values instead of reliable and well-defined ones, and which allows the precise modelling of the elementary process which occurs when sunlight comes upon a solid opaque surface.

1.3 Outline of the Present Approach

Within the present approach, not the reflected but the *absorbed radiation* is determined, namely by measuring the temperature courses of coloured quadratic plates (10 x 10 cm, usually 20 mm thick) with a known thermal specification when sunlight of a known intensity comes *vertically* onto these plates. They are embedded in Styrofoam, and covered with a thin transparent foil acting as an outer window to minimize erratic cooling by atmospheric turbulence. Thereby, the colours as well as the plate material are varied (aluminium, wood, brick and stone). As a reference material, aluminium is used being optimal due to its high heat conductivity and high heat capacity leading to a low heating rate and a homogeneous heat distribution. For enabling a correct orientation, the plate modules are positioned on an adjustable carrier. During the heating time of preferably 30 minutes, the equilibrium

temperature was normally not reached, but the heating-rate could easily be determined by graphically assessing the initial slope.

In order to study the *cooling down behaviour*, separate measurements have been made with preheated plates in a darkened room, the results being mathematically analysed. Hence, this method is solely based on thermal measurements using Hg-thermometers but omitting electronic instruments, except a »solarmeter« for measuring the intensity of the incident light during the warming-up process. If certain boundary conditions are fulfilled (constant atmospheric temperature, relatively thin plates and high thermal conductivity), the cooling-down process can be exactly expressed by a mathematical equation. Moreover, a stringent mathematical combination of the warming-up and the cooling-down process is feasible allowing to model the temporal energy transfer occurring between a solid surface layer and the contiguous air, and thus to study the influence of the colour and of the thermal admittance of the plate, as well as the temporal course of the temperature up to its limiting value.

The clearing of the relevant colour dependent termini is of special importance whereby partly novel designations and definitions are introduced. In particular, as initially mentioned, it is proposed distinguishing between the *(relative) surface albedo* a_s being colour dependent and related to a white surface exhibiting an albedo of 1, and the *solar reflection coefficient* α_s being related to the total energy flux of the incident light, and being coupled to the *solar absorption coefficient* β_s by the relation $\alpha_s = 1 - \beta_s$. Furthermore, the term *solar colour factor* b_s is introduced amounting the ratio between the solar absorption coefficients of the plates with the relevant colour and the white colour, or, easier, the ratio between the respective heat absorption rates.

Finally, some comparing albedo-measurements were made using a *light-meter* being directed towards wooden boards which have been coloured alike the original plates, a white plate serving as the reference.

1.4 Equipment, Procedure and Materials

The *warming-up experiments* were carried out using small coloured quadratic plates (10 x 10 cm^{-2} and about 20 mm thick) from different materials (aluminium, wood, brick and stone) when sunlight of a known intensity (approx. 1000 Wm^{-2}) was coming vertically onto these plates (i.e. perpendicular to the plates). Each plate was equipped with a Hg glass tube thermometer being inserted in centrally provided holes, and embedded in Styrofoam being covered with a thin transparent PVC-foil (0.07 mm) acting as an outer window, as schematized in Fig. 1.1. The vertical positioning of the thermometer facilitated controlling the perpendicular arrangement of the module by regarding its shadow. However, in some appropriate cases the thermometer was attached laterally. At plate-materials with a low thermal conductivity (e.g. from brick or, in particular, from wood), the additional insertion of an aluminium foil into the thermometer holes was advantageous to enhance the thermal distribution.

Using a suitable panel comprising the plate modules and being directed by a mounting on a monopod at back, up to six measurements could be made simultaneously, as shown in Fig. 1.2. The direction of the sun irradiation was determined by an aluminium tube being adjustably mounted on a tripod and measured by a goniometer. Prior to the experiment, all the modules were covered with aluminium-mirrored foils, avoiding a premature warming-up, and being removed at intervals of 10 seconds thereby starting the process. The temperature readings were made every five minutes. During the experiment lasting normally 30 minutes, the sky had to be cloud-free, and the modules were currently adjusted to the irradiation direction by stepwise revolving the padding on which the equipment has been established. The irradiation intensity was measured by a certified KIMO Solar-meter SL 100. The solar experiments have been made on a balcony in Glattbrugg (near Zurich/Switzerland, about 450 meters above sea level) during several summer days, and preferably early in the afternoon. The atmospheric pressure was between 960-980 hPa, and the relative humidity between 50-60%.

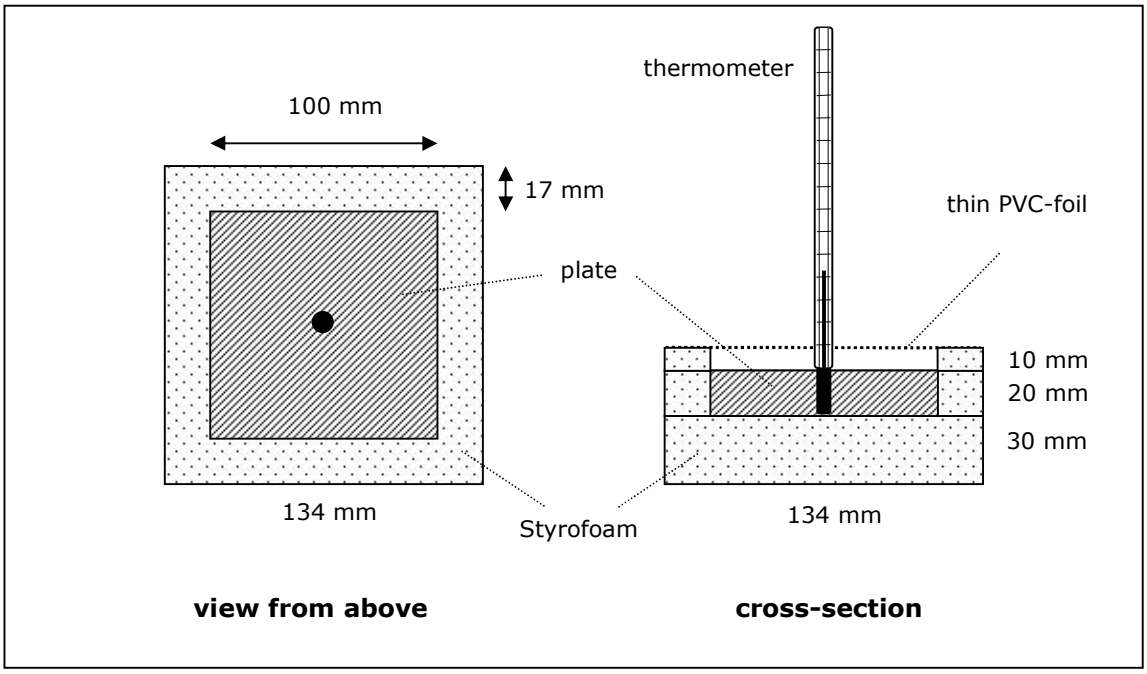

Fig. 1.1. Plate embedded into Styrofoam

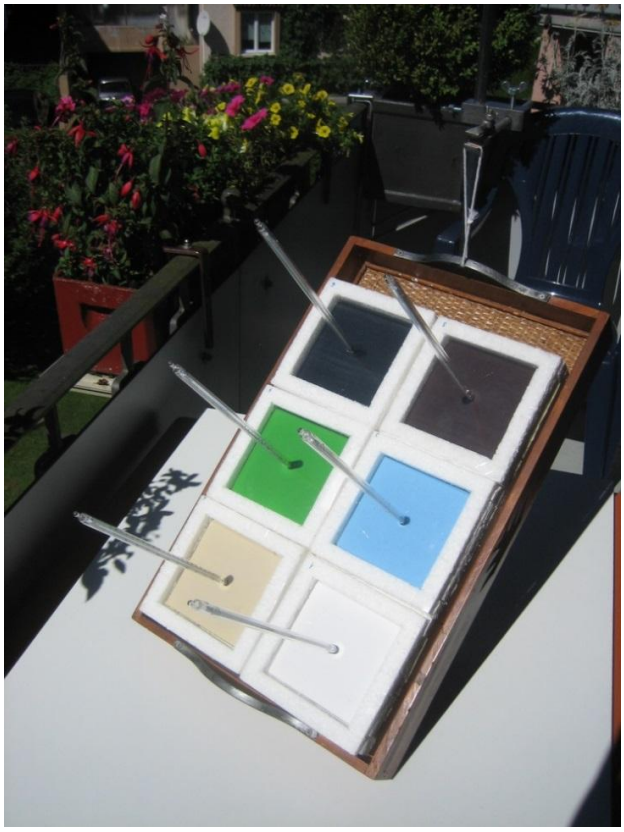

Fig. 1.2. Panel comprising six modules

The *cooling-down experiments* were made in a partly darkened room with a known ambient temperature between 20 – 25°C using the same modules. However, they were carried out partly, i.e. bit by bit. Initially, each plate was heated in an oven up to a temperature above 60°C, and the start of the experiment was given when the temperature of the plate had reached 60.0°C. Afterwards, temperature readings were made at regular intervals, for aluminium of 15 minutes, and for wood or brick of 5 minutes (since the latter ones cooled down more rapidly).

The relevant features of the applied *materials* are listed in the table below:

Type	**thickness [mm]**	**mass (middle) [g]**	**density [gcm^{-3}]**	**spec. heat capacity [Jg^{-1}K^{-1}]**	**total heat capacity [JK^{-1}]**	**heat conductivity [Wm^{-1}K^{-1}]**
aluminium (al)	20.0	537.5	2.70	0.902	485	236
wood (wo)	17.5	80.5	0.50	1.83	147	(0.1-0.2)
brick (br)	14.5	245	2.06	(0.84)	(206)	(0.5-1.4)
stone (st)	20.5	527.5	2.60	(0.79)	(417)	(2.8)

The brick-plates were sawed out from fresh red brick-pieces (being not weathered), and the (single) stone-plate was also sawed out from a natural granite boulder found in the Alps. The mass variance of the plates was minimal. The densities of spruce-wood, brick and the granite-stone plates were determined using the usual water buoyance method. The heat capacity of spruce-wood was determined using a calorimeter. The other values, being not very reliable and thus enclosed in brackets, are taken from literature.

The following *colours* have been applied (being not specified more precisely):

white (wh)	bright brown (lb)	vanilla (va)	bright blue (bl)
bright green (gr)	brick-red (re)	dark brown (db)	black (bk)

1.5 Results and Interpretations

1.5.1 Solar warming-up experiments

The primary experiments were made with two series of six colours using plates from aluminium and spruce-wood. The results are displayed in Figs. 1.3 and 1.4. The warming-up rates, expressed in grades per time (minutes), were determined by graphically evaluating the initial (linear) slope.

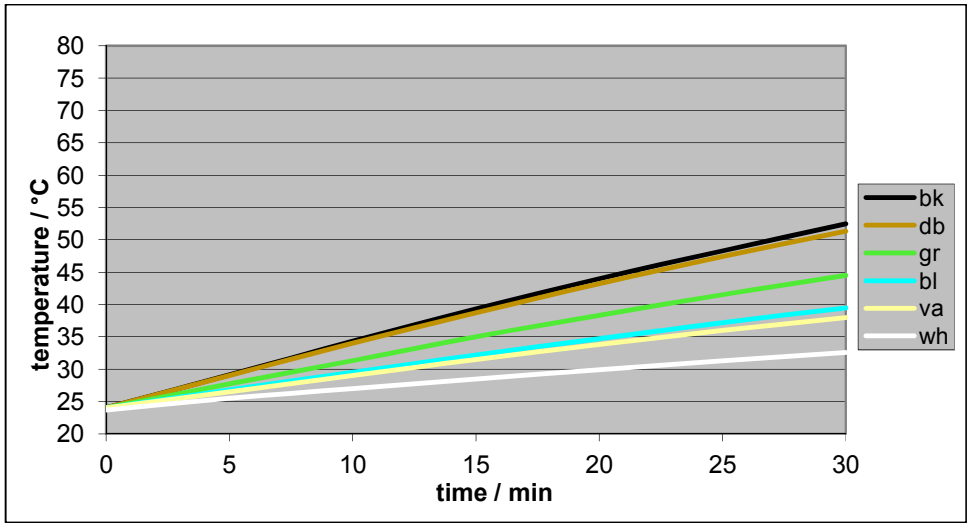

Fig. 1.3. Warming-up of aluminium at 1040 Wm^{-2} 2013-09-04, 12:58 h
Initial slopes [°/min]: wh 0.31 / va 0.52 / bl 0.58 / gr 0.77 / db 1.02 / bk 1.08

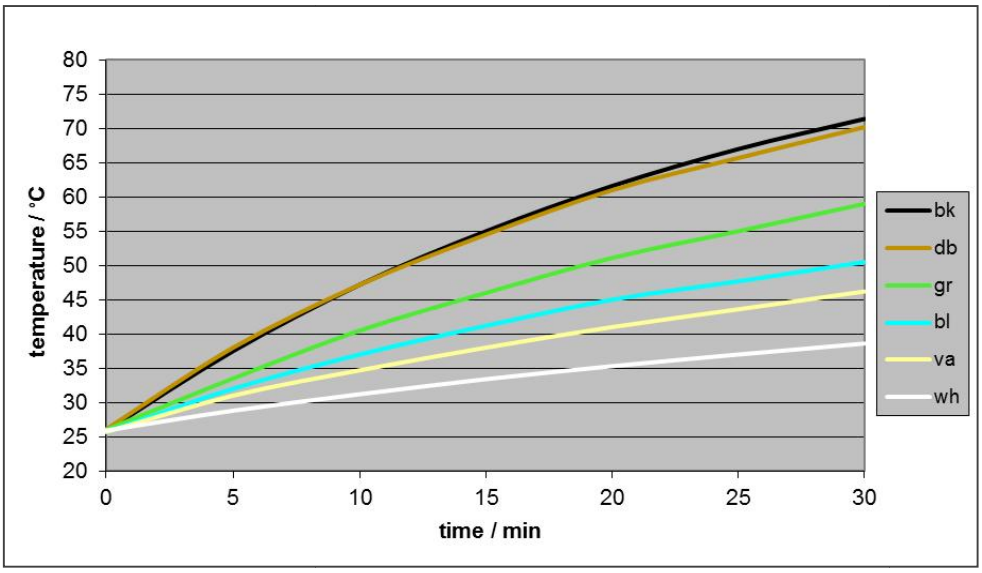

Fig. 1.4. Warming-up of wood at 970 Wm^{-2} 2013-09-06, 12:43 h
Initial slopes [°/min]: wh 0.60 / va 1.02 / bl 1.20 / gr 1.57 / db 2.35 / bk 2.45

Regarding these figures, firstly it is salient that the warming-up rates are much larger for wood than for aluminium. Secondly, the *relative courses* of the colour dependent rates are quite similar in both cases, the dark brown one being nearly equal to the black one, and the light green one being considerably high. And thirdly, in particular with wood and with dark colours, the rate courses were not linear all the more the temperature rose. A similar order is evident in the case of brick plates (Fig. 1.5), also exhibiting high warming-up rates, whereby partly other colours were applied.

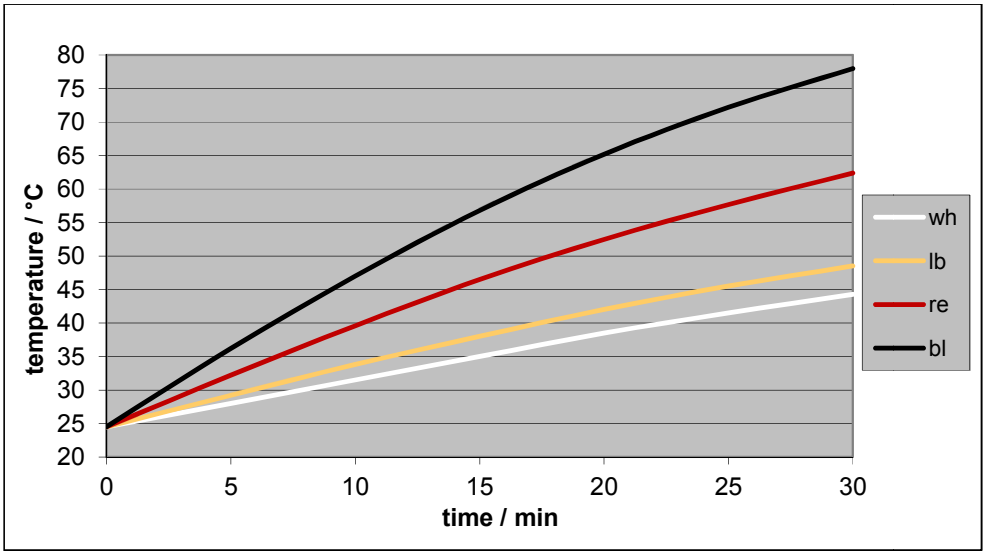

Fig. 1.5. Warming-up of brick plates at 1050 Wm^{-2} 2013-09-04, 14:52 h
Initial slopes [°/min]: wh 0.70 / lb 0.98 / re 1.61 / bk 2.37

Formally, *the initial warming-up rate* is determined by the *irradiation density* of the sunlight, the *solar absorption coefficient* of the relevant colour, and the *thermal admittance* of the plate. Within the initial linear range, the resulting temperature is given by

$$\frac{T - T_0}{t} = \Phi \cdot \beta_s / C_A \tag{1.4}$$

T = temperature of the plate [K] or [°C]
T_0 = starting temperature of the plate [K] or [°C]
t = time [s]
Φ = irradiation density on the surface [Wm^{-2}] where 1 W = 1 Js^{-1}
β_s = solar absorption coefficient
$C_A = c_m \cdot \rho \cdot d \cdot 10^4$ = thermal admittance of the plate [$Jm^{-2}K^{-1}$]
c_m = mass specific heat capacity of the plate material [$Jg^{-1}K^{-1}$]
ρ = density of the plate material [gcm^{-3}]
d = thickness of the plate [cm]

The evident differences of the warming-up rates between aluminium, on one hand, and wood as well as brick, on the other hand, may be basically explained by the differences of their thermal admittances, whereas the deviation of the linearity at the ends of the curves is due to the thermal radiation being emitted by the plates insofar as the temperature difference to the environment increases.

Inserting the values given in the table, the following *thermal admittances* are obtained (in $Jm^{-2}K^{-1}$):

aluminium 48'700 stone 41'700 brick 20'600 wood 14'700

Inserting the above thermal admittances and using the expression of the slope given in formula (1.4), the (colour dependent) *solar absorption coefficients* β_s and, as a consequence, the *solar reflection coefficients* $\alpha_s = 1 - \beta_s$ can be calculated yielding for aluminium plates the values being plotted in the Figs. 1.6 and 1.7, and being best suited as standards due to their high thermal admittance as well as their thermal conductivities.

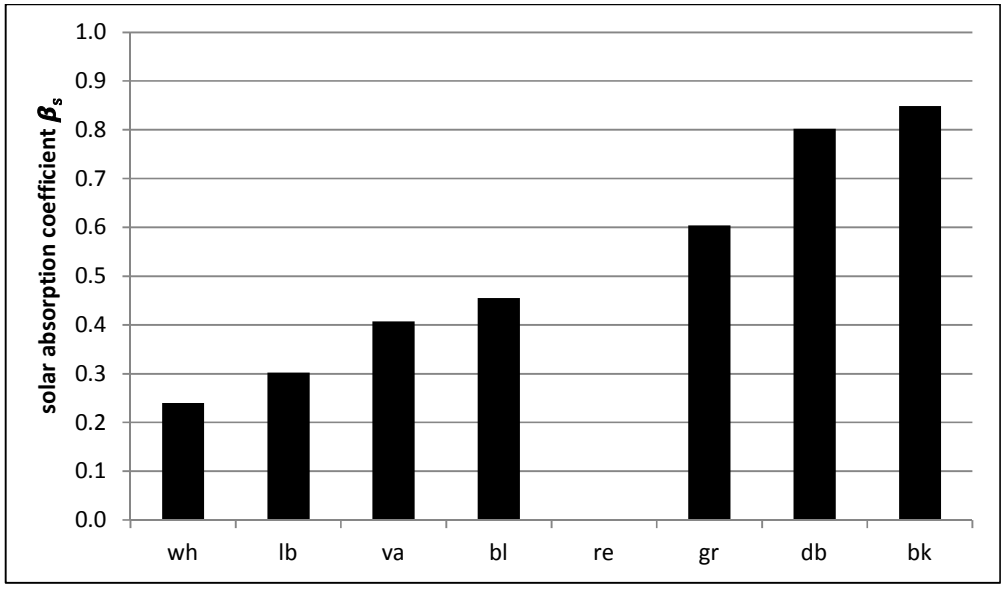

Fig. 1.6. Solar absorption coefficients β_s on aluminium (colour code p. 10)

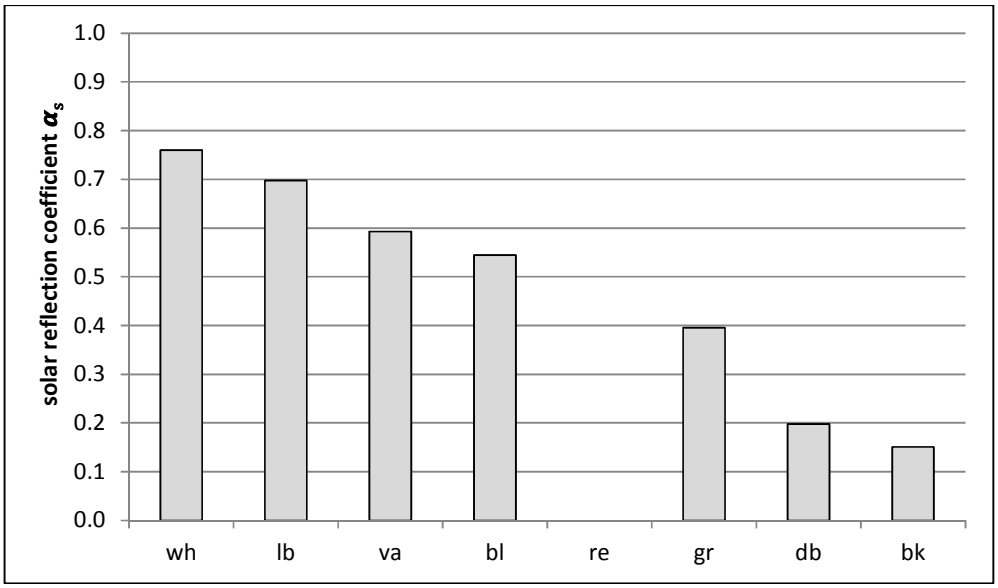

Fig. 1.7. Solar reflection coefficients α_s on aluminium (colour code p. 10)

Hence, the white solar absorption coefficient is 0.24, and the black absorption coefficient 0.85, corresponding to solar reflection coefficients of 0.76 and 0.15.

Using the values of the solar reflection coefficients given in Fig. 1.7, and relating them on the white surface assuming it as 1.0, for the real surface albedos a_s you get the values of Fig. 1.8, the black colour exhibiting a value of 0.20.

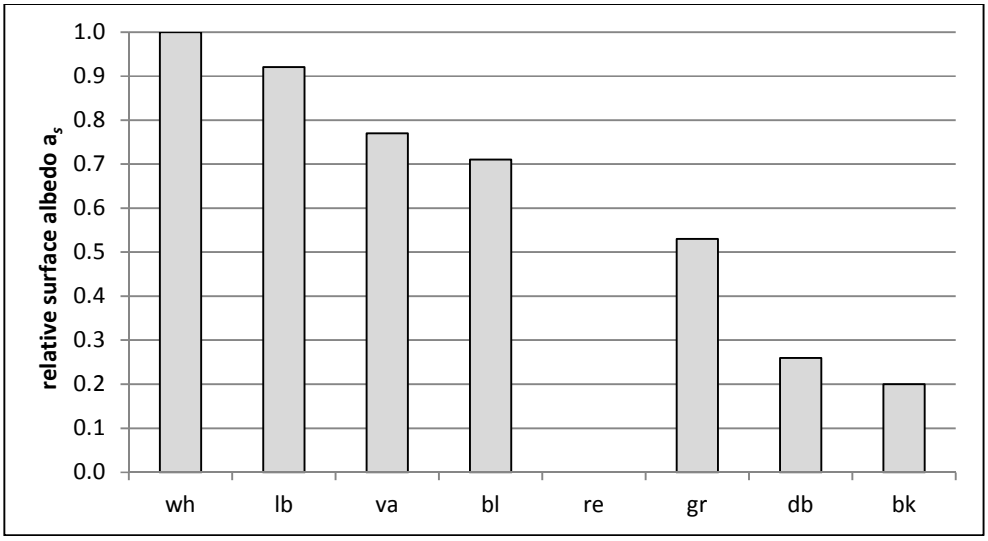

Fig. 1.8. Relative surface albedos a_s on aluminium (colour code p. 10)

Applying that procedure and using the averages of at least two differently measured values being normalized to the intensity of 1000 Wm^{-2}, the following *radiate colour factors* b_s have been found being compared in Fig. 1.9, in the case of aluminium the *black colour factor* exhibiting the value of approx. 3.5.

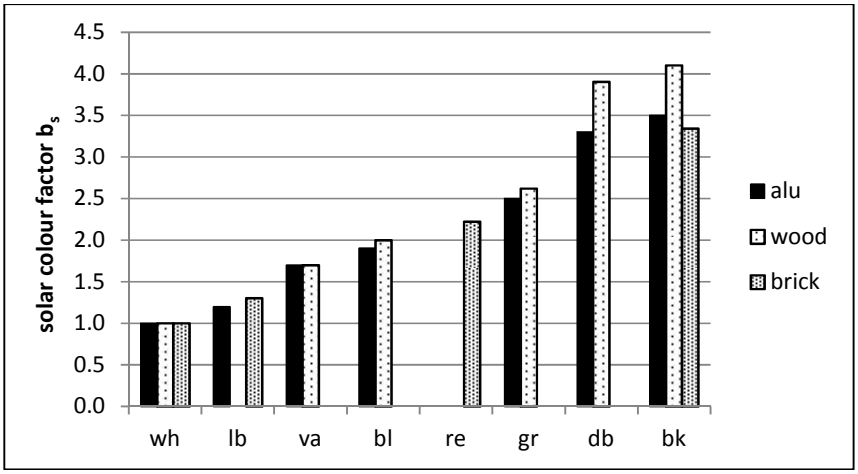

Fig. 1.9. Solar colour factors b_s on different materials (colour code p. 10)

However, comparing the warming-up rates at the different materials, there emerges the inconsistency that for each colour, e.g. for black, the warming-up rates were not just inversely proportional to the thermal admittances; i.e. for *wood* the warming-up rate was considerably smaller than theoretically expected, namely about 0.60 times as large. For *brick*, this factor was less small, namely 0.91, while for *granite-stone* it was 0.95. But that may be explained by the low heat-conductivity, particularly of wood, leading to a *vertical temperature gradient* within the plate accompanied by an enhanced surface temperature compared to the measured average one, particularly with dark surfaces.

1.6 Cooling-down Experiments

The procedure has already been described briefly. The primary observation was that, apparently contrary to *Kirchhoff's Radiation Law*, the long-wave radiate emission was completely *independent of the colour* of the plate but *dependent on the material*, as evident from Fig. 1.10. Moreover, the ordinarily applied thin transparent PVC-foil (0.07 mm) had a considerable influence on the cooling down rate, as evident from Fig. 1.11. The temporal course was not linear but converging to an equilibrium temperature being equivalent to the ambient room temperature. Thus for these experiments, differing from real natural conditions, the temperature of the ambient atmosphere was constant.

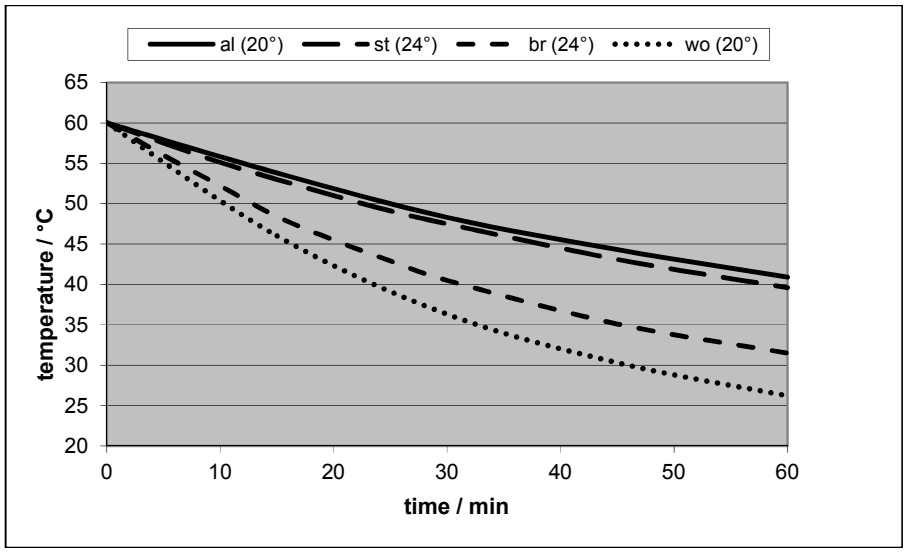

Fig. 1.10. Cooling-down of different materials, with foil
(in brackets: ambient temperature)

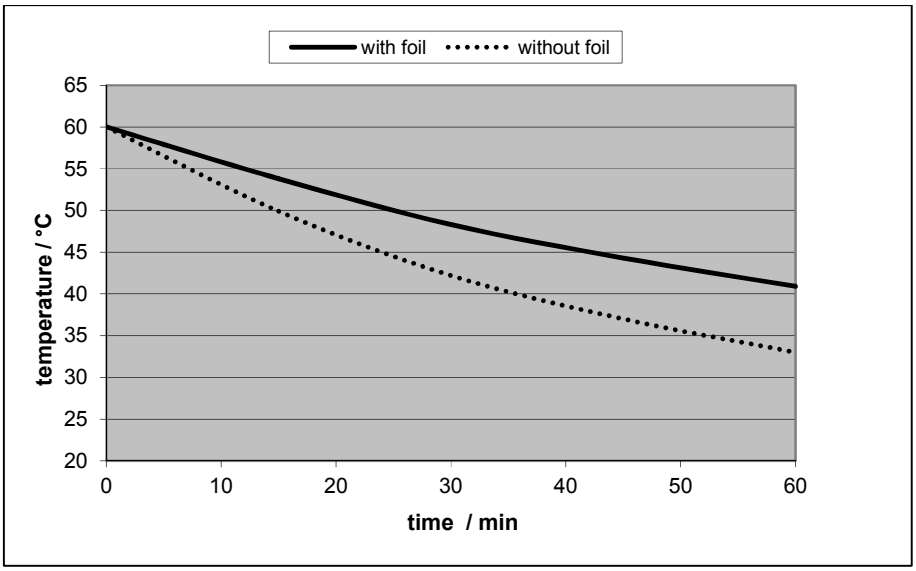

Fig. 1.11. The isolating effect of a foil for aluminium

Assuming an interference of heat diffusion and of radiation and thus using, as explained in the introduction, *Newton's Law* (1.3) instead of the modified *Stefan-Boltzmann Law* (1.2), a mathematical modelling may start from the following differential approach, valid for a given plate area:

$$-m \cdot c_m \frac{dT}{dt} = B \cdot A(T - T_{am}) \tag{1.5}$$

wherein t = time
T = (surface) temperature of the plate
T_{am} = ambient (room) temperature
B = heat transfer coefficient [$Wm^{-2}K^{-1}$]
A = surface area [m^2]

The further abbreviations are listed together with formula (1.4).

This differential equation can be resolved as follows:

$$T = T_{am} + (T_{in} - T_{am}) \cdot e^{-\frac{B \cdot A}{m \cdot c_m} t} \tag{1.6}$$

wherein T_{in} = initial (surface) temperature of the plate

Instead of the absolute temperatures, given in °K, the °C values may be used.

In order to determine the heat transfer coefficient *B* from experimental data, the logarithmic form of equation (1.6) may be used, delivering a linear plot:

$$\ln(T_{in} - T_{am}) - \ln(T - T_{am}) = \frac{B \cdot A}{m \cdot c_m} t \tag{1.7}$$

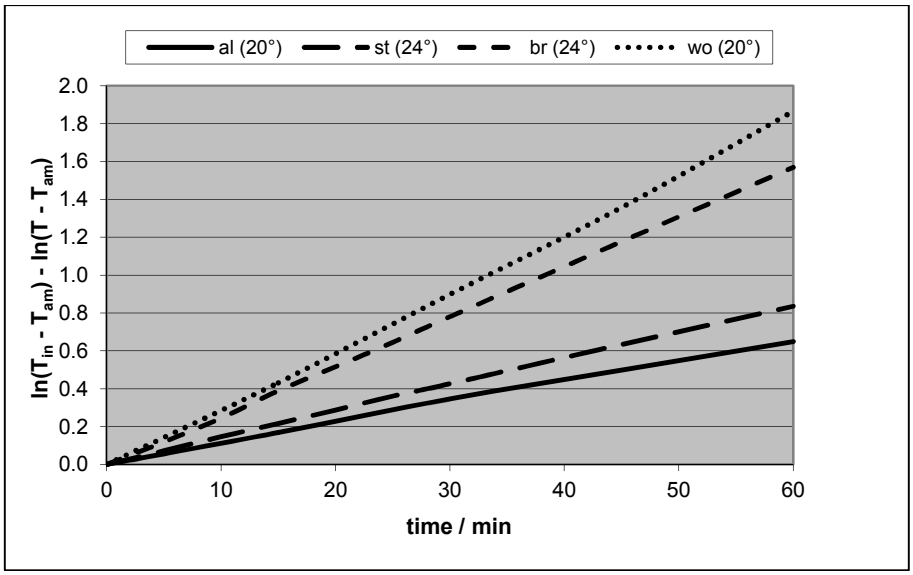

Fig. 1.12. Logarithmic plots of the cooling-down data, with foil
(in brackets: ambient temperature)

Inserting the heat capacity values listed in respective table, the evaluation of the logarithmic plots of Fig. 1.12 yields the following values for the *heat transfer coefficients B* [$Wm^{-2}K^{-1}$], with foil:

Aluminium (al):	8.8
Stone (st):	9.7
Brick (br):	9.0
Wood (wo):	7.4

The relatively small deviations for stone and for brick compared to the value for aluminium, being the most reliable one, may be due to inaccuracies of the heat capacity values. Moreover, it may be considered that the measurements for stone and for brick have been made at another time and on another day of the year, hence the (room) atmosphere could have been slightly deviating. However, the greater deviation of the value for wood is probably due to its reduced heat conductivity, but being smaller than in the case of the warming-up experiment (accordance factor: 0.84 compared to 0.60, cf. the table on page 10). Overall, the results are enough satisfying and suggest a *general heat transfer coefficient* of approx. 9 $Wm^{-2}K^{-1}$. In the case of the *absence of a foil*, the heat transfer coefficient increased by the factor 1.7, being determined analogously using the results of Fig. 1.11. Thus, for flat plates, the heat transfer coefficient comes up to more than 15 $Wm^{-2}K^{-1}$ even when the atmosphere is quiet, i.e. when there is no significant turbulence. This means that, at a temperature difference of 10°, the heat flux at the air/ground interface would be 150 Wm^{-2}, that value being in good accordance with the values of Asaeda et al. (1996) for pavements, as cited incipiently.

However, the theoretical value of 6 $Wm^{-2}K^{-1}$ resulting from the modified and simplified *Stefan-Boltzmann Law* (cf. 1.2 Introduction, formula (1.2)) is much lower than the here measured values even in the presence of a foil, meaning that the apparent heat transfer coefficient is significantly larger than the theoretical one predicted by the modified Stefan-Boltzmann Law. This fact is certainly due to an additional heat transfer by heat diffusion through the air. Moreover, no evidence could be found for the existence of an additional emissivity coefficient ε being commonly implemented in the modified Stefan-Boltzmann relation (1.2), implying an even smaller heat transfer since it is principally assumed to be smaller than 1. But in spite of the uncertainties due to the variable atmospheric conditions, it may be stated that, when the heat conductivity within the solid surface layer is sufficient, *the apparent heat transfer coefficient is usually at least two and a half times as large as the modified Stefan-Boltzmann Law predicts.* But when the material specific heat conductivity is low compared to the layer-thickness, it certainly gets rate-determining distorting that regularity.

1.7 The Combination of the Warming-up and the Cooling-down Process

When a plate is exposed to solar irradiation of a constant intensity, its temperature initially rises linearly but, in the course of time, a counter reaction occurs due to the increasing thermal emission, leading to a decrease of the warming-up rate until an equilibrium temperature is reached. Two processes were studied separately, the first one at the starting range where the temperature increase was nearly linear, and the second one separately in a darkened room where no simultaneous warming-up occurred. Now the two effects shall be mathematically combined to a time-temperature-curve disclosing the overall process.

Thereto, the *warming up rate* $\dot{T}_{\uparrow}$ may be expressed by differentiation of equation (1.4):

$$\dot{T}_{\uparrow} = \partial T_{\uparrow} / \partial t = \Phi(1-\alpha_s)/C_A = k_1 \tag{1.8}$$

On the other hand, the *cooling down rate* $\dot{T}_{\downarrow}$ is delivered by equation (1.5):

$$\dot{T}_{\downarrow} = \frac{dT_{\downarrow}}{dt} = -\frac{B \cdot A}{m \cdot c_m}(T - T_{am}) = -k_2(T - T_{am}) \tag{1.9}$$

where the two constants k_1 and k_2 have been introduced for the sake of convenience. The *total temperature rate* is given by the sum of the two single temperature rates:

$$\dot{T} = \dot{T}_{\uparrow} + \dot{T}_{\downarrow} = k_1 - k_2(T - T_{am}) = k_1 + k_2 T_{am} - k_2 T \tag{1.10}$$

This differential equation (1.10) is resolvable yielding the explicit form (1.11):

$$T = T_{am} + \frac{k_1}{k_2}\left(1 - e^{-k_2 t}\right) = T_{am} + \frac{\Phi(1-\alpha_s)}{B}\left(1 - e^{-\frac{B \cdot A}{m \cdot c_m} t}\right) \tag{1.11}$$

When $t = \infty$, T has reached a limes being calculated by equation (1.12):

$$T_{\lim} = T_{am} + \frac{\Phi(1-\alpha_s)}{B} \tag{1.12}$$

Hence, according to formula (1.12), the limiting temperature is *independent of the thermal admittance* or the heat capacity, respectively, but solely dependent on the irradiation density Φ, the solar reflection coefficient α_s, and the heat transfer coefficient *B*. E.g. in the case of the black aluminium plate, exhibiting a solar reflection coefficient of 0.15 and a heat transfer coefficient of 8.8 $Wm^{-2}K^{-1}$ (in the presence of a cover-foil), and at a solar irradiation density of 1000 Wm^{-2}, the maximal temperature enhancement is approx. 95°(K or C), whilst in the case of the white aluminium plate, exhibiting a solar reflection coefficient of 0.76, the maximal temperature enhancement is approx. 27°(K or C). If the ambient temperature T_{am} is assumed to be 25°C, the resulting limiting temperatures are 120° (for the black plate) and 52°(for the white plate), respectively.

The Figs. 1.13 and 1.14, being derived from equation (1.11), illustrate the influences of the surface colour (black and white), the thermal admittance and the cover foil, solely inserting aluminium plates but being variously thick (20 mm or 10 mm). From Fig. 1.13 (with B = 8.8 $Wm^{-2}K^{-1}$), it is evident that the limiting temperature for the black plates is considerably higher than for the white plates. But in the cases of the thinner plates, the processes are proceeding faster than in the case of the thicker plates, exhibiting a larger (twice as much) thermal admittance. In principle, the situation being outlined in Fig. 1.14 (with B = 15 $Wm^{-2}K^{-1}$) is similar, but the limiting temperatures are generally lower due to the absence of the cover foil leading to accelerated heat emission.

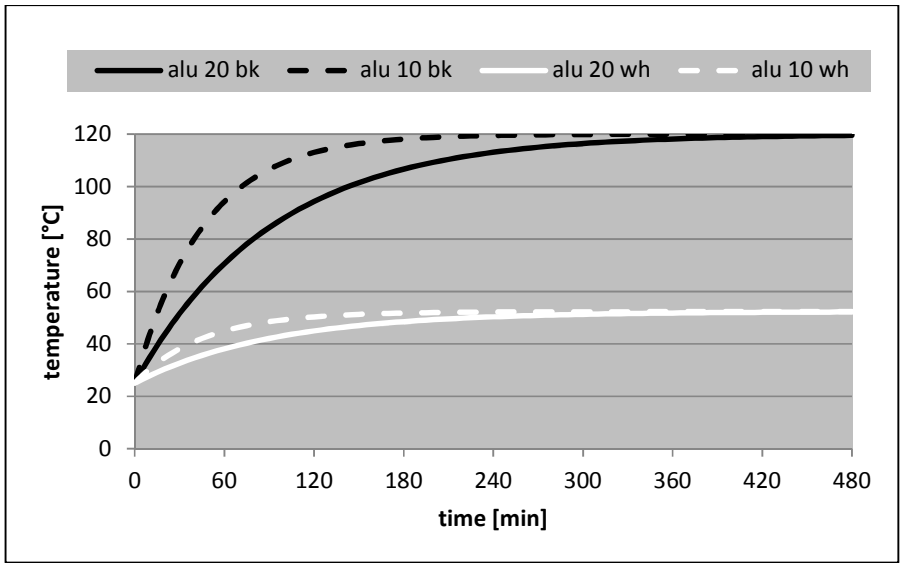

Fig. 1.13. Temperature courses with foil (at 1000 Wm^{-2}, calculated)

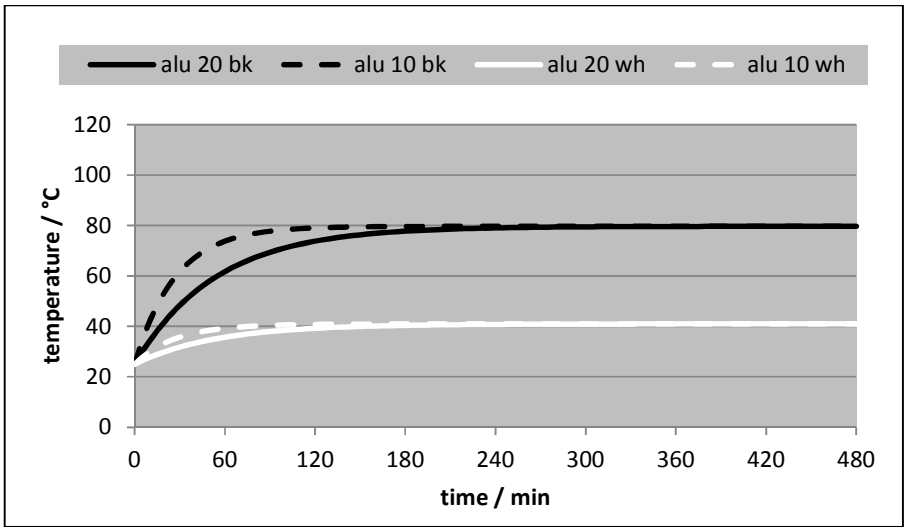

Fig. 1.14. Temperature courses without foil (at 1000 Wm^{-2}, calculated)

Analogously and for comparison, the temperature courses of differently coloured at aluminium-plates (Fig. 1.15), as well as at brick-plates (Fig. 1.16), may be calculated (with foil). These plots reveal that the heating-rates of the aluminium-plates are much smaller than those of the brick-plates – namely due to the larger thermal admittance -, while the limiting temperatures are equal in both cases. And, as being already evident from the previous diagrams, the green colour implicates a relatively high limiting temperature due to its relatively low albedo or solar reflection coefficient, respectively.

In addition, the given formulas allow an exemplary lining-up of the warming-up and the subsequent cooling-down process. Comparing blackened stone and blackened brick, e.g., such a possible two-step combination is showed in Fig. 1.17 where the warming-up curves are based on real measurements (at 1020 Wm^{-2}), and the cooling-down curves are calculated by formula (1.6) using the given material constants, assuming an ambient temperature of 24.5°C. Thereby it has to be remembered that the stone-plate was considerably thicker than the brick-plate (20.5 compared to 14.5 mm).

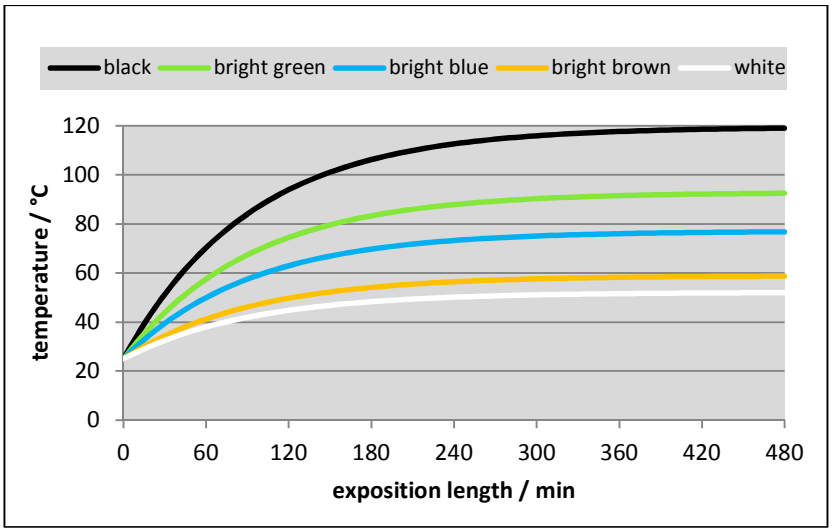

Fig. 1.15. Temperature courses at differently coloured aluminium-plates

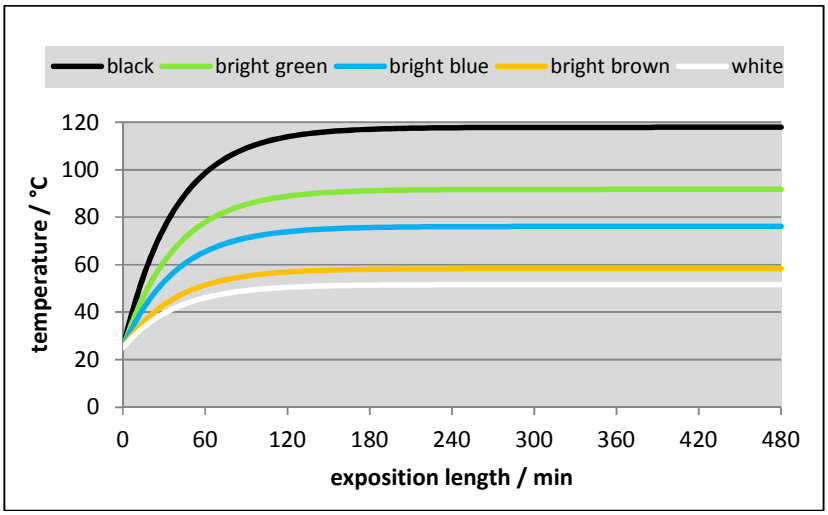

Fig. 1.16. Temperature courses at differently coloured brick-plates

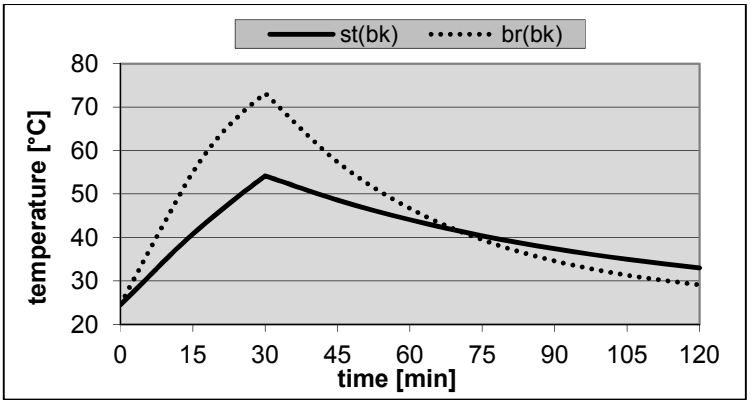

Fig. 1.17. Two-step combination for stone and for brick

1.8 Comparing Reflection Measurements by a Light-meter

As herewith demonstrated, this caloric method permits a quite exact determination of the relevant key values, as well as a mathematic description of the basic processes. However, it requires an accurate preparation of well-defined materials and the availability of the convenient equipment, being thus not suitable for field-measurements. Moreover, its relation to the conventional method of measuring the reflected radiation has not been empirically proven. Therefore, finally an easy device shall be proposed exhibiting both requirements. However, instead of the pyranometer for measuring the reflected radiation operating in the range of 280-2800 nm as being recommended in the quoted ASTM Standard E1918-06, a normal *light-meter* has been used, operating in the visible light range and being customary for photography and delivering the measured values in lux. Naturally, it would solely allow the determination of *relative albedo-values,* i.e. being related to a white surface, but they may be compared with the albedo-values which have been evaluated by the caloric method. Since only the visible light is affected, temperature and wind are irrelevant. However, the measurements must always be made from the same position while the solar irradiance must be constant, which may be checked by a pyrheliometer. Nevertheless, as has already been objected, the precision of this method will presumably not be high, the more so as mirror-like reflection may occur.

Fig. 1.18 shows an appropriate assembly for an albedo-measurement by a light-meter, using a white plastic-coated wooden board (60 x 70 cm) which has been painted with the respective colours. For this comparison, exactly the same colours were applied as for the previous experiments, namely white, vanilla, bright-green and black. For being able to adjust the board perpendicularly to the solar radiation by regarding the shadow, a small coloured bar (from aluminium) is attached near the bottom edge of the board. The inclination angle of the board depends on the time of the year and of the day, and was in this case about 25°. For avoiding the interference by its shadow, the light-meter has to be positioned laterally. As a light-meter, the Illuminometer i-346 from Sekonic was used, while the already used KIMO Solarmeter SL 100 served to measure the sunlight intensity.

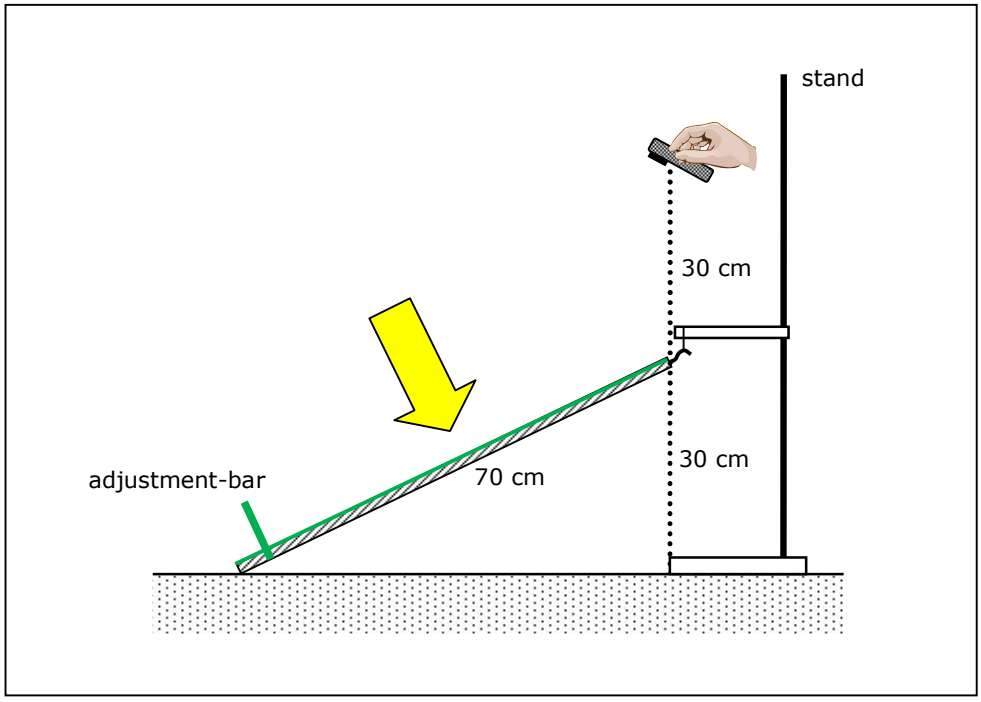

Fig. 1.18. Assembly for the albedo-measurement by a light-meter

1.9 Results

The measurements have been made in July around two o'clock at a solar irradiance intensity of about 1040 Wm^{-2}. Thereby, the following values were obtained, being compared below with the values which have been earlier received by the caloric method:

Method	white	vanilla	bright-green	black
direct / light-meter [lx]	58'500	15'000	28'000	47'500
indirect (relative albedo)	1.000	0.770	0.530	0.200

Using these results, the albedo-values referring to the light-meter can easily be calculated delivering the comparison being illustrated in Fig. 1.19, and revealing a remarkably good accordance of the two methods. However, the direct measurement delivers solely the relative values. For determining the absolute values concerning the solar reflection coefficient, a calibration on the basis of the caloric method is necessary.

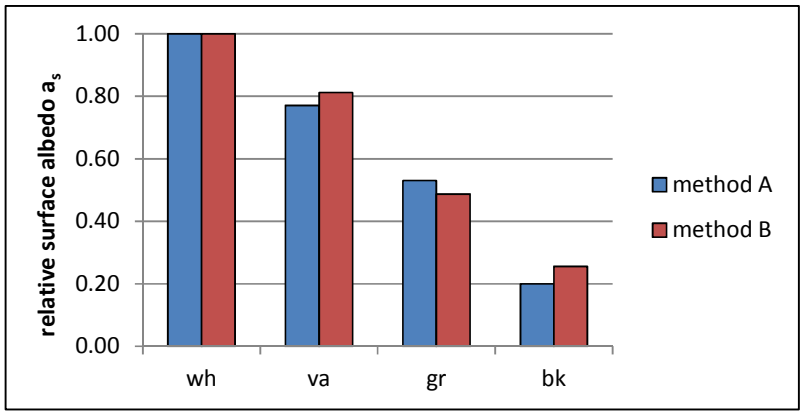

Fig. 1.19. Method-comparison by means of the albedo-values

1.10 Conclusions

Due to the mathematical analysis of the diverse warming-up and cooling-down experiments, the following statements can be made: The warming-up rate of a solid plate depends on the intensity of the solar radiation, on the surface-colour of the plate and thus on its solar absorption coefficient, and on its thermal admittance being given by the heat capacity of the plate, its thickness and its density. On the other hand, the cooling-down rate depends on its temperature difference to the surroundings, on the thermal admittance of the plate, and on the heat-transfer coefficient but not on the surface-colour. Moreover, the heat-conductivity of the material may be relevant. Thereby, the heat-transfer coefficient depends on the atmospheric conditions at the surface such as air-convection but apparently not on material features (except the thermal conductance), while the Stefan-Boltzmann Law appeared to be invalid under atmospheric conditions. The limiting temperature depends on the intensity of the solar radiation, on the surface-colour of the plate and thus on its solar absorption coefficient, on its thermal admittance, and on the heat-transfer coefficient. For these experiments, the atmospheric influences usually have been minimized by attaching a thin transparent foil providing an outer window. However, they are not quantized in such a way that they would enable a complete modelling of microclimates. The same is true with respect to the thermal conductance of the soil which has a considerable impact on microclimates.

ACKNOWLEDGEMENT

The present work has been carried out independently but not without the professional supports of Dr. Harald v. Fellenberg, of Dr. Philipp Hasler and, in particular, of Dr. Andreas Rüetschi.

REFERENCES

Adams JB, Jones RL (1970): Spectral reflectivity of lunar samples. *Science 167*, 737-739

Asaeda T, Thanh Ca V, Wake A (1996): Heat storage of pavement and its effect on the lower atmosphere. *Atmos. Envir. 30*, 413-427

Black JF (1963): Weather control: Use of asphalt coatings to tap solar energy. *Science 139*, 226-227.

Boltzmann L (1884): Ableitung des Stefan'schen Gesetzes betreffend die Abhängigkeit der Wärmestrahlung von der Temperatur aus der electromagnetischen Lichttheorie. *Ann. Phys. Chem. 22*, 291-294

Burkhart G, Detrie T, Swiler D (2001): When black is white. *Paint and Coatings Industry Magazine*, January 2001

Coulson KL, Bouricins CM, Gray EL (1965): Optical reflection properties of natural surfaces. *J. Geophys. Research 70*, 4601-4611

Coulson KL, Reynolds W (1971): The spectral reflectance of natural surfaces. *J. Appl. Meteor. 10*, 1285-1295

Coulson KL (1975): Solar and terrestrial radiation. Academic Press 1975

Doulos L, Santamouris M, Livada I (2004): Passive cooling of outdoor urban spaces. The role of materials. *Solar Energy 77*, 231-249

Dulong MM, Petit (1817): Des Recherches sur la Mesure des Températures et sur les Lois de la communication de la chaleur; *Annales de Chimie et de Physique*, *Ser. 2/7*, 225-264 ("Des Lois du Refroidissement"); 337-367 ("Du Refroidissement dans l'air et dans les gaz")

Hagishima A, Tanimoto J (2003): Field measurements for estimating the convective heat transfer coefficient at building surfaces. *Building and Environment 38*, 873-881

Johnson GT, Watson ID (1984): The determination of view-factors in urban canyons. *J. Clim. Appl. Meteorol. 23*, 329-335

Levinson R, Berdahl P, Akbari H (2005): Solar spectral properties of pigments – Part I: model for deriving scattering and absorption coefficients from transmittance and reflectance measurements. *Solar Energy Materials & Solar Cells 89*, 319-349; Part II: survey of common colorants, *Solar Energy Materials & Solar Cells 89*, 351-389

Levinson R, Akbari H, Berdahl P (2010): Measuring solar reflectance – Part I: Defining a metric that accurately predicts solar heat gain. *Solar Energy 84*, 1717-1714; Part II: Review of practical methods. *Solar Energy 84*, 1745-1759

Meschede D (2002): Gerthsen Physik. Springer-Verlag Berlin Heidelberg, 21. Aufl. 2002

Nkemdrim LC (1972): A note on the Albedo of surfaces. *J. Appl. Meterology 11*, 867-874

Pomerantz M, Akbari H, Berdahl P, Konopacki SJ, Taha H, Rosenfeld AH (1999): Reflective surfaces for cooler buildings and cities, *Philosophical Magazine Part B 79(9)*, 1457-1476

Schwerdtfeger P (1976): Physical principles of micro-meteorological measurements. *Developments in Atmospheric Science 6*, Elsevier 1976

Stefan J (1879): Über die Beziehung zwischen der Wärmestrahlung und der Temperatur. *Sitzungsberichte der mathematisch-naturwissenschaftlichen Classe der kaiserlichen Akademie der Wissenschaften 79*, 391-428

Synnefa A, Santamouris M, Livada I (2006): A study of the thermal performance of reflective coatings for the urban environment. *Solar Energy 80*, 968-981.

Synnefa A, Santamouris M, Apostolakis K (2007): On the development, optical properties and thermal performance of cool colored coatings for the urban environment. *Solar Energy 81*, 488-497

Visconti G. (2001): Fundamentals of physics and chemistry of the atmosphere. Springer-Verlag Berlin Heidelberg 2001

Zerlaut G (1989): Solar radiation instrumentation. Solar Resources, R. L. Hulstrom, editor, MIT Press, Cambridge, MA. 1989, 173-308

2. THE THERMAL BEHAVIOUR OF GASES UNDER THE INFLUENCE OF INFRARED-RADIATION

2.1 Summary

In contrast to the usual spectroscopic methods, the temperature of a gas embedded in a tube was measured here and not the intensity loss of the radiation. In order to minimize the interference by the tube, light-weight building materials were used, preferably Styrofoam, transparent plastic foils and aluminium foils. Sunlight as well as IR-bulbs were employed as radiation sources, whereby near-IR is predominant and not medium-IR as it is usually assumed. Different gases were tested, not only air and carbon-dioxide but also the noble gases argon, helium and neon. In each case, a temperature increase was detected up to a limiting value. While the warming-up rate was independent of the gas type, the limiting temperature turned out to be gas-specific. Surprisingly – and contrary to the expectation of the greenhouse theory -, the limiting temperatures of air, pure carbon-dioxide and argon were nearly equal while the light gases neon and, particularly helium, exhibited significant lower limiting temperatures. Applying the kinetic gas theory, and assuming a direct correlation between limiting temperature and radiative emission power, a stringent dependency of the product on mean kinetic energy and collision frequency could be deduced. Moreover, the adsorption degree could be calculated, appearing as very low. The absorption was assumed as a result of vibration of the atomic electron shell, induced by the electromagnetic waves. Comparing the results in sunlight to those obtained in artificial light, the effective wavelength could be assessed delivering the value of 1.9 µm. Therefore, the greenhouse theory has to be questioned.

2.2 Introduction

The starting point of this research was the generally accepted »greenhouse theory« assuming that the recent climate change is mainly due to the growing amount of the so-called greenhouse gases in the atmosphere, particularly of carbon dioxide. This theory takes its source in the comparison of the Earth atmosphere with the glass of a green house, made by Fourier in 1827, first advocated by Tyndall in 1863 and later by Arrhenius in 1896/1901. In modern times, the topic was taken up particularly by Möller (1956), Plass (1956 a,b) and Curtis (1956), followed by a great number of publications delivering several climate models, which differed already significantly in the mid-nineties (Schlesinger 1997).

In view of the atmospheric warming, each climate model or theory must exhibit two major parts: the influence of the direct incident solar light, and the thermal output of the Earth surface. The theoretical description of the latter one appears to be inherently difficult since different effects are involved, such as the surface albedo, the heat transfer at the surface and its IR-radiative emission. Hitherto, several theories are known, designated by the generic term »radiative transfer«. Thereto, basic comprehensive treatises thereto are given by Tien (1968) and by Cess and Tiwari (1972).

However, these theories are not within the scope of the present paper which is primarily focussed on empiric measuring methods in a laboratory-like scale, solely concerning incident radiation, and at most finding a theoretical interpretation of the results. Thereto, not only natural (solar-) light is of interest but also artificial light. Of course, for characterizing the radiation sources, Planck's law may be used being valid for black bodies. Thereby, as to IR-radiation, it is important to distinguish between *near IR* (λ = 0.8 – 3 µm), emitted at high temperatures (> 1000 K), and *medium IR* (λ = 3 – 50 µm) occurring at lower temperatures as usual thermal radiation, while IR-radiation with larger wavelengths (λ = 50 – 1000 µm) is conveniently denoted as *far IR*.

The fact that the extra-terrestrial solar constant is considerably larger than the terrestrial one (namely 1367 Wm^{-2} instead of approx. 1000 Wm^{-2}), even in the absence of clouds and haze, provides evidence that – in addition to the Raleigh scattering - infrared solar radiation is absorbed. This expectation may be sustained by the resemblance of the respective spectra suggesting an intensity decrease over the whole spectral range, and not solely in the visible one. According to the greenhouse theory, the absorption of IR-radiation is solely due to greenhouse-gases such as carbon-dioxide or water vapour but not to pure air since thereto no spectral absorbance had been observed.

As a consequence, in the absence of such greenhouse gases the atmosphere would be expected to absorb no IR-radiation at all.

As initially mentioned, prior gas absorption measurements in the laboratory were made by Tyndall (1861, 1863 and 1872), always applying artificial light. He used various apparatus which may be understood as wideband spectrometers for gases. The favoured one, described in Tyndall (1861), consisted of a brass tube (length 1.2 m, diameter 6 cm) which was filled with various gases at different pressures but which could also be evacuated allowing measurements in the vacuum. The ends of the tube were capped with slabs of rock salt crystal (sodium chloride), a substance known to be highly transparent to heat radiation. A standard Leslie cube from copper, coated with »lamp-lack« and filled with boiling water, emitted radiation that traversed the tube and interacted with the gas before entering one cone of a differential thermopile. Radiation from a second Leslie cube passed through a screen and entered another cone. The common apex of the two cones, containing a differential thermopile junction, was connected to a galvanometer which measured small voltage differences. The intensity of the two radiation sources entering the two cones could be compared by measuring the deflection of the galvanometer which was proportional to the temperature difference across the thermopile. Different gases in the tube, as well as different gas pressures, caused varying amounts of deflection of the galvanometer needle. Tyndall didn't detect any adsorption by pure air, unlike in the case of carbon-dioxide or of other strongly absorbing gases particularly of an »olefiant« gas, at least when he worked at lower temperatures, while at higher temperatures he found a weak absorbance by air.

About forty years later, a similar apparatus was used by Arrhenius (1896, 1901), focusing on the carbon-dioxide adsorption of infrared radiation and using a 50 cm long iron tube but two different IR-sources, namely - besides a Leslie-cube at 100°C – a hollow body from smutted copper, being chilled down to -80°C by a mixture of dry ice and ether. He varied the pressure, but within such a low range that no significant deviation from linearity appeared.

However, due to the comparatively low temperature of the heat source these kinds of radiation sources imply solely the emission of *medium-wave IR* which isn't typical for sunlight, at least not to a considerable extent. Tyndall couldn't know that, since Wien's distribution law (1896), and even less Planck's radiation law (1900), were not known at that time. But his observation of a weak absorbance by air at higher temperatures could mean that air doesn't absorb medium-wave IR-radiation while it becomes absorbing at lower IR-radiation waves.

Moreover, Knut Ångström (1900) made another experiment using an apparatus consisting of two 40 cm long glass-tubes, arranged side by side within a wider tube made from wood, the latter one serving as a visible thermal insulation, and exhibiting plates from fluorspar, on one end, and thermocouples on the opposite end. When one tube was filled with air, and the other with pure carbon-dioxide, and when the tubes were oriented perpendicularly to the sun beam, practically no temperature difference could be found. This means: both gases either didn't absorb any sunlight – or they absorbed it to the same extent.

A further false conclusion is drawn by making the assumption that all the radiative energy absorbed by the gas will be transformed into heat, for it is conceivable that gas atoms or molecules may be electronically excited due to the absorption of electromagnetic radiation but emitting it without transforming it in thermal motion. Since this emission will occur in any direction – and not only in the direction of the sensor of the apparatus - intensity loss will nevertheless be detected while the emitted radiation is absorbed by the material of the sample tube. For this purpose, the temperature of the enclosed gas should therefore be measured, rather than the intensity loss of the radiation beam. But such measurements are not easy to carry out since a considerable interference with the tube material has to be expected, due to its large heat capacity compared to the heat capacity of the gas. A further difficulty arises when artificial light or radiation is applied, as it was the case in Tyndall's experiments, since a normal intensity-loss is to be expected then, even in the absence of a medium.

With respect to practical measurements, the general interest was more and more geared to monochromatic spectroscopic methods for analytical applications, using artificial light sources and photodetectors, the light usually being resolved by a prism in combination with a frame. In astronomy as well as in meteorology, the direct analysis of natural light, in particular of solar light, still plays a certain role (Zerlaut, 1989; Bird, 1989), whereby the measuring of the absolute intensities is needed much more here. But while the over-all intensity (given in Wm^{-2}) may be easily determined by temperature measurements at a blackened cavity - or by electronical instruments (bolometers) being gauged by such blackened cavities -, wave-specific measurements are much more delicate, particularly when infrared radiation is affected, since the medium for splitting the radiation may absorb parts of it, which is leading to systematic measuring errors. For instance, for the "spectro-bolometer" used by Langley (1884) interference due to the glass-prism may occur since glass absorbs IR-light. Even grating infrared spectrometers, e.g. the one described by Thompson et al. (1994) may exhibit some intrinsic deficiencies since glassy materials such as glass-lenses and glass-prisms are necessary for focussing the beam, not least the ones of the telescope. When gases are concerned, the circumstances are even more intricate, especially when they absorb only slightly, and when the absorption bandwidth is wide so that an absorption effect may be overlooked.

Normally, molecule-spectra of gases are calculated by quantum-mechanical methods. The relating theory, outlined e.g. in the textbook of Boeker and van Grondelle (2011), is complex and shall not be discussed in detail here, except one item: the statement that any IR-activity of molecules or atoms requires a shift of the electric dipole moment, so that two-atomic homo-nuclear molecules are always IR-inactive, must be regarded as a theorem and not as principal natural law, since numerous examples of nonpolar substances are known where an interaction with electro-magnetic radiation occurs, e.g. at halogens where even coloured – and thus visible - light is absorbed.

Hitherto, apparently no thermal measurements have been made with gases in the presence of IR-radiation, in particular of sunlight, except of those being provided for didactic purposes as the one of Sirtl (2010) but delivering no scientifically evaluable results. Therefore, it seemed advisable to seek a method for measuring the thermal behaviour of gases under the influence of IR-radiation within special tubes, in particular of air and of carbon-dioxide but also of noble gases such as argon, helium and neon. Thereby, sunlight as well as artificial light (IR-lamps) shall be applied.

2.3 Objectives, Concept and Apparatus

The primary objective of this investigation was to verify empirically the common assumption that carbon-dioxide – unlike the main air components nitrogen and oxygen - absorbs infrared light, being thus significantly accountable for the so-called greenhouse effect. For this purpose, and contrary to any previous measuring concepts, not the intensity of the radiation beam should be studied – as by spectroscopic methods - but its particular influence on gases, thus on matter, i.e. their thermal behaviour in the presence of a light-beam. At that time, it was not evident that solely the near-IR should be focused.

Compared with solid bodies, thermal measurements on gases are much more delicate due to their low heat capacity letting suppose a considerable interference of the vessel walls in which the gas is embedded, apart from the fact that gases may move when a temperature gradient arises. Hence, a large ratio between the gas volume and the surface of the vessel must be intended, as well as a low heat capacity of the vessel material. Therefore, it doesn't astonish that no effect could be detected when erstwhile materials and apparatus were used. But it is all the more astonishing that such measurements have not been made in recent times.

Preliminary tests for the present investigation were made using square twin-tubes from Styrofoam (3 cm thick, 1 m long, outer diameter 25 cm), each being equipped with three thermometers at different positions, and being covered above and below by a thin transparent foil (preferably a 0.01 mm thick Saran-wrap). The tubes were pivoted on a frame in such a way that they could be oriented in the direction of the solar light (Fig. 2.1). One tube was filled with air, the other with carbon-dioxide. Incipiently, the tubes were covered on the tops with aluminium-foils being removed at the start of the experiment.

Fig. 2.1. Twin-tubes from Styrofoam

The primary experimental result was quite astonishing in many respects. Firstly: The content gases warmed within a few minutes by approximately 10°C up to a constant limiting temperature. This was surprising - at least in the case of air – for no warming-up should occur since sunlight is colourless and allegedly being not able to absorb any IR-light. However, the existence of a limiting temperature is conceivable since an emission of heat radiation has to be expected insofar as the temperature rises. Secondly: The limiting temperatures were more or less equal at any measuring point. This means that the intensity of the sun beam was virtually not affected by the heat absorption in the gas tube since the latter one was comparatively weak. And thirdly: Between the two tubes no significant difference could be detected. Therefore, already owing to this simple experiment a significant effect of carbon-dioxide on the direct sunlight absorption can be excluded since it is unlikely that the minor carbon-dioxide concentration in the air of approx. 0.04% should have the same effect as pure carbon-dioxide. However, even pure air (and perhaps also other colourless gases) seems to absorb IR-light – an effect which, so far, has obviously not been taken account of since it is very weak.

Indeed, in the open atmosphere such a warming-up cannot usually be perceived since the warmed air rises immediately, cooling itself. Moreover, this direct warming-up-effect is superimposed by the much stronger one via the ground-surface. However, it seemed appropriate to study this effect more precisely with the aim of getting quantitative results, and insight of the theoretically ascertainable coherences. For this purpose, the subsequent experiments were made with artificial light, i.e. with IR-lamps, exhibiting a higher amount of IR and being better reproducible (Fig. 2.2). Furthermore, different gases were employed (ambient air, a 4:1 N_2/O_2-mixture, CO_2, Ar, Ne, He) while the apparatus was improved step by step. Finally, the results being obtained in artificial light were compared with the results obtained in solar light allowing an approximate statement about the wavelength of the effective radiation.

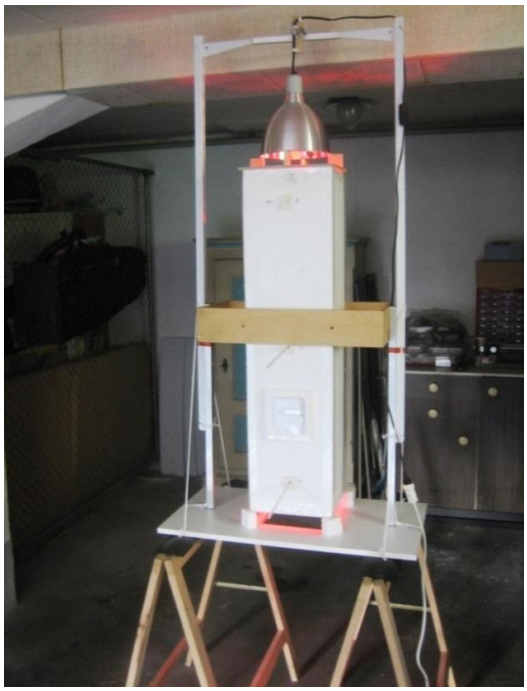

Fig. 2.2. Equipment with IR-lamp

The preparation of the – single - measuring-tube is of great importance since it can influence the reliability of the results. Initially, there was no clue at all as to what will happen when such a tube is irradiated by an IR-lamp of the type being used for terraria (150 W, 100 W and 50 W). At least it was clear that an irradiation from above would guarantee an optimum immobility of the gas since the gas expansion would be larger at the hotter upper region than in the lower region. Moreover, in the case of artificial light a decrease of intensity from top to bottom was to be expected since this case differs from the general case of punctuate light source where the intensity decreases inversely proportionally to the square distance, letting suppose another intensity course due to the channelling of the radiation within the tube. In order to be able to study this, three temperature measuring points were provided, positioned 10, 50 and 90 cm from the edge. The temperatures were measured with Hg-thermometers (approx. 8.5 mm thick) which were inserted into the Styrofoam walls and sealed by foamed plastics. To ensure a definite distance to the light source, a spacer (5 cm) from wood was mounted between tube and reflector of the lamp, while a square opening in the bottom board prevented a reflection of the passing radiation, and the tube was mounted on sockets from Styrofoam. The measuring gas, supplied from a professional steel-cylinder via a reducing valve, was injected through the bottom thermometer-hole while the top hole was opened for letting out the previous gas. For monitoring the filling degree by means of the relative humidity of the ambient air, a hygrometer was provided 30 cm beyond the lower edge. The filling process lasted normally one hour or more, usually reaching 3-5% rel. humidity. In the case of carbon-dioxide, the reducing valve had to be warmed with a hair dryer because of the cooling due to the gas expansion.

It would be confusing to list all the numerous amendments which have been made over time. Solely the most important variants shall be mentioned being compiled in Fig. 2.3. Usually, the amendments were made due to experimental results which will be reported subsequently in detail. Thereby, mainly the thermal course along the tube was focused regarding the fact that the tube walls or their laminations, respectively, may influence the thermal behaviour by absorption, emission and conduction of heat. Hereto, several kinds of glossy aluminium foils were employed. A further problem arose because of the bad gastight sealing character of Styrofoam, particularly when helium was used, needing an additional adhesive splicing foil (in Fig. 2.3 marked in green). In respect of the many variables (six different gas fills, and three different lamp intensities), it was not feasible to run the whole experimental program every time, in particular since - for studying the pressure

influence - some experiments were made in a room of a hotel being situated on a mountain at 2100 meter above sea-level, and furthermore the final outdoor measurements in sunlight didn't allow the application of other gases than ambient air since the complete filling with another gas would have needed too much time, accompanied by a considerable shift of the solar altitude. Nevertheless, several valuable results could be obtained when the apparatus was not yet optimal, especially since *argon* had turned out to be suited as a reference gas.

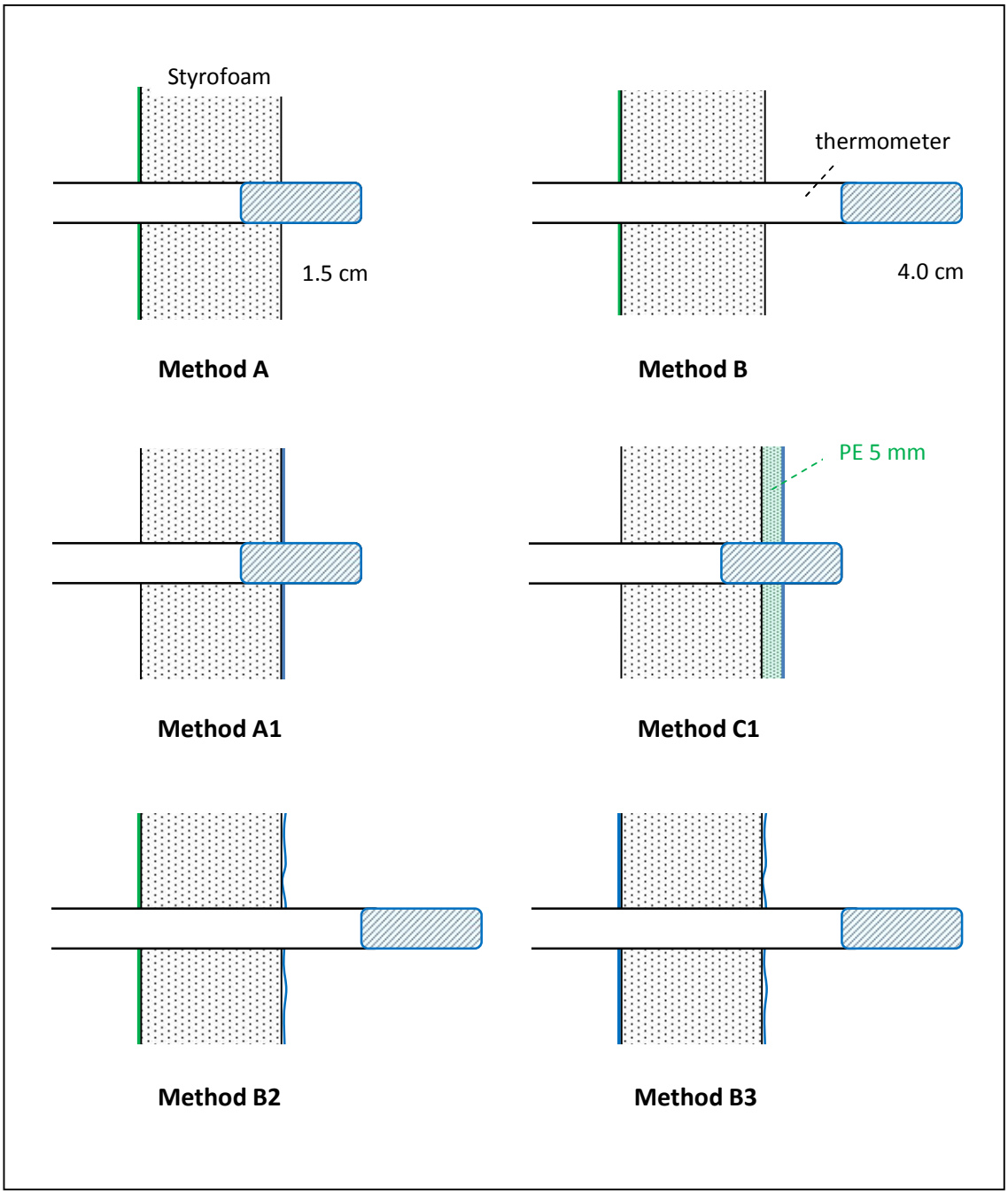

Fig. 2.3. Drafts of the Styrofoam-wall including thermometer, coated with additional layers
(Blue coloured: aluminium-foils; green coloured: plastic materials; both specified in the text)
Additional method: Method C ≡ method C1 without the adhesive aluminium-foil

Altogether *four types of aluminium-foils* were used, in Fig. 2.3 being always marked in blue: For mirroring contact-tips of the thermometers, a common 0.015 mm thick aluminium-foil was applied. The thickness of the aluminium component of the adhesive foils was the same while the total thickness was 0.18 mm for method A1, and 0.26 mm for C1. At methods B2 and B3, a very thin foil (metallized plastic, 0.015 mm) was employed being commonly used for freeze protection. The optimal furniture was realized in method B3, shown in Fig. 2.4, but it wasn't available for any experiments, solely for the least ones.

Fig. 2.4. Solar-tube according to method B3

As IR-bulbs, "Basking Spots" from »exo-terra« in three sizes, according to three intensities (150 W, 100 W, and 50 W), were used, being inserted in an »Arcadia« reflector. Due to the different sizes of the bulbs, the distances between the lower surfaces of the bulbs and the base of the reflector were different, namely 5 cm, 7.5 cm, and 9 cm.

Some additional but inconsistent information is delivered by the producer: On the one hand, a colour-temperature of 1500 K is indicated, besides being poorly defined. In particular, the relative spectral power distribution, being displayed in Fig. 2.5, does not correspond to that colour-temperature but to a much higher one, namely to 3450 K. This may be checked by a calculation using Planck's formula, written in simplified terms as

$$I \approx \frac{1}{\lambda^5 \left(e^{\frac{hc}{k\lambda T}} - 1 \right)} \tag{2.1}$$

whereby $\frac{hc}{k} = 0.01439 mK$

The resulting curve, being displayed in Fig. 2.6 and exhibiting a peak-maximum at a wavelength of about 0.85 µm, describes the curve given by the producer quite well – except for its left branch - whereas the difference to the 1500 K curve, exhibiting a maximum at 1.9 µm as shown in Fig. 2.7, is large. Such a high temperature of the glowing filament seems possible with respect to the melting point of tungsten being 3680 K and thus being higher than the here estimated colour-temperature of 3450 K. However, with respect to the glass of the bulb there arise considerable doubts. But even the 1500 K specification seems questionable since red heat corresponds to approx. 1000 K. Anyway, there remains an uncertainty regarding the producer's declaration, notably since no information is given about the measuring method.

The irradiation intensity of the sunlight was measured by a certified KIMO Solarmeter SL 100. Most experiments were made at about 450 meters above sea level during several summer days, and preferably early in the afternoon. The atmospheric pressure was approx. 0.948 bar (real value), and the relative humidity between 50-60%.

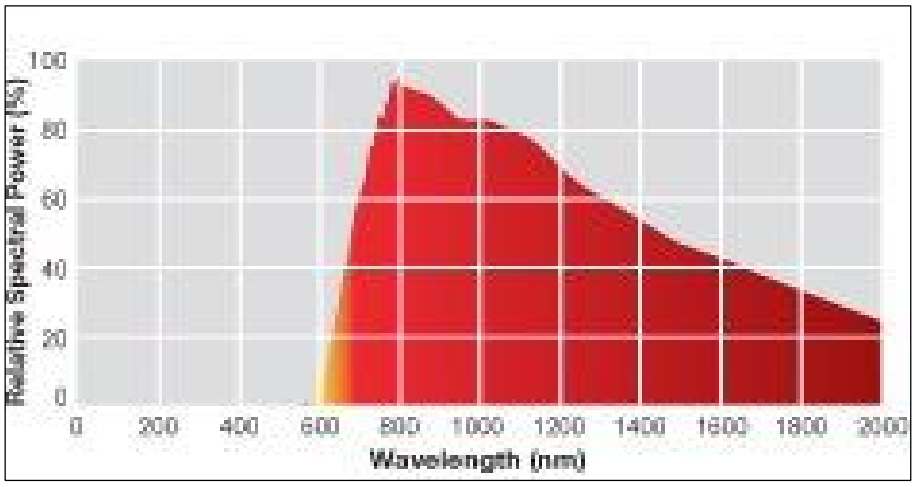

Fig. 2.5. Relative spectral power, according to producer's information

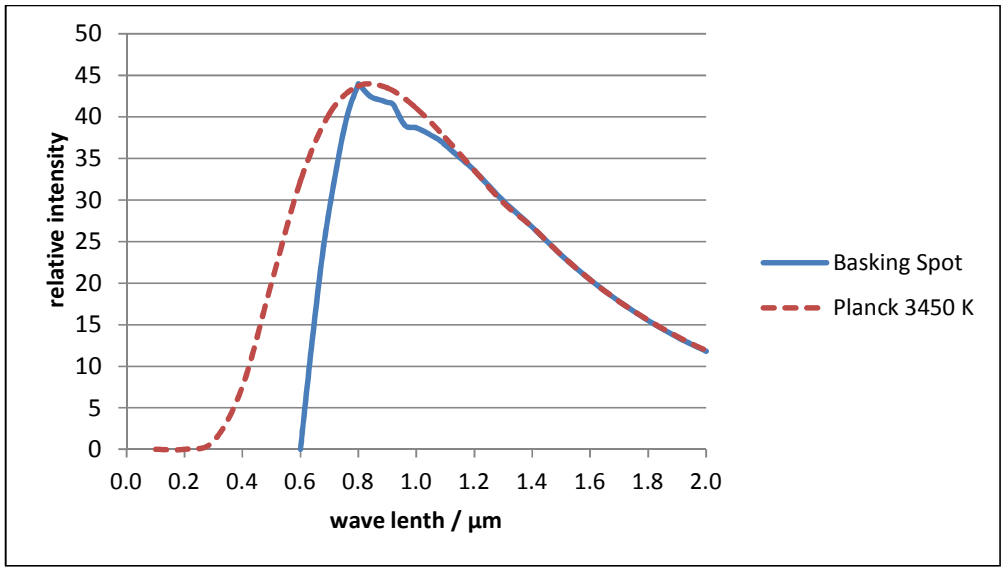

Fig. 2.6. Comparison of producer's information with a Planck calculation

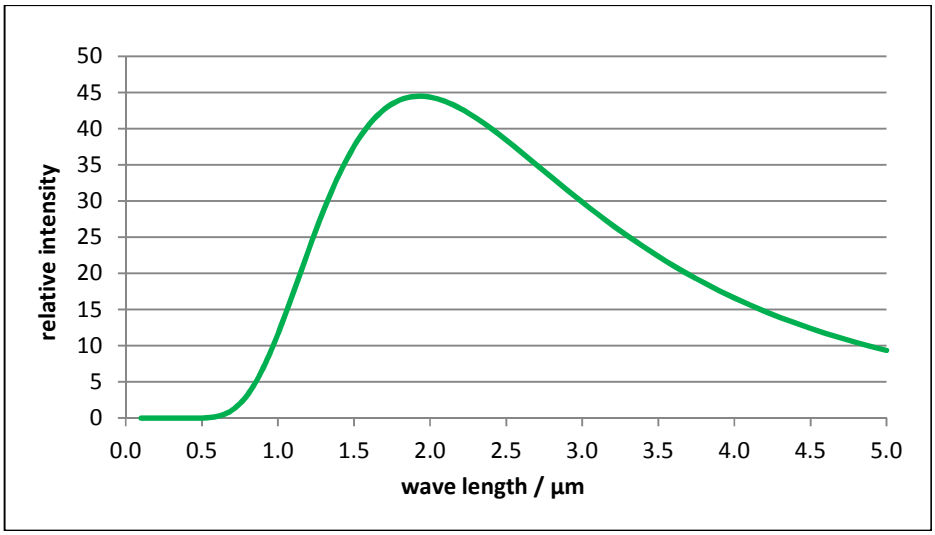

Fig. 2.7. Relative spectral power at 1500 K according to Planck's calculation

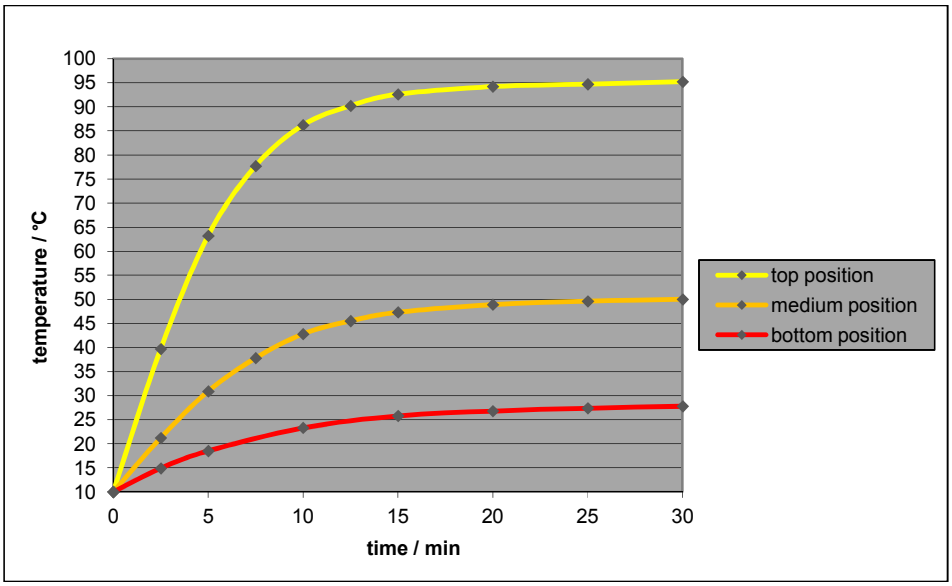

Fig. 2.8. Temporal courses at the three temperature positions with 150 W in air
(Method being analogous to method A, but with bare thermometer-contact-tips)

2.4 Experimental Results

2.4.1 The influences of the apparatus features

The tests for optimizing the apparatus were made with equipment similar to the one shown in Fig. 2.2, and using a 150 W spot. Initially, solely ambient air was used. As obvious from the time-temperature-diagram displayed in Fig. 2.8, a constant limiting temperature was reached at any measuring point. Since the limiting temperature at the supreme measuring point was quite high, possibly harming the Styrofoam, and since low air humidity was intended, the initial tests were made in a room at a low ambient temperature. But all the following tests were made at room temperature with argon as a reference gas, behaving similarly to air.

The occurrence of such limiting states is certainly due to equilibria between absorption and emission rates. But unlike in the case of solar radiation, (alleged for comparison in Fig. 2.14), in the case of artificial radiation the limiting temperatures at the three measuring positions (in every case being indicated by the three colours yellow, orange and red) differed more or less, depending on the texture of the tube. In order to make these distinctions more visible, and in addition to the examples given in Figs. 2.9a – 2.13a, the respective diagrams in Figs. 2.9b – 2.13b reveal the limiting temperatures as a function of the measuring position. Comparing these examples, the optimum variant can be expected where the slope of the limiting temperature curve is minimal while the limiting temperature at the medium position is maximal.

In Fig. 2.9, the effect of mirroring the thermometer-contact-tips by aluminium-foils is revealed whereby in both cases the thermometers were positioned alike in method A. (The first case is identical with the example given in Fig. 2.8). Obviously, the mirroring of the thermometers induces a general reduction of the heating-up rates, as well as of the limiting temperatures. Hence it may be concluded that the differences must be due to the glass layers enclosing the mercury bulbs of the thermometers. The interferences were considerably large, so that all subsequent measurements were made using mirrored thermometer-contact-tips.

Fig. 2.10 reveals the influence of the horizontal thermometer position illustrated in Fig. 2.3 (methods A and B). When the contact-tips of the thermometers were positioned closer to the Styrofoam wall, the temperatures were generally lower. This fact suggests that the wall absorbed some heat, in spite of its low heat capacity, inducing interference, and letting appear method B as the preferable one. However, since method A implies a lower slope of the limiting temperature curve, and since the heat stress on the Styrofoam tube is lower, too, several measurements comparing the influence of different gases were made applying this method, particularly since – unaware of the effects of completely different gases – such measurements had to be carried out without having the final perfect apparatus available.

The attachment of a self-adhesive aluminium-foil inside the walls (method A1) lead to a considerable flattening of the temperature-path curve, as it is evident from Fig. 2.11. This may be explained by a less warming-up of the walls due to the reflection of the aluminium foil, and therefore reducing their counter-radiation towards the contact-tips of the thermometers. On the other hand, the initial energy loss of the radiation beam becomes lower inducing a smoother pathway of the radiative intensity.

However, as it may be seen from Fig. 2.12, when the heat capacity of the wall was enhanced, as it was the case when massive polyethylene plates were applied (method C), the warming-up of the enclosed gas is considerably reduced due to the high heat capacity of these plates, while the covering of the plates with aluminium foils (method C1) generated similar conditions as in the absence of such plates (method A1, cf. Fig. 2.11).

As a consequence, maximally undisturbed results may be obtained using aluminum-mirrored Styrofoam walls whereby the aluminium-foil should be as thin as possible to avoid a lengthways heat conduction. A further advantage is a deepened attachment of the (mirrored) thermometers. Additionally, a plastic foil should be provided, avoiding the diffusion of the embedded gas (method B2, Fig. 2.13). For outdoor experiments, i.e. for experiments with solar radiation, it is advantageous to apply additional aluminium-foils on the outsides of the tube preventing an unintentional influence of the dispersed daylight (method B3, Fig. 2.14).

In summary, it can be said that a mirroring of the inside surfaces of the tube engenders a linearization and a flattening of the time-temperature curves meaning that the intensity loss of along the tube is minimal, getting inversely proportional to the distance and not – as usual for open artificial radiation – inversely proportional to the square of the distance. Hence, the optimal method for quantitative analyses is given by method B2 (or for outdoor measurements by method B3). However, for basic comparing purposes, the more simple method A was used, but preferably choosing the medium measuring point since this one delivered similar results as method A1 (cf. Fig. 2.11a). Regarding the three thermometric measuring points, it generally seemed conceivable to neglect the thermal conductivities of the gases in consideration of the relatively large distances.

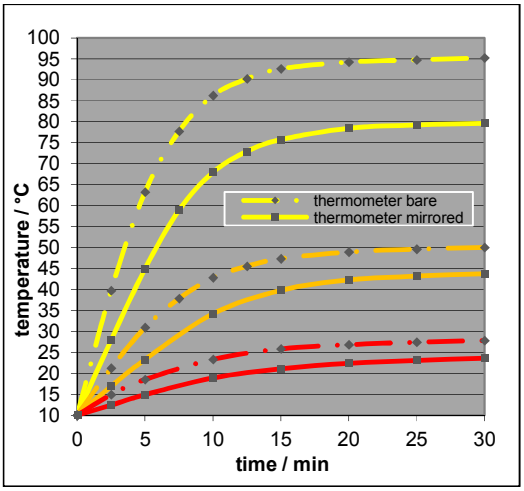

Fig. 2.9a. Thermometer-contact-tip/150W/air

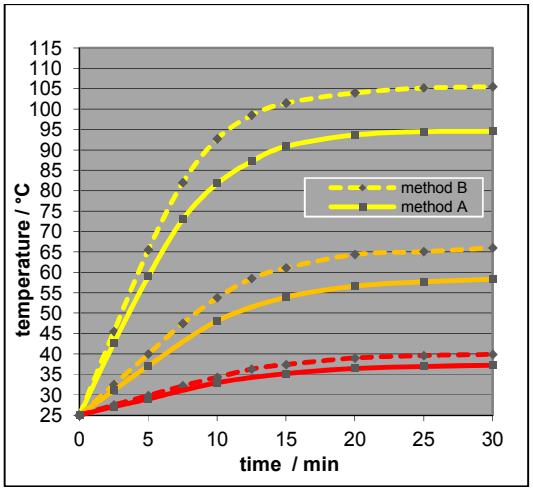

Fig. 2.10a. Thermometer positions/150W/argon

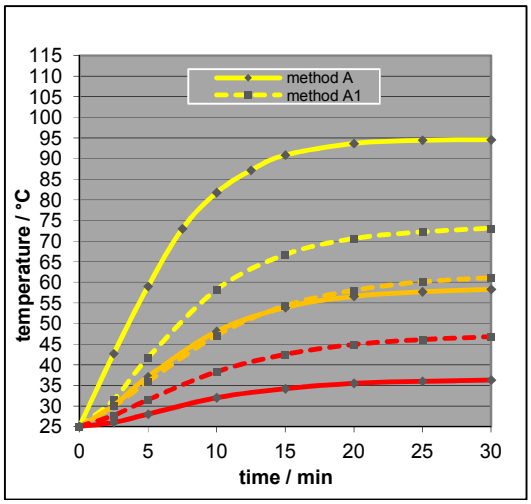

Fig. 2.11a. Alu adhesive foil/150W /argon

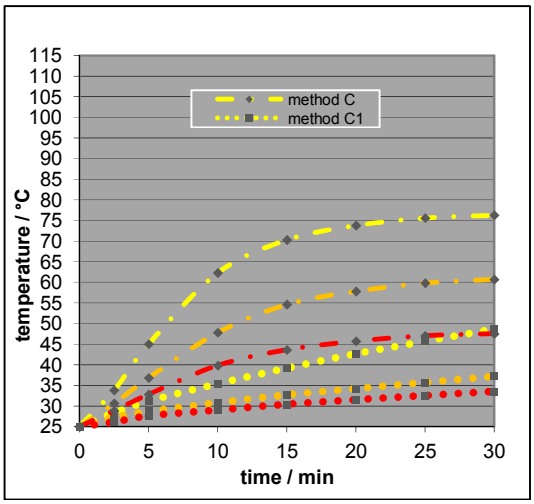

Fig. 2.12a. Alu adh. foil on PE-plate /150W/argon

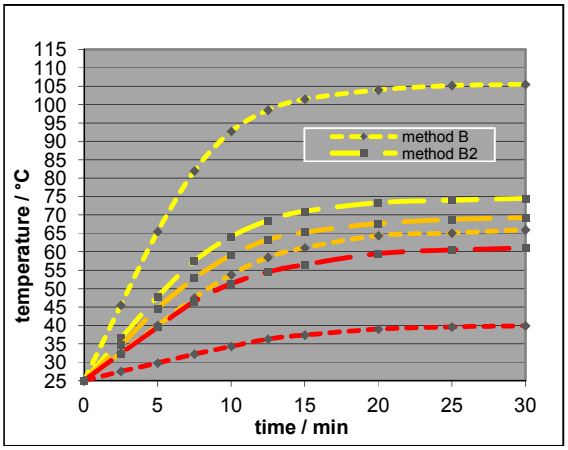

Fig. 2.13a. Alu light /termomet. deep/150W/Ar

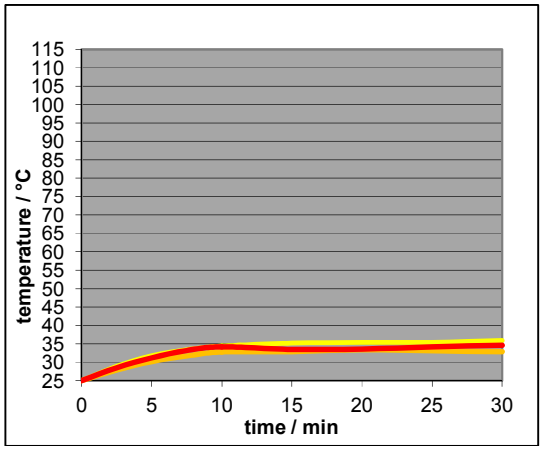

Fig. 2.14a. Method B3/solar tube/outdoor/ air

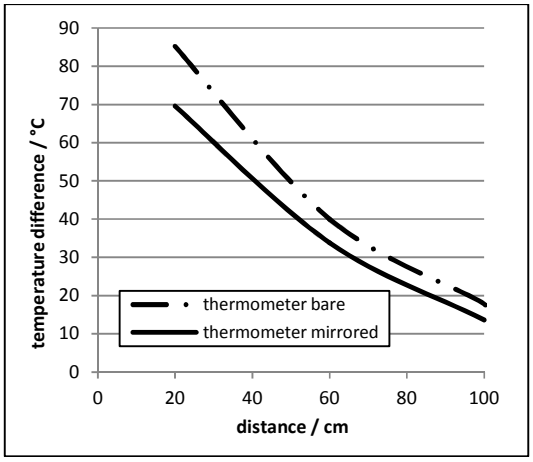

Fig. 2.9b. Thermometer-contact-tip/150W/air

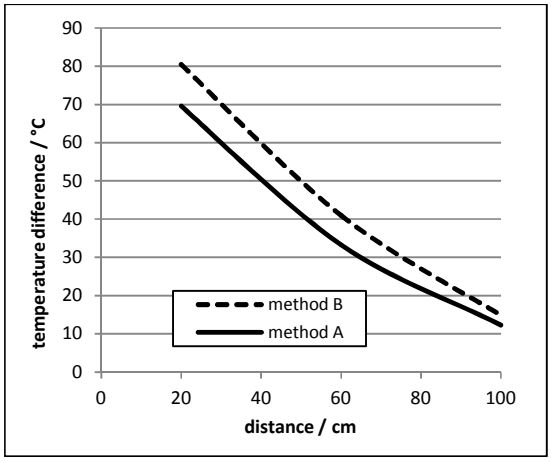

Fig. 2.10b. Thermometer positions/150 W/argon

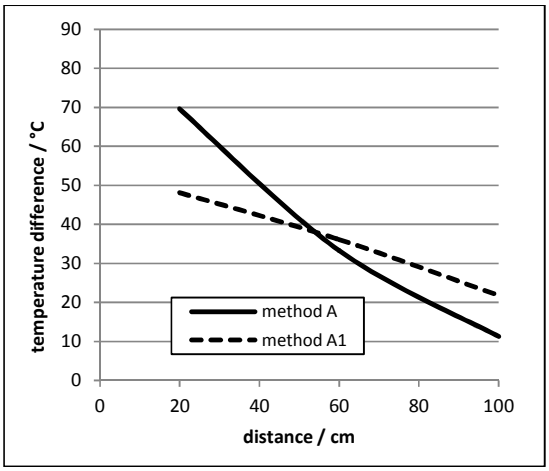

Fig. 2.11b. Alu adhesive foil/150W/argon

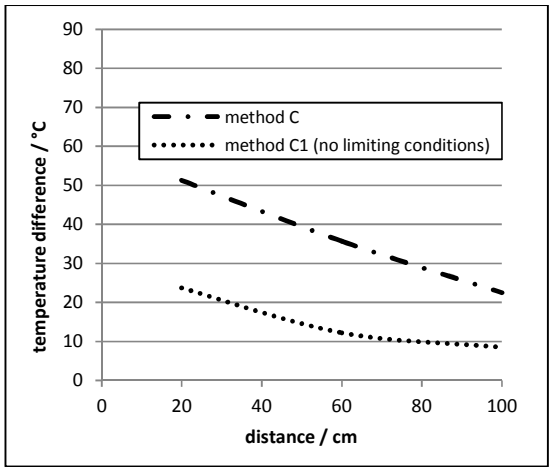

Fig. 2.12b. Alu adh. foil on PE-plate/150W/argon

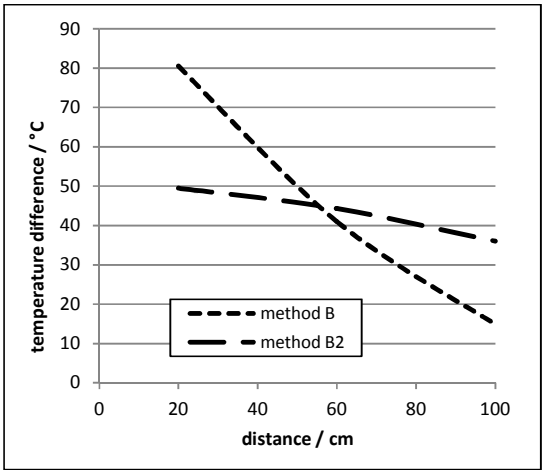

Fig. 2.13b. Alu light/termomet. deep/150W/Ar

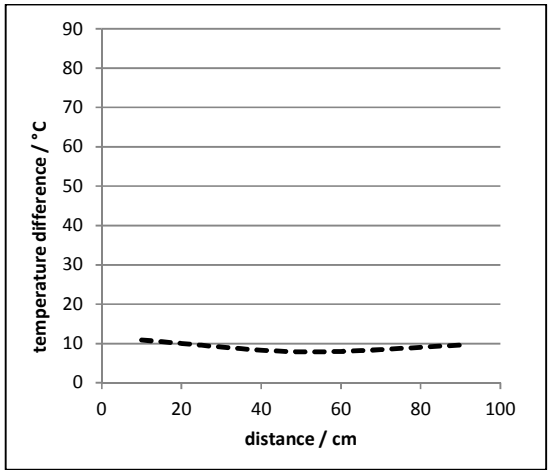

Fig. 2.14b. Method B3/solar tube/outdoor/air

As the comparison of Figs. 2.15, 2.16 and 2.17 yields, the pattern of the temperature-time courses is independent of the lamp intensity, while – of course – the initial slopes as well as the limiting temperatures are different. Hence the accuracy of the measurements cannot considerably be improved by the choice of the lamp intensity.

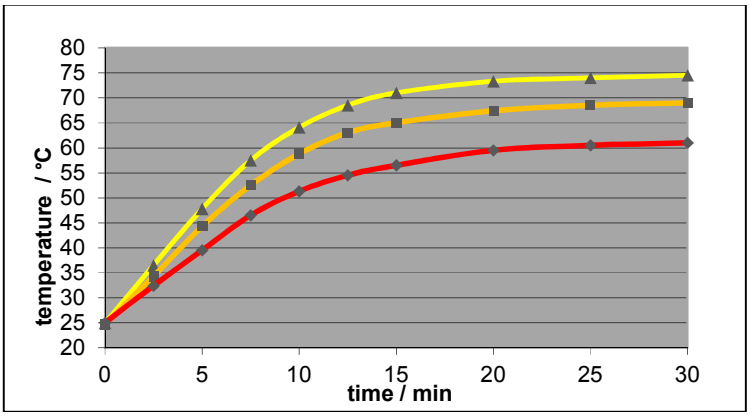

Fig. 2.15. Temporal courses with the 150 W lamp / method B2 / argon

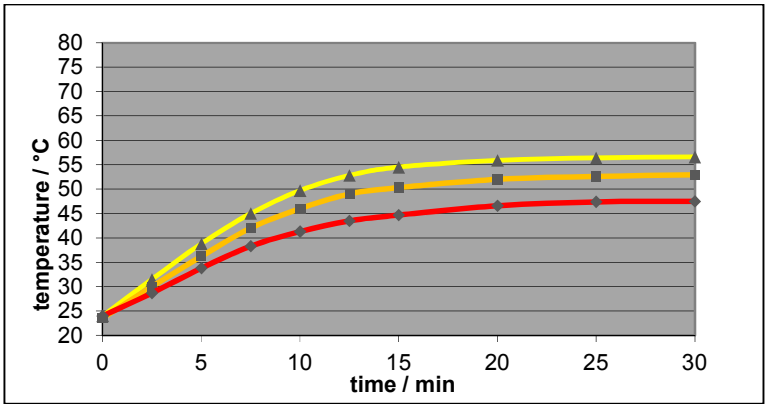

Fig. 2.16. Temporal courses with the 100 W lamp / method B2 / argon

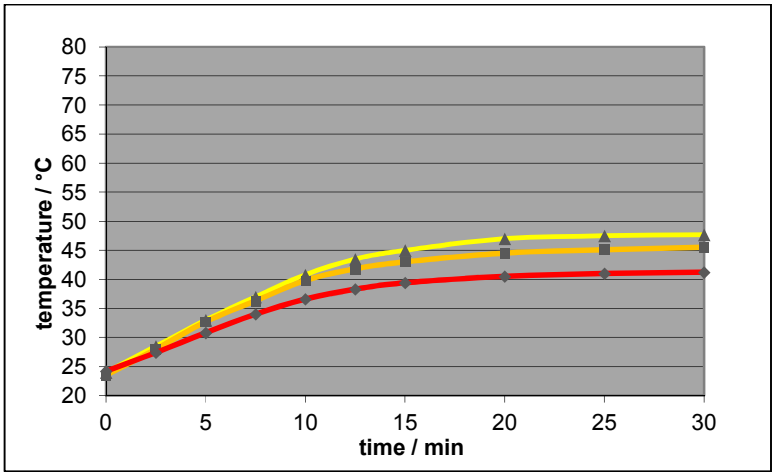

Fig. 2.17. Temporal courses with the 75 W lamp / method B2 / argon

2.5 The Dependence on the Kind of Gas and on the Gas Pressure

The influence of the several gas kinds, as well as of the atmospheric gas pressure, was studied by means of artificial IR-light measurements since the reproducibility as well as the temperature enhancement was higher than in the case of the sunlight measurements. Since the greater part of the measurements had been accomplished before the method-optimization had been finished (delivering method B2), mostly the results basing on the less reliable and only semi-quantitative method A were available for comparisons, preferably with the 150W spot, and regarding the medium time-temperature curve, while for most quantitative analyses the results of methods B2 and B3 were used.

As Fig. 2.18 reveals, the limiting temperatures of argon and (pure) carbon-dioxide were almost equal while the one of room air was slightly lower. The initial slopes were equal in any case. A nitrogen/ oxygen mixture (4:1), which is not displayed here, delivered nearly the identical result as room air. Hence, the rough initial observation which was made using twin-tubes in the presence of sunlight could be approved. Moreover, there is no doubt that air and even noble gases such as argon absorb IR-light, while the absorbance of pure carbon-dioxide happens in the range of the absorbance of air, the latter one being not considerably influenced by traces of further gaseous components, such as water vapour.

Significantly larger differences of the limiting temperatures appeared when the noble gases argon, neon and helium were compared, as revealed in Fig. 2.19. However, the initial slopes were equal in any case. Thereby it is interesting to know that the molar heat capacities of these gases are equal.

The comparison of Figs. 2.19 and 2.20, i.e. the comparison of the methods A and B2, yields approximately the same ratio between the limiting *absolute* temperatures of argon and helium (331: 314 = 1.054 at Fig. 2.19, instead of 342: 323.5 = 1.057 at Fig. 2.20) while the warming-up rates differed which may be explained by the stronger interference between gas and tube in the case of method 16. In Fig. 2.19, the equity of the initial slopes is even more obvious. The similarity of the absolute limiting temperature ratios between argon and helium with respect to the methods A and B2 enables the appraisal of the respective ratio between argon and neon according to Fig. 2.19, delivering the value 331 : 323 = 1.025, or adjusted analogously to the argon/helium results 1.025 · 1.057 : 1.054 = 1.028.

For studying the influence of the gas pressure, it is necessary to change the ambient pressure since it is not possible to evacuate or pressurize the measuring tube due to the low stability of the Styrofoam and of the cover foils. The simplest way for realizing this is displacing the measuring station on a mountain, and e.g. renting a hotel room there. In our case, the two levels of the measuring stations – namely about 450 m and 2100 m above sea level – enabled a pressure decrease of about 20 percent, i.e. from 0.97 to 0.79 bar. But as Figs. 2.21, 2.22 and 2.23 reveal (corresponding to measurements using all the three lamps 150, 100 and 75 W) no significant pressure dependence could be found.

2.6 Theoretical Interpretation of the Results

2.6.1 The determination of the absorption degree

The course of the time/temperature curves can be explained by a linear growth within the initial phase where the gas is continuously warmed-up, on the one hand, and a final constant limiting phase where its radiative emission rate is equal to the warming-up rate, on the other hand. Hence, for determining the absorption degree, solely the linear initial phase has to be regarded, while the values of the limiting temperatures promise to deliver information about the radiative behaviour of gases.

Obviously, for calculating the heat absorbance of a gas, its molar heat capacity c_p is relevant, exhibiting the unit J/mol·K. Instead of K (Kelvin), also centigrade may be inserted. The multiplication by the measured initial heating rate yields a *molar power* [W/mole]:

$$P_{absorb} = c_p \cdot \frac{\Delta T}{\Delta t} \tag{2.2}$$

whereby T = temperature [K] or [°C], and t = time [s].

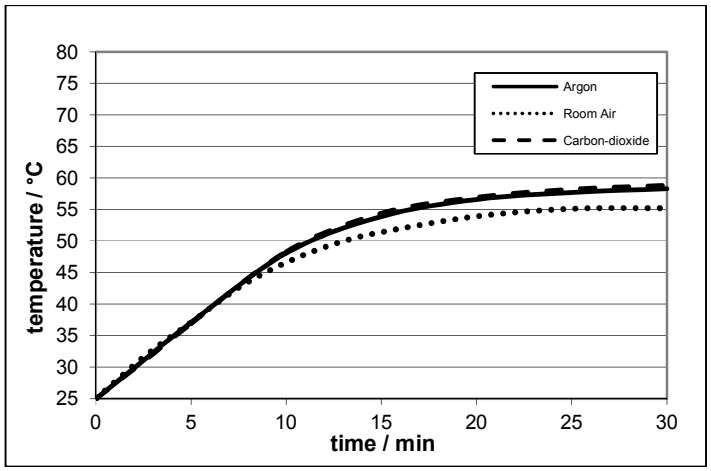

Fig. 2.18. Comparison of argon, air and CO_2 (method A, 150 W, medium pos.)

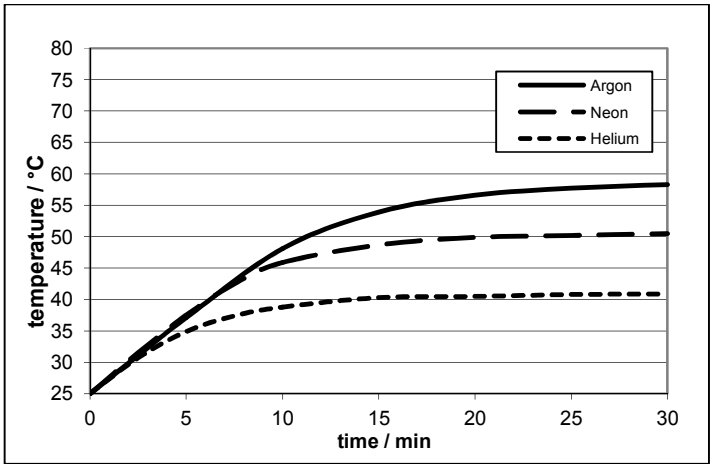

Fig. 2.19. Comparison of argon, neon and helium (method A, 150 W, medium pos.)

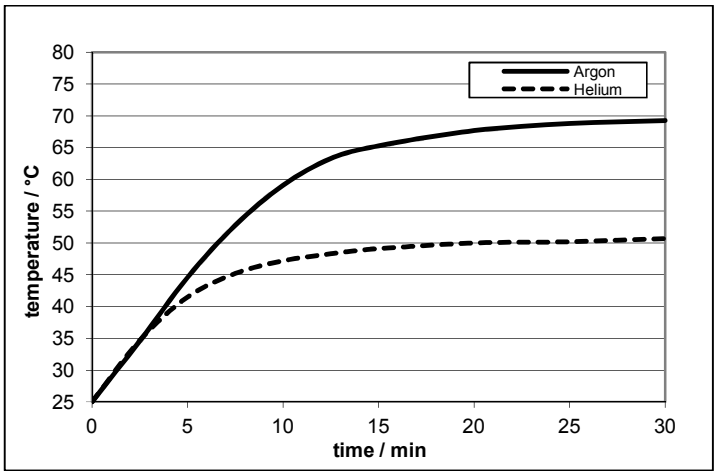

Fig. 2.20. Comparison of argon and helium (method B2, 150 W, medium pos.)

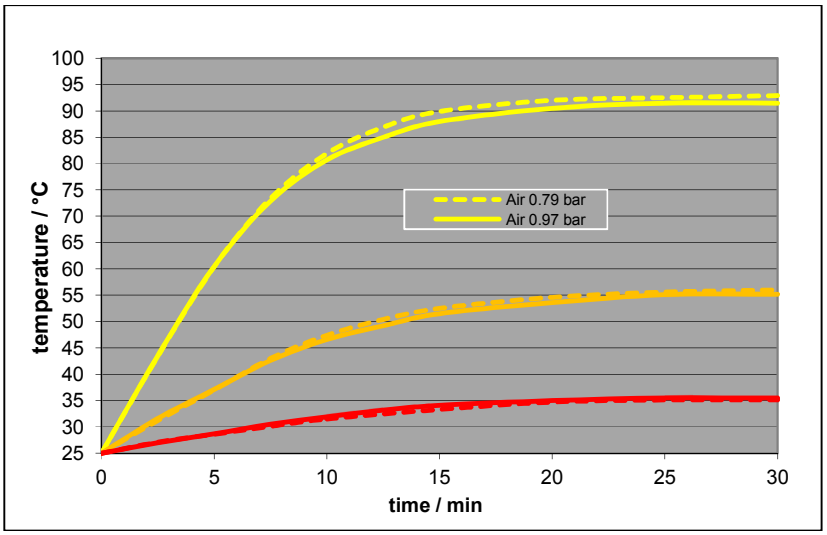

Fig. 2.21. Comparison of air at different pressures (method A, 150 W)

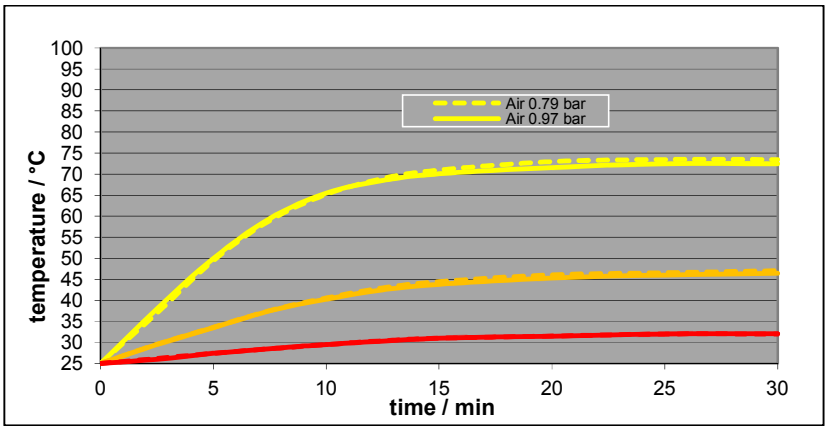

Fig. 2.22. Comparison of air at different pressures (method A, 100 W)

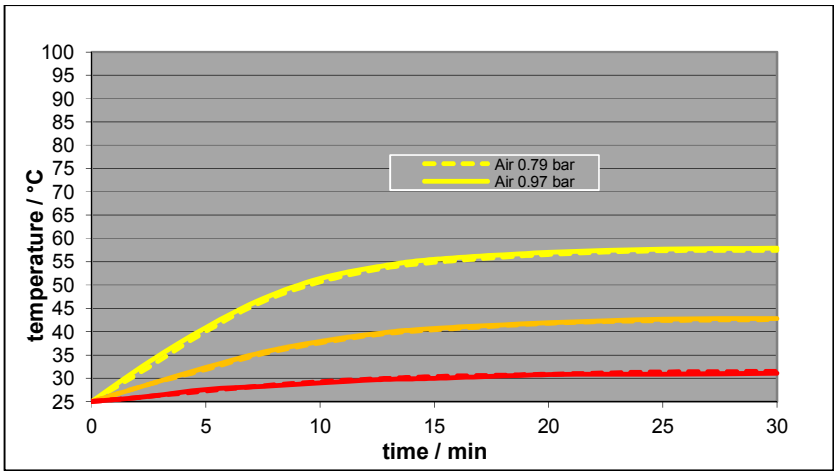

Fig. 2.23. Comparison of air at different pressures (method A, 75 W)

Using for example the values for argon being evaluable from Fig. 2.20 (yielding a warming-up rate of 20°/5 min = 0.0667 K/s, and exhibiting a molar heat capacity of 20.85 J/mol·K), the molar absorption power gets 1.39 W/mole, or, converted into litres, approx. 0.062 W/l. Assuming at this point a lamp-power of about 120 W, the absorption degree is solely 0.012/mole or 0.00053/l – so it is not surprising, that this effect has so far been overlooked!

The determination on base of medium values, or of the warming-up rate at the medium measuring point, can be considered reasonable for guaranteeing a result which is as accurate as possible. Admittedly, the result is not highly exact, in particular since the lamp intensity at the reference point had to be estimated. However, at least the order of magnitude is correct. Moreover, this approach delivers the explanation why the warming-up rates of argon and of helium (and of similar gases) are equal - namely since their molar heat capacities are equal.

2.7 The Radiative Emission of Gases in View of the Kinetic Gas Theory

Comparing the time/temperature curves of argon and helium in Fig. 2.20, a significant difference of the limiting temperatures is evident while the initial slopes are equal. If we assume a temperature dependency on the emission rate, and if we furthermore assume that the limiting temperature condition is given by the equity of warming-up power and emission power, we can conclude that the radiative emission rates of the two gases must be different, the one of helium being smaller than the one of argon. And since the molar heat capacities of the two gases are virtually equal, this difference must be due to one or more other factors. Thereby, the atomic mass seems to play a certain role. However, the atomic mass ratio of these elements is much greater than the ratio of the absolute temperatures, namely 40 : 4 = 10 instead of 342 : 323.5 = 1.057, so that a direct proportionality has to be left out of consideration.

In order to explain this, it is necessary to draw on the kinetic gas theory which has already been successfully applied on the heat conductivities of gases, and which is described in any textbooks. Thereto, it seems reasonable to consider the emission power as being proportional to the arithmetic product of *the mean kinetic energy* of the gas particles and their *collision-frequency*. For both terms there exist mathematical expressions:

$$\overline{E}_{kin} = \tfrac{1}{2} m \overline{w}^2 = \tfrac{3}{2} k_B T \qquad (2.3) \qquad \rightarrow \qquad \overline{w} = \sqrt{\frac{3RT}{M}} \qquad (2.4)$$

$$\bar{z} = \frac{\overline{w} \cdot \sigma \cdot p \cdot \sqrt{2}}{k_B \cdot T} \qquad (2.5) \qquad \rightarrow \qquad \overline{E}_{kin} \cdot \bar{z} = 3p \cdot \sigma \cdot \sqrt{\frac{3RT}{2M}} \qquad (2.6)$$

Symbols:

$\overline{E}_{kin}$	mean kinetic energy
$\overline{w}$	mean velocity
$\bar{z}$	mean collision-frequency
m	particle mass (atom or molecule)
M	mole mass
σ	cross sectional area of a particle (atom or molecule)
p	pressure
R	ideal gas constant (= 8.314 J/K·mol)
k_B	Boltzmann constant (= R/N_L = $1.38 \cdot 10^{-23}$ J/K)
N_L	Avogadro constant (= $6.023 \cdot 10^{23}$)

When two gases are compared, their absorption powers can be assumed to be equal, and since the emission power is equal to the absorption power, at constant pressure the term $\sigma\sqrt{3RT/2M}$ should be constant; i.e. the comparison of two gases yields the relation

$$T_1/T_2 = M_1(\sigma_2)^2 / M_2(\sigma_1)^2 = M_1(r_2)^4 / M_2(r_1)^4 \tag{2.7a}$$

Therein r_1 and r_2 indicate the atomic radii of the compared gases. However, this relation is difficult to verify since there are some uncertainties with respect to the cross sectional areas even when noble gases are considered: On the one hand, the atomic radii are not well defined so that the literature values are diverging; and on the other hand, solely a minimal deviation of the radius values leads to a large deviation of the temperature ratio due to the forth power of the atomic radii. However, the *inverse way* where the radius ratio is calculated on basis of the temperature ratio seems to be promising, hence representing a determination method for the atomic radii of noble gases according to the rearranged formula

$$r_2/r_1 = \sqrt[4]{(M_2/M_1)\cdot(T_1/T_2)} \tag{2.7b}$$

Nevertheless, it presupposes the knowledge of one atomic radius serving as a reference. When we use argon as the reference assuming its atomic radius r_{Ar} = 1 Å = 0.1 nm, we get for helium and neon, when using the temperature ratios given in chap. 2.3., the following values:

r_{He} = 0.57 Å and r_{Ne} = 0.85 Å

Since these results are plausible it seems to be advisable to assume that the above approach, and thus the formula (2.6) for describing the radiative emission of gases, is correct. Obviously, it is completely different from Stefan's formula which is solely valid for solid black bodies.

Moreover, there arises the question of proportionality between the »collision power«, given by equation (2.6), and the effective emission power being relevant to the power equilibrium at the limiting temperature condition. Thereby, it must be kept in mind that the mean kinetic energy being formulated in equation (2.3) solely concerns a *single* particle, and not the particle ensemble being present in a thermodynamic system. For this purpose, the basic kinetic relation about the ideal gas equation must be used:

$$p\cdot V = n\cdot R\cdot T = \tfrac{2}{3}\, n\cdot N_L\cdot \overline{E}_{kin} \tag{2.8}$$

(n = mole number, V = Volume)

As a consequence, the molar collision power $P_{collision}$ is given by the equation (2.9):

$$P_{collision} = \tfrac{2}{3}\, N_L\cdot \overline{E}_{kin}\cdot \bar{z} = 2N_L\cdot\sqrt{\frac{3RT}{2M}}\cdot p\cdot\sigma \tag{2.9}$$

Moreover, proportionality between that collision power and the emission power may be assumed, represented by a proportional factor ε:

$$P_{emission} = \varepsilon\cdot P_{collision} \tag{2.10}$$

When the equilibrium temperature is attained, the molar emission power, given by equation (2.10), should be equal to the molar absorption power, given by equation (2.2). When *argon* is adduced as an example, at 1 bar pressure (= 10^5 Nm^{-2}) the numeric values are T = 342 K (according to Fig. 2.23), and σ = $3.14\cdot10^{-20}$ m^2, yielding a $P_{collision}$-value of $1.23\cdot10^{12}$ W/mole. The comparison with the empiric

$P_{absorbance}$-value which has previously been obtained using equation (2.2), namely 1.39 W/mole, delivers the extremely low ε-value of $1.13 \cdot 10^{-12}$. For now, this result cannot theoretically be explained. Probably, it is connected with the question of what happens when two atoms collide, letting suppose that atomic electron shells are caused to vibrate being accompanied with electron excitations. However, the pressure independence of the process, displayed in the Figs. 2.21-2.23, can be easily explained by considering the pressure-dependence of the heat capacity of the gas.

2.8 Estimate of the Effective Wavelength-Range

A rough estimate of the effective wavelength-range appears feasible by comparing the absorbance rates due to sunlight and artificial light, for their spectra are not congruent but overlapping. When both spectra are plotted in the same diagram in such a way that the ratio of their integrated intensities corresponds to the ratio of the real intensities, the effective wavelength may be determined by graphically evaluating the wavelength where the ratio of the warming-up rates is equal to the ratio of the respective spectral intensities. Hereto, methods B2 and B3 were used with air fillings and using the 75 W Basking spot (implying a local radiation density of approx.1500 Wm^{-2}, while the one of sunlight was 1000 Wm^{-2}), yielding - at the medium measuring point - warming-up rates of 1.4°/min for sunlight and 2.1°/min for artificial IR-light, and thus a ratio of 1.5. But while the solar spectrum can be adopted from literature, the uncertainties with respect to the spectrum of the Basking spot, as mentioned in chap. 2.3, make it appear meaningful to consider any variant (c.f. Figs. 2.24 a-c), and delivering the wave lengths 0.8, 1.45 and 1.9 µm, where solely the last one seems to be plausible.

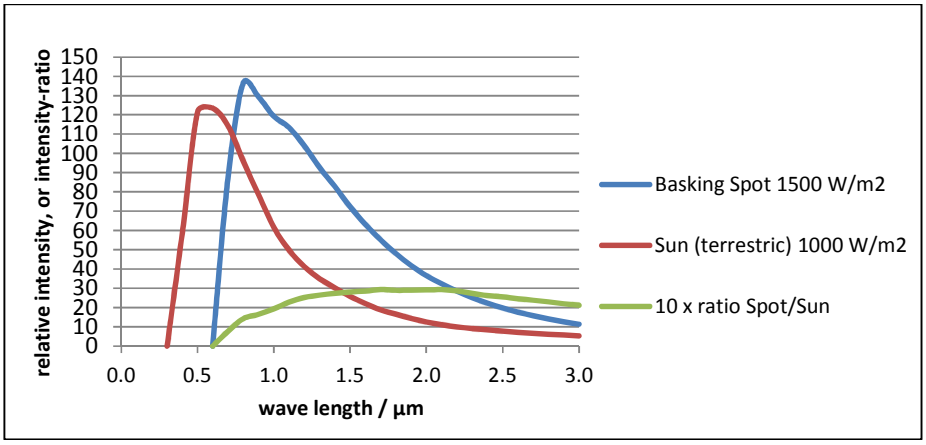

Fig. 2.24a. Comparison of sunlight with spotlight according to the producer specification

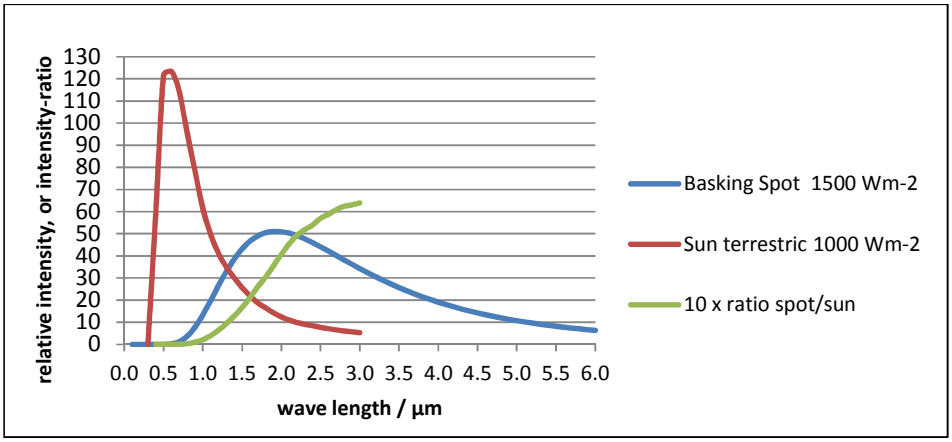

Fig. 2.24b. Comparison of sunlight with spotlight being calculated for 1500 K (Planck)

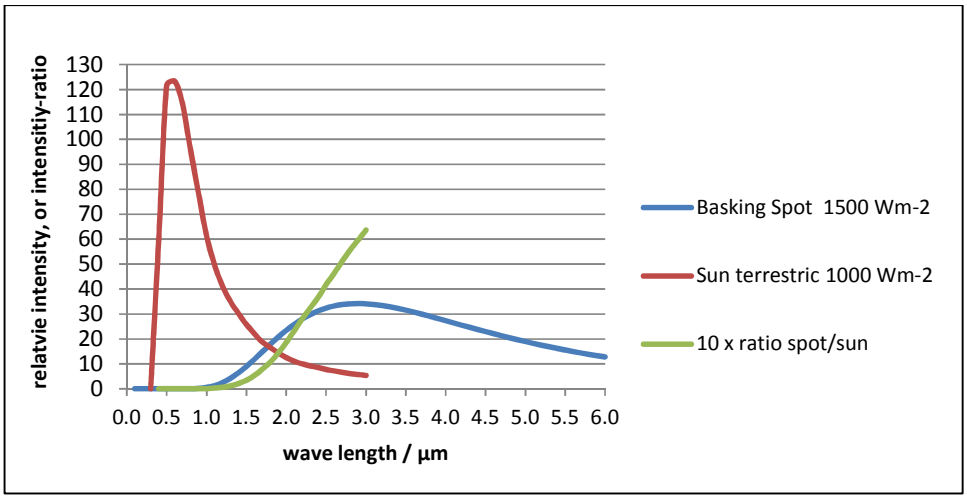

Fig. 2.24c. Comparison of sunlight with spotlight being calculated for 1000 K (Planck)

2.9 The Determination of the Radiative Heat Coefficient

Finally, the question as to which portion of the radiation energy is transformed into heat energy shall be answered. For such a comparison, both energies must be known but being preferably focused on a single particle, and not on the whole ensemble. Since we know now the effective wavelength, namely 1.9 µm, delivering the respective wave frequency according to the relation $\lambda \cdot \nu = c$ (speed of light), we can easily calculate the respective energy by using Einstein's relation (2.11)

$$E_{rad} = h \cdot \nu \qquad (2.11) \qquad \rightarrow \qquad E_{rad} = \frac{h \cdot c}{\lambda} = 1.05 \cdot 10^{-16}\ \text{J} \qquad (2.12)$$

On the other hand, the mean kinetic energy calculated employing formula (2.3) may be interpreted as the heat energy, delivering the value $6.6 \cdot 10^{-21}$ J (with T = 300 K). Therefore, defining the quotient of the two energies as the radiative heat coefficient, we obtain the very low value $6.3 \cdot 10^{-5}$, i.e. the amount of radiative energy being transformed into kinetic heat energy is very small. The order of magnitude of this coefficient wouldn't change significantly if the adsorption wavelength were in the middle IR-range. Indeed, this low yield is characteristic for gases differing considerably from the one of black bodies, which may be explained vividly by the large difference in density and the reduced intermolecular interaction.

2.10 Conclusions

The here described method employing one or two comparatively large tubes from Styrofoam, preferably mirrored by aluminium foils, and being covered on both ends with thin plastic foils, enables temperature measurements at gases under the influence of solar light as well as of artificial IR-light using special bulbs with a reflector. The temperatures are measured at three positions, allowing studying the path dependence on the radiation intensity. Due to a hygrometer being laterally embedded in the tube, the filling degree of a gas can be checked. Usually, immediately after the start, the temperature rises linearly but later on, it tends to a constant limiting temperature, which is due to the equilibrium of the thermal absorption rate and the radiative emission rate. The initial slope of the temperature/time curve enables determining the warming-up rate and the thermal absorption degree, regarding the heat capacity of the gas, while the limiting temperature delivers the empirical coherence between the (absolute) temperature and the emission power of the gas.

Thereto, the following remarks have to be made with respect to an atomic model concept: It has to be emphasized that the thermal absorption degree may be probably not equal to the radiative absorption degree since presumably not the whole adsorbed radiation energy is transformed into heat, i.e. into kinetic energy, but it may be temporarily stored within the atoms or molecules in the form of exited electronic vibrational states. For determining the radiative absorption degree, solely spectroscopic methods would be suitable. However, at very low absorption degrees, as is the case here, such methods appear to be not enough sensitive due to the relative low absorbance compared to the whole radiation intensity, and due to the possible interference with lenses and prisms in the IR-range. But above all, for atmospheric considerations solely the thermal behaviour is relevant, and that one cannot be strictly derived from spectroscopic features because of the above-mentioned reason.

Moreover, the knowledge of the limiting temperatures - and of the fact that different gases may deliver different limiting temperatures – the conclusion can be drawn that the radiative emission depends on the atomic features of the gas, namely on the mass and on the size. Indeed, based on the kinetic gas theory, a mathematical formulation could be found delivering a direct correlation between limiting temperature and radiative emission power, given by the product of mean kinetic energy and collision frequency, delivering the power-dimension W. On the other hand, the warming-up rate turned out to be independent of the gas type.

Since sunlight as well as IR-bulbs were employed as radiation sources, near-IR was expected to be predominant and not medium-IR as it is commonly assumed. Comparing the results in sunlight and in artificial light, the effective wavelength could be assessed delivering the value of 1.9 µm.

Surprisingly – and contrary to the expectation of the greenhouse theory -, the limiting temperatures of air, pure carbon-dioxide and argon were nearly equal while the light gases neon and, particularly, helium exhibited significant lower limiting temperatures. Thanks to this empirical evidence, the greenhouse theory has to be questioned. The warming-up of the lowest layer of the troposphere has to be understood as the result of the warming-up of the Earth's surface, mainly depending on its albedo (Barrett (1995)).

ACKNOWLEDGEMENT

The present work has been carried out independently but not without the professional support of Dr. Andreas Rüetschi (physicist, from the Swiss Federal Institute of Technology, Zurich).

REFERENCES

Ångström K (1900): Ueber die Bedeutung des Wasserdampfes und der Kohlensäure bei der Absorption der Erdatmosphäre. *Ann. Phys. 308(12)*, 720-732

Arrhenius S (1896): On the influence of carbonic acid in the air upon the temperature of the ground. *Phil. Mag. 41(5)*, 238-276

Arrhenius S (1901): Ueber die Wärmeabsorption durch Kohlensäure. *Ann. Phys. 309(4)*, 690-705

Barrett J (1995): The roles of carbon dioxide and water vapour in warming and cooling the Earth's troposphere. *Spectrochimica Acta. 51A(3)*, 415-417

Bird R. (1989): Spectral Terrestrial Solar Radiation, in: Solar Resources, Ed. by R.L. Hulstrom, Cambridge, MA, MIT Press. 1989, VIII: 310-333

Boeker E, van Grondelle R (2011): Environmental Physics. Wiley (Third Edition) 2011

Cess RD, Tiwari SN (1972): Infrared Radiative Energy Transfer in Gases. *Adv. Heat Transf. 18*, 229-283

Curtis AR (1956). The computation of radiative heating rates in the atmosphere. *Proc. R. Soc. London. Series A, Math. Phys. Sci. 236*, 156-159

Fourier M (1827): Mémoire sur les temperatures du globe terrestre et des espaces planétaires; *Mémoires de l'Académie Royale des Sciences de l'institut de France 7*, 569-604

Langley SP (1884): Professional papers of the signal service: Researches on solar heat and its atsorption by the earth's atmosphere. US. Army. Signal Corps, William Babcock Hazen 1884.

Möller F. (1956): The pattern of radiative heating and cooling in the troposphere and lower stratosphere. *Proc. R. Soc. London. Series A. Math. Phys. Sci. 236*, 148-156

Plass GN (1956a): The carbon dioxide theory of climatic change. *Tellus 8*, 140-154

Plass GN (1956b): Effect of carbon dioxide variations on climate. *Am. J. Phys. 24*, 376-387

Schlesinger ME, Andronova NG, Entwistle B, Ghanem A, Ramankutty N, Wang W, Yang F (1997): Modelling and simulation of climate and climate change, in: Proceedings of the International School of Physics *«Enrico Fermi»*, Course CXXXIII, Società Italiana di Fisica Bologna-Italy 1997, 389-429

Sirtl S (2010): Absorption thermischer Strahlung durch atmosphärische Gase, Wissenschaftliche Arbeit für das Staatsexamen in Physik; 2010. Available: http://hpfr02.physik.uni-freiburg.de/arbeiten/diplomarbeiten/ sirtl_staatsexamen_2010.pdf

Tien CL (1968): Thermal radiation properties of gases, in: Hartnett J.R. and Irvine T. (Eds.). *Adv. Heat Transf. 5,* 253-324

Thompson RI, Epps HW, Winters G, Womack W, Mentzell E (1994). GRIS: The grating infrared spectrometer. Public Astron. *Soc. Pac. 106*, 94-100

Tyndall J (1861): On the absorption and radiation of heat by gases and vapours, and on the physical connexion of radiation, absorption, and conduction. *Phil. Mag. 22*, 169-285

Tyndall J (1863): On the radiation through the earth's atmosphere. *Phil. Mag. 25*, 200-206.

Tyndall J (1872): Contributions of molecular physics in the domain of radiant heat. Logmans, Green, and Co. 1872, 446

Zerlaut G (1989): Solar radiation instruments, in: Solar Resources, ed. by R.L. Hulstrom, Cambridge, MA, MIT Press. 1989, VIII: 173-308

3. THE THERMAL RADIATION OF THE ATMOSPHERE AND ITS ROLE IN THE SO-CALLED GREENHOUSE EFFECT

3.1 Summary

Knowledge about thermal radiation of the atmosphere is rich in hypotheses and theories but poor in empiric evidence. Thereby, the Stefan-Boltzmann relation is of central importance in atmosphere physics, and holds the status of a natural law. However, its empirical foundation is little, tracing back to experiments made by Dulong and Petit two hundred years ago. Originated by Stefan at the end of the 19th century, and theoretically founded afterwards by Boltzmann, it delivers the absolute temperature of a blackbody – or rather of a *solid opaque body (SOB)* – as a result of the incident solar radiation intensity, the emitted thermal radiation of this body, and the counter-radiation of the atmosphere. Thereby, a similar character of the blackbody radiation – describable by the expression $\sigma \cdot T^4$ - and the atmospheric counter-radiation was assumed. But this appears quite abstruse and must be questioned, not least since no pressure-dependency is provided.

Thanks to the author's recently published work - proposing novel measuring methods -, the possibility was opened-up not only to find an alternative approach for the counter-radiation of the atmosphere, but also to verify it by measurements. This approach was ensued from the observation that the IR-radiative emission of gases is proportional to the pressure and to the square root of the absolute temperature, which could be bolstered by applying the kinetic gas theory. The here presented verification of the modified counter-radiation term $A \cdot p \cdot T^{0.5}$ in the Stefan-Boltzmann relation was feasible using a direct caloric method for determining the solar absorption coefficients of coloured aluminium-plates and the respective limiting temperatures under direct solar irradiation. For studying the pressure dependency, the experiments were carried out at locations with different altitudes. For the so-called *atmospheric emission constant* A an approximate value of 22 $Wm^{-2}bar^{-1}K^{-0.5}$ was found. In the non-steady-state, the total thermal emission power of the soil is given by the difference between its blackbody radiation and the counter-radiation of the atmosphere. This relation explains to a considerable part the fact that on mountains the atmospheric temperature is lower than on lowlands, in spite of the enhanced sunlight intensity. Thereto, the so-called greenhouse gases such as carbon-dioxide do not have any influence.

3.2 Introduction

Thermal and IR-radiative measurements at gases encounter several principal difficulties: Firstly, gases need to be embedded in a vessel from a solid material which may considerably influence and overlay the thermal behaviour due to its higher heat capacity. Secondly, thermal-radiative energy transfer – i.e. electromagnetic interaction - may be influenced by simple heat conduction as well as by gas convection. And thirdly, the coexistence of radiative energy and of heat energy complicates the situation since one component may be partly converted into the other, and vice versa. Thereby it has to be realized that heat energy is due to atomic or molecular translational motion, rotation and nuclear vibration, while radiative energy is due to electronic oscillations at atoms or molecules. The first aspect concerns thermodynamics, implying non-quantized processes, while the second aspect affects quantum mechanics and thus energetically quantized processes. Planck's distribution law bridged the two domains applying the coherence between temperature and entropy (Planck, 1900a-c). However, it is confined to boundary conditions, for instance to equilibrium states between emission and absorption intensities. But in particular, it concerns so-called blackbodies, and not implicitly gases. Overall, this domain appears to be the most intricate one in physics – apart from nuclear physics -, calling for considerable expertise, while, on the other hand, it is in everyone's interest in so far as it affects the climate and thus the day-to-day life.

It must be noted that contemporary atmospheric physics is rich in theories and hypotheses but poor in experimental evidence which in fact should deliver the final proof of the truth – and not the credence in authorities, as *Robert Boyle* claimed already in the 17th century. Notably, the large part of basic

radiation experiments was made in the 19th century. In particular, *Beer* formulated his absorption law for liquids in 1852 (which is not identical with the nowadays assumed absorption law named after him), using an oil-lamp as a light source (Beer, 1852), while *Tyndall* published in 1861 absorption experiments with carbon-dioxide in comparison to air, using Leslie-cubes as thermal radiation sources, cf. Fig. 3.1 (Tyndall, 1861). *Stefan*, the eponym of the Stefan-Boltzmann Law, did not make own experiments but solely interpreted the results of *Dulong* and *Petit* which had already been published in 1817, using the equipment shown in Fig. 3.2 (Stefan, 1879; Dulong and Petit, 1817). *Lummer* and *Pringsheim* published their empiric results concerning blackbody radiation in 1899 (Lummer and Pringsheim, 1899) which allowed verifying Planck's quantum theory, established in 1900.

As to these basic experiments, the predominance of photometric and spectroscopic methods is remarkable while caloric methods were still neglected. In fact, the spectroscopic methods are even the only methods which were used in recent research, particularly in connection with satellite measurements. Thereby, the intensity loss of IR-radiation is detected after passing through a medium – in our case a gas, in particular atmospheric air -, while the possible temperature change of the medium is disregarded. But this method exhibits two principal weaknesses which will later be discussed on the basis of the author's recently published work: It is not sure whether – or to which extent – the absorbed radiation is converted into heat. Moreover, very weak radiative absorbance by the gas may be disregarded due to the insufficient sensibility of the apparatus, in spite of the fact that for spectroscopic measurements prisms and lenses are needed which partly absorb IR.

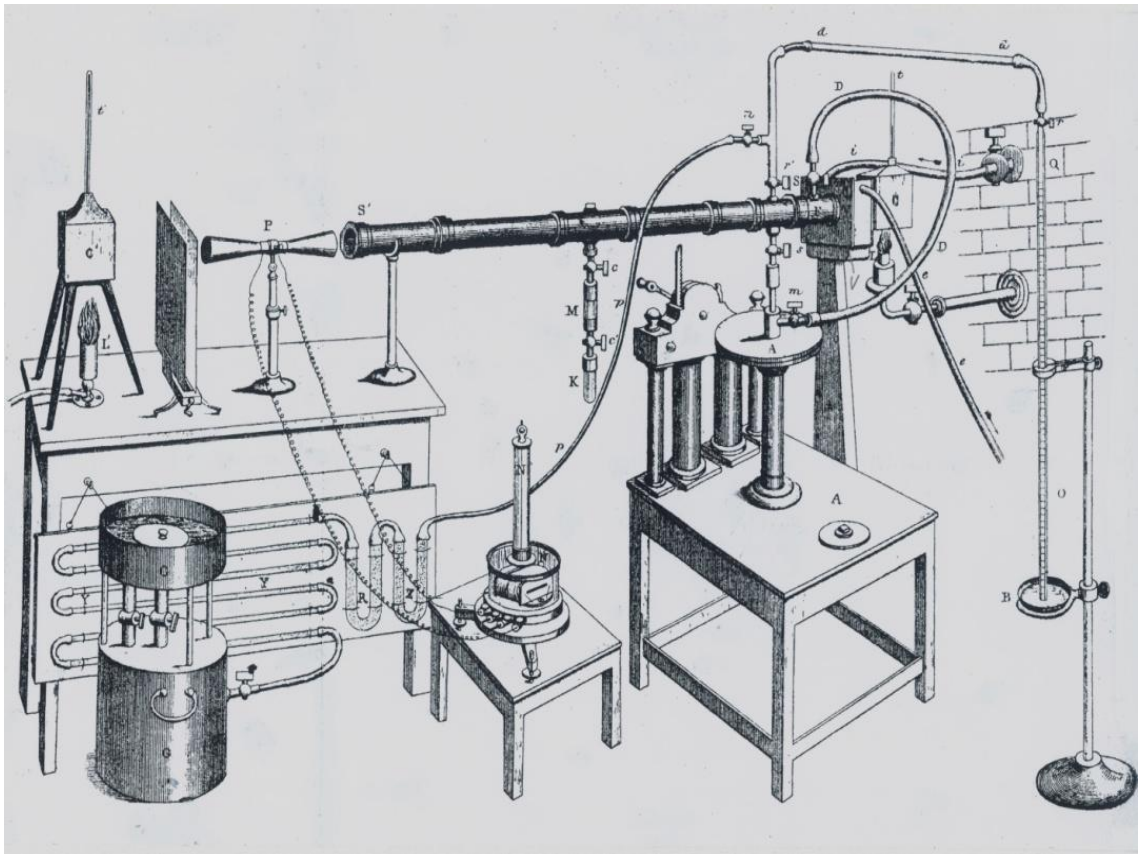

Fig. 3.1. The preferred apparatus of Tyndall (1861) using a Leslie-cube as a thermal radiation source (to the right) and another Leslie-cube as a reference (to the left)

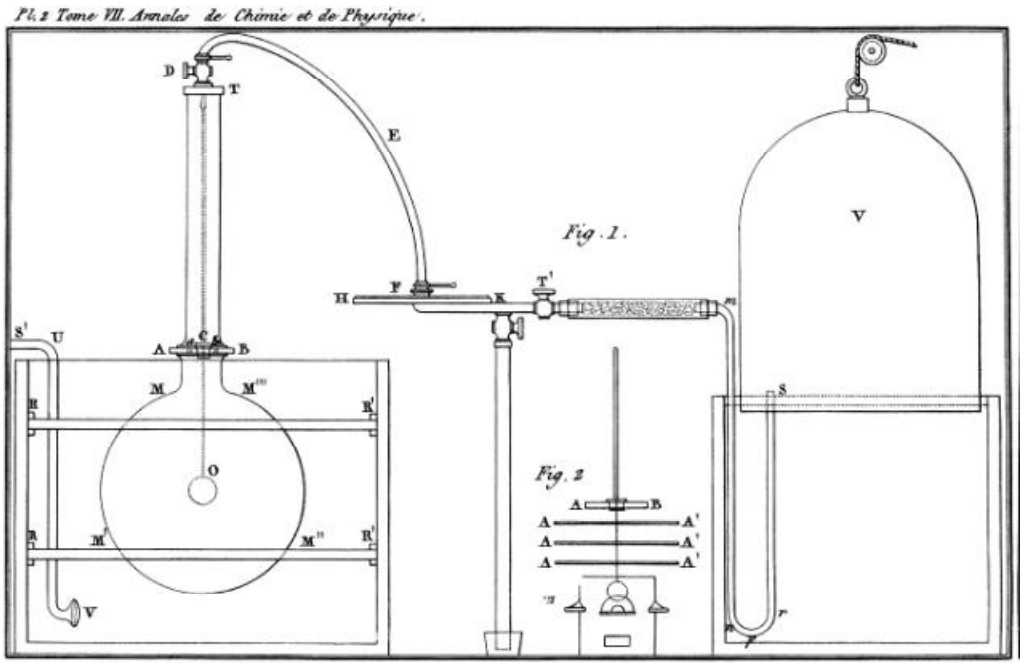

Fig. 3.2. The equipment of Dulong and Petit (1817)

Besides the application in bolometers, the sole method implicating caloric measurements is the one which concerns the *Stefan-Boltzmann relation*. As already mentioned, Stefan's (1879) approach was based on earlier experiments of Dulong and Petit (1817), using the equipment shown in Fig. 3.2, while Boltzmann delivered the theoretical explanation five years later (Boltzmann, 1884). Subsequently, the respective constant could be exactly computed using Planck's theory. The said relation is of central importance in atmosphere physics holding the status of a physical law, even if some doubts are justified. Nevertheless it represents the pivot of the present treatise.

The Stefan-Boltzmann relation comprises three decisive conceptions:

Firstly, it makes use of the radiation law which is valid for blackbodies under vacuum, given by (3.1):

$$I = \sigma \cdot T^4 \tag{3.1}$$

where I = radiation intensity [Wm^{-2}], T = absolute temperature [K]

The Stefan-Boltzmann constant σ can empirically be determined, but - as above mentioned - also theoretically be computed, yielding (3.2), cf. Meschede, 2002:

$$\sigma = 2\pi^5 k^4 / 15c^2 h^3 = 5.75 \cdot 10^{-8} Wm^{-2} K^{-4} \tag{3.2}$$

where k = Boltzmann constant, c = light velocity, h = Planck constant

Secondly, it is supposed that in the presence of the atmosphere – or of another blackbody –, which is held at a constant temperature T_{atm}, *atmospheric counter radiation* takes place, which leads to a reduction of the total radiation of the blackbody, yielding the reduced value I^* according to (3.3). Thereby, the same radiation law is assumed for this counter-radiation as for a blackbody:

$$I^* = \sigma(T^4_{blackbody} - T^4_{atm}) \tag{3.3}$$

And thirdly, radiation equilibrium is assumed between the intensities of the incident solar radiation Φ and the total blackbody radiation (3.4), implying a steady state where a constant limiting temperature of the black body is reached:

$$\Phi = \sigma(T^4_{blackbody,\lim} - T^4_{atm}) \tag{3.4a}$$

or rearranged $$\sigma \cdot T^4_{blackbody,\lim} = \Phi + \sigma \cdot T^4_{atm} \tag{3.4b}$$

Hence, the Stefan-Boltzmann relation was applied to the whole atmosphere – or rather to its lowest layer -, which obviously does not exhibit any surrounding walls, as it was the case for the measurements of Dulong and Petit. Instead, it is held together by the gravity of the Earth. However, this implies a considerably inhomogeneity - even when cloud and dust effects are neglected -, not only because of the vertical pressure and temperature gradients, but also because of horizontal gradients caused by the ball shape of the Earth, which leads to latitude-dependant solar irradiation intensities. In addition, differences in altitude, due to mountains, as well as diurnal and seasonal fluctuations contribute to permanent but not consistent motions which hardly admit steady-state conditions.

When, instead of a blackbody, a coloured *solid opaque body* (abbrev. *SOB*) is used, these equations can be modified to the equations (3.5a) and (3.5b) since the thermal emission power of a coloured solid opaque body turned out to be equal to the thermal emission power of a blackbody (Allmendinger, 2016a):

$$\Phi \cdot \beta_s = \sigma(T^4_{SOB,\lim} - T^4_{atm}) \tag{3.5a}$$

or rearranged $$\sigma \cdot T^4_{SOB,\lim} = \Phi \cdot \beta_s + \sigma \cdot T^4_{atm} \tag{3.5b}$$

yielding formula (3.6) for calculating the limiting temperature of an irradiated coloured SOB:

$$T_{SOB,\lim} = \sqrt[4]{\frac{\Phi \cdot \beta_s}{\sigma} + T^4_{atm}} \tag{3.6}$$

Therein, β_s indicates the *solar reflection coefficient*, expressing the portion of absorbed irradiation. But normally, instead of this solar absorption coefficient, the complementary *solar reflection coefficient* α_s (or the «albedo») is used which entails its *indirect* determination according to the relation $\beta_s = 1 - \alpha_s$. Since this may lead to uncertainties due to scattering of the reflected radiation, a method for the *direct* determination of the solar reflection coefficient β_s was developed by the author, measuring the warming-up of coloured solid opaque plates (Allmendinger, 2016a). Thus, it spares you the trouble of determining the albedo, in particular since it is suitable to empirically assess the Stefan-Boltzmann relation.

In any case it should be realized that the incident solar intensity Φ and the ambient surface air temperature T_{atm} are not independent of one another, apart from the fact that the latter one is ill-defined. However, this interdependency is not distinctly computable because of the variety of relevant further parameters and processes. Moreover, in reality the limiting temperature of superficial materials is hardly ever reached, not least because of the diurnally alternating altitude of the sun and, in particular, because of the cooling-down of the Earth surface during night. In the latter case, the intensity of the incident solar intensity becomes zero. Instead, a radiative emission of the solid opaque body – representing the soil – is to be anticipated, thus equation (3.5b) turns into equation (3.7):

$$\Phi_{emission,soil} = \sigma \cdot T^4_{soil} - \sigma \cdot T^4_{atm} \tag{3.7}$$

However, the cooling-down experiments described in Allmendinger (2016a) did not verify this equation. As an explanation, the different characters of the two participants have to be taken into account: in the case of solid materials, primarily the properties of the *surface* are relevant, while in the case of gases the relevant processes occur *inside*, i.e. within their whole extension range. This means, that the former processes occur *two-dimensionally,* while the latter ones are *three-dimensional*. It seems to be obvious that the atmosphere acts altogether *incidentally* like a solid thermal radiator, suggesting that it behaves like a solid opaque body. However, it can be assumed that, if the atmosphere were less extensive, its back-radiation power would probably be weaker, due to the reduced atmospheric pressure. As a consequence, an alternative approach such as

$$\Phi \cdot \beta_s = \sigma \cdot T_{SOB,\lim}^4 - f(p_{atm}, T_{atm}) \tag{3.8}$$

should be taken into consideration, exhibiting the presently unknown term $f(p_{atm}, T_{atm})$, being a function of atmospheric pressure and temperature, appears reasonable but difficult to derive and verify. It is one of the main goals of this treatise to find a formal expression for this term. The recently reported and below described discovery of near-infrared absorption by gases delivered the key for finding such an expression. Since this novel method and its results cannot be assumed to be generally known, it will be recapitulated in chap. 3.3. But first of all, the method for the direct determination of the solar absorption coefficient will be described, allowing the empirical verification of the proposed atmospheric term by variation of the atmospheric pressure due to different sea levels.

3.3 A Novel Method Suited for the Validation of the Stefan-Boltzmann Relation

A *direct* determination method for the solar absorption coefficient has been recently published by the author where the temperature rise of coloured plates in the presence of vertical incidental solar light is measured (Allmendinger, 2016a). The plates were 10 x 10 cm^2 large and normally 20 mm thick. To avoid heat losses laterally and at the bottom, the plates were embedded in Styrofoam, and covered with a thin transparent foil acting as an outer window to minimize erratic cooling by atmospheric turbulence (Fig. 3.3). The preferred reference material was *aluminium.* It guarantees a high measurement precision, on the one hand due to its high specific heat capacity, reducing the thermal interference with the mounting material, and on the other hand due to its high thermal conductivity facilitating the heat dispersion in the plate and thus minimising the temperature difference between surface and bulk. For comparison, additionally other materials were used (wood, brick, and stone).

For the warming-up experiments several coloured plates were orientated exactly vertically to the incoming sunlight. In order to enable a correct orientation, the plate modules were positioned on an adjustable carrier (Fig. 3.4). The temperatures were measured at regular intervals of 5 minutes using Hg-thermometers being centrally inserted in holes. The heating-rates could easily be determined by graphically assessing the initial slopes of the time/temperature curves. The sky had to be cloudless during the experiment. For detecting the intensity of the solar insolation, a suitable electronic apparatus was used. The time/temperature-plots for differently coloured plates are shown in Fig. 3.5. Considering the heat capacities of the plates, the specific solar reflection coefficients β_s could be calculated.

As expected, such plates being exposed to direct sunlight will not be warmed up ad infinitum but only up to a *limiting temperature*. Thus the time/temperature-curves will flatten sooner or later, losing their initially linear character. This phenomenon is already briefly perceptible when, instead of aluminium, plates from wood are inserted which exhibit a lower heat capacity implying a quicker warming-up. Obviously, this can be explained with the emission of thermal radiation effecting cooling-down, since it is temperature dependent, and growing till its intensity is equal to the intensity of the absorbed incident solar radiation.

With the plates used it was not possible to reach the limiting temperature ranges since the measuring period was too short. However, it was possible to study the cooling-down effect *separately* in a darkened room, using the same embedding as the one which had been used for the warming-up

measurements, but starting from an elevated temperature being achieved by preheating the plates in an oven (Fig. 3.6). As expected, the cooling-down rates depended on the material, in particular on its heat capacity. But unexpectedly, they did *not* depend on the surface colour. This was surprising since it seemed to contradict the well-known theorem of *Kirchhoff* which states that the absorbency of a surface is equal to its emissivity. However, Kirchhoff's statement was made at a time when, for instance, the quantization of electromagnetic radiation was not yet known (Kirchhoff, 1860, 1861). Therefore, the body must not necessarily be black, it is sufficient that it is opaque. Hence, Planck's distribution law is not exclusively valid for blackbodies, but also for *any solid opaque body*.

As the analysis yielded, the cooling-rates were proportional to the temperature difference between plate and ambient air, leading to exponential curve-courses which were exactly describable with a mathematic formula. It exhibits the so-called *heat transfer coefficient B* which can be determined from experimental data. It depends on the experimental conditions, in particular on the surrounding atmosphere, but *not* on the specific properties of the plates. Using the respective apparatus, a general heat transfer coefficient of approx. 9 $Wm^{-2}K^{-1}$ was obtained. In the case of the absence of a foil, the heat transfer coefficient increased up to 15 $Wm^{-2}K^{-1}$. However, as it seems obvious, the heat conductivity of the material is decisive, too, but scarcely implementable.

Combining the differential equations for the warming-up rate and the cooling-down rate, a differential equation for the overall-process was obtained. Its solution yielded equation (3.9):

$$T = T_{atm} + \frac{\Phi \cdot \beta_s}{B}\left(1 - e^{-\frac{B \cdot a}{m \cdot c_m} t}\right) \tag{3.9}$$

whereby a = area of the plate, m = mass of the plate, and c_m = its mass specific heat capacity. When $t = \infty$, T has reached a limes which is computable by equation (3.9):

$$T_{\lim} = T_{atm} + \frac{\Phi \cdot \beta_s}{B} \tag{3.10}$$

Hence, according to formula (3.10), the limiting temperature is *independent of the heat capacity*, but solely dependent on the irradiation density Φ, the solar absorption coefficient β_s, and the heat transfer coefficient B, while the ratio of the limiting temperatures (in °C) is equal to the ratio of the β_s-values.

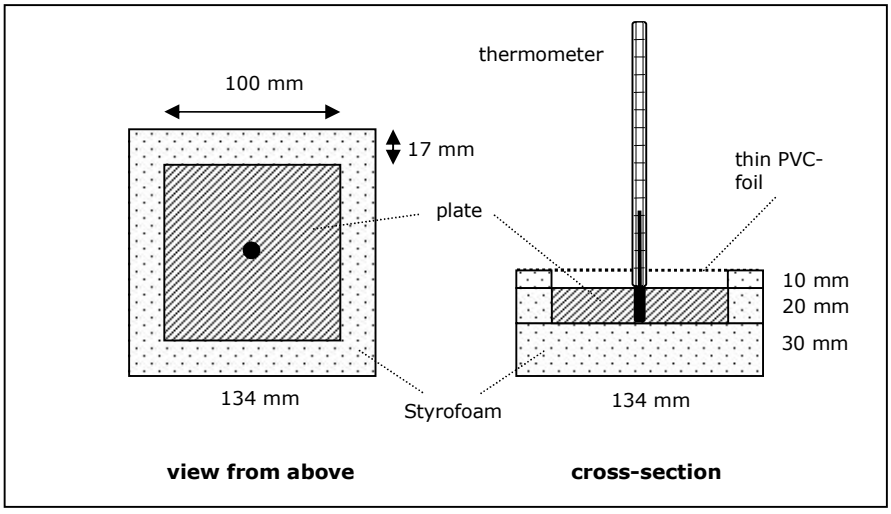

Fig. 3.3. Coloured plate embedded into Styrofoam and covered by a transparent foil (Allmendinger, 2016a)

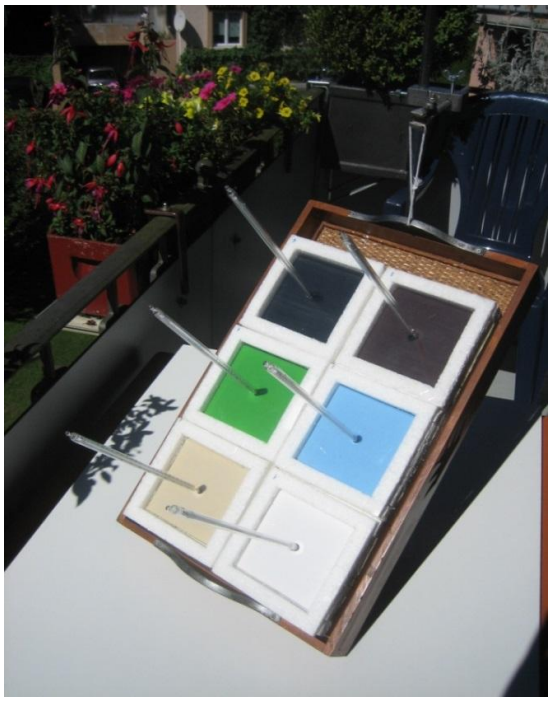

Fig. 3.4. Panel comprising six differently coloured modules according to Fig. 3.3 (Allmendinger, 2016a)

Using formula (3.9), the temperature courses at differently coloured aluminium-plates were calculated applying this model and plotted in Fig. 3.7. Respective plots for similarly coloured plates exhibiting lower heat capacities reveal larger heating rates but identical equal limiting temperatures. Although this modelling method cannot deliver exact results since the heating-up and the cooling-down process were not carried out under the same conditions, the results of this modelling appear nevertheless plausible and in principle accurate.

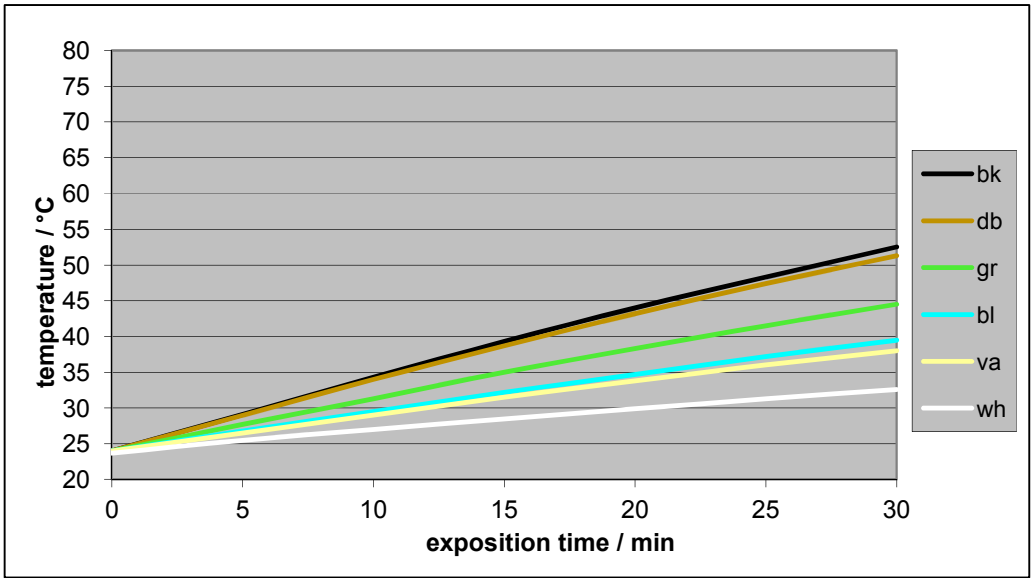

Fig. 3.5. Warming-up of aluminium at 1040 Wm^{-2} (Allmendinger, 2016a)
(wh = white, va = vanilla, bl = blue, gr = green, db = dark brown, bk = black)

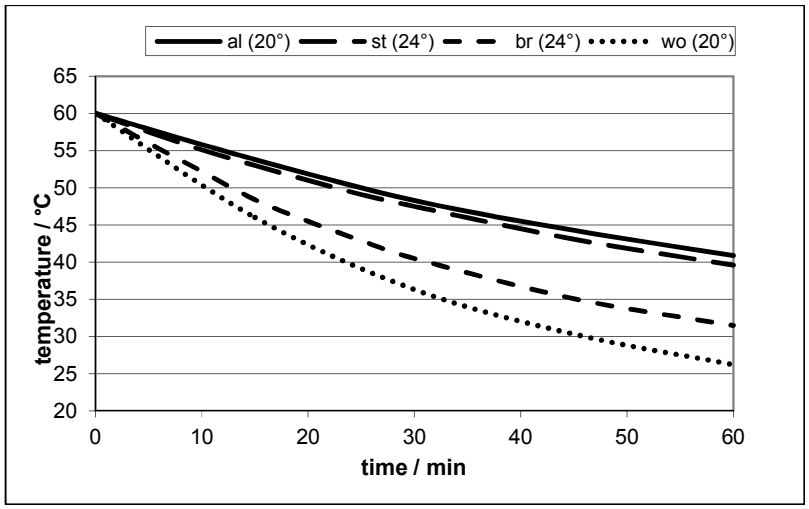

Fig. 3.6. Cooling-down of different materials, with covering foil (Allmendinger, 2016a)
(al = aluminum, st = stone, br = brick, wo = wood; in brackets: ambient temperature)

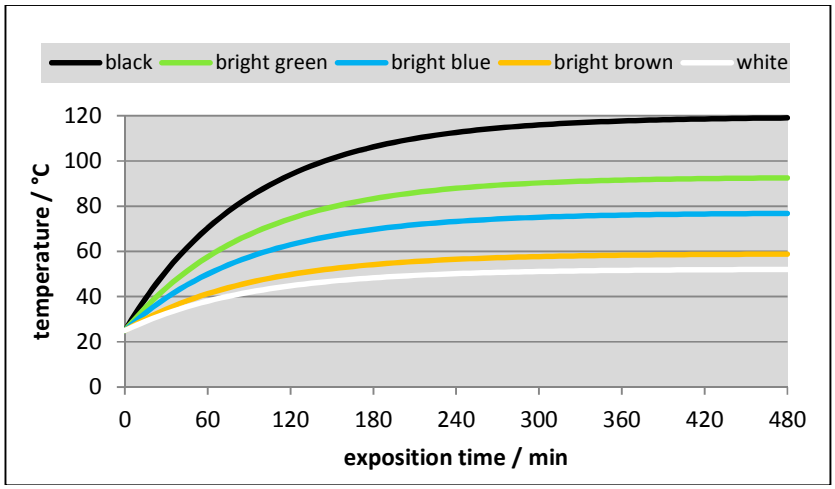

Fig. 3.7. Temperature courses at differently coloured aluminium-plates (20 mm thick) (Allmendinger, 2016a)

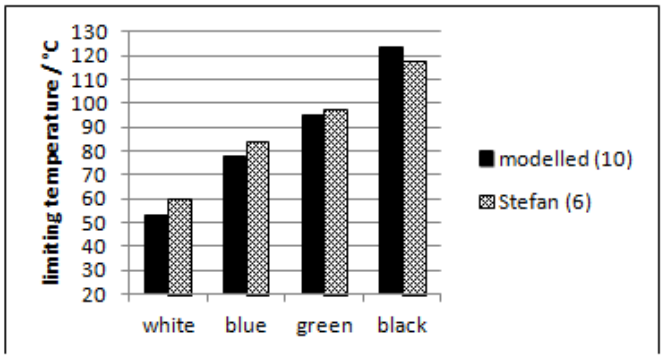

Fig. 3.8. Comparison of the calculated values according to eq. (3.10) and (3.6) based on the edge data for β_s and T_{am} given in Allmendinger (2016a)

In principle, this method is suitable for verifying the Stefan-Boltzmann relation by comparing the limiting temperatures for different colours using formulas (3.6) and (3.10). For that purpose, in Fig. 3.8 the results of the two computation methods are compared for the four colours white, blue, green and black, based on the edge data of the original own measurements quoted in Allmendinger (2016a). They are consistent to such an extent that the validity of the Stefan-Boltzmann relation seems to be proved.

However, it should be regarded that the measurements of Dulong and Petit, evaluated by Stefan, were made in closed vessels - and not in contact with the open atmosphere. Similarly, the author's own cooling-down experiments, whose results allowed the computational simulation of the limiting temperatures, were made in a closed room. Thus in both cases the counter-radiation might be induced by the surrounding walls, i.e. by solid opaque bodies, and *not* - or not only - by open air. As a consequence, a stringent empirical proof is solely possible if the coloured plates are irradiated by sunlight as long as their temperatures have reached the limiting values, and this is preferably achieved by using thinner plates with smaller heat capacities. Hence, the first and preliminary purpose of the present treatise consists in delivering experimental data for assessing the modelled values given in Allmendinger (2016a) by using 8 mm thick aluminium plates instead of the ones that are 20 mm thick.

In view of the above alleged objections which, in spite of the apparent evidence, suggest a principal questioning of the Stefan-Boltzmann relation, a second purpose arises consisting in establishing and verifying a hypothesis which immediately suggests itself through a result of a further method which was published recently by the author (Allmendinger, 2016b). It concerns the measurement of IR-absorption and IR-emission by gases and will be shortly described below. Its results promise an application to the atmospheric counter-radiation, which will lead to a modification of the Stefan-Boltzmann relation concerning its air radiation term.

3.4 The Basic Work about the IR-adsorption and IR-emission by Gases and Its Hypothetical Application to the Atmospheric Radiation

The starting point of the here referenced author's research (Allmendinger, 2016b, 2017a) was the common greenhouse theory. According to this, the atmosphere is solely warmed-up due to absorption of thermal Earth radiation by so-called greenhouse gases, in particular by carbon-dioxide, while pure air is assumed to be incapable of absorbing any IR(infrared)-radiation, be it the near-IR of the incident solar-radiation (wavelength $\lambda < 3\mu m$), or the medium-IR of the thermal Earth radiation ($\lambda > 3\mu m$). At least the former assumption must be questioned in view of the fact that the intensity of the incident solar light is considerably reduced by the atmosphere: As it is well-known, there is a significant difference between the *extra-terrestrial solar constant* (measured on the top of the atmosphere) and the *terrestrial solar constant* (measured on the Earth surface). For the extra-terrestrial one, commonly the average value 1360-1366 Wm^{-2} is assumed (see for instance Visconti, 2001; Boeker and van Grondelle, 2011), while for the terrestrial one approximately 1000 Wm^{-2} are measured, but dependant on the altitude (see later). The primary, basic investigations were made with solar light and - particularly - with artificial IR-light exhibiting mainly near-IR (Allmendinger, 2016b), while additional measurements concerning thermal radiation, i.e. medium-IR, were carried out with a hotplate (Allmendinger, 2017b).

Compared to solid bodies, thermal measurements on gases are much more delicate. Due to their low heat capacity they suggest a considerable interference with the vessel walls in which the gas is embedded, apart from the fact that gases may move when a temperature gradient arises. Hence, a large ratio between the gas volume and the surface of the vessel must be intended, as well as a low heat capacity of the vessel material. Therefore, it is not surprising that no effect can be detected when heavy materials and apparatus are used, as it was the case with the photometric measurements made by Tyndall (1861) using apparatus shown in Fig. 3.1, or by his followers Svante Arrhenius (1896) and Knut Ångström (1901), in spite of the fact that no caloric measurements were made but solely photometric ones.

Therefore, the author's experiments were made using very light building materials, namely square tubes from Styrofoam (3 cm thick, 1 m long, outer diameter 25 cm), covered above and below with a thin transparent foil (0.01 mm thick Saran-wrap). At an advanced stage, the Styrofoam was sealed

with adhesive foils and mirrored with aluminium foils. For the measurements with solar light, one or two tubes were pivoted on a frame so that they could be exactly oriented in the direction of the light (Fig. 3.9). For the measurements with artificial light, an *IR-spot* with a reflector was mounted above the vertically aligned tube (Fig. 3.11), while for the thermal radiation measurements a *hotplate* was positioned on the bottom of the tube (Fig. 3.13).

When artificial infrared light or thermal radiation was applied, normally a temperature gradient along the measuring tube appeared, in contrast to the use of solar light which did not exhibit such an intensity decrease (Fig. 3.10). This effect was detected by providing three temperature-measuring points in the distance of 40 cm. In spite of this disadvantage, most measurements were made with artificial light since it enabled higher intensities and better reproducibility. The deviations could be minimized by mounting internal mirroring with aluminium foils along the tube walls. This effect had always been disregarded at former IR-measurements with gases, apart from the fact that not the temperature enhancement of the gas was measured but solely the intensity loss of the applied light ray.

Fig. 3.9. Solar-tube according to Allmendinger (2016b)

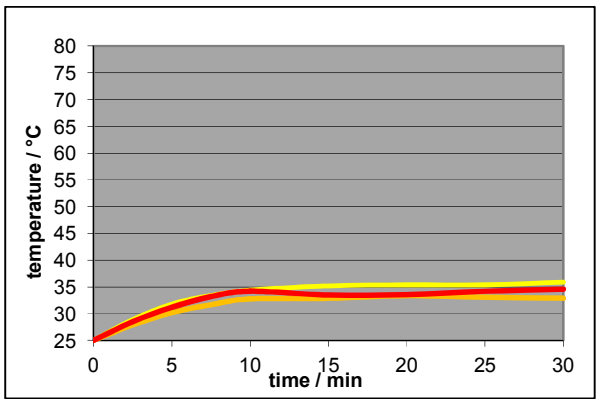

Fig. 3.10. Time/temperature curves for solar light at three different temperature-positions, detected with the solar tube shown in Fig. 3.9

The time-temperature curves of irradiated gases proceed alike to those of irradiated SOBs, always reaching *limiting temperatures*. Analogously, it may be assumed that a limiting temperature is attained when a steady equilibrium exists between the intensity of the absorbed radiation, on the one side, and of the emitted radiation, on the other side. Thus the knowledge of the limiting temperature values enables making statements about the radiation emissivity of the respective gases. Surprisingly, *any* gas was up-warmed, even noble gases did so (Fig. 3.12), while – contrary to the prediction of the conventional greenhouse theory – no significant difference could be found between pure carbon-dioxide, air and argon. In the case of thermal radiation emitted by a hotplate, comparing air with carbon-dioxide, a similar behaviour was found (Fig. 3.14). However, that test assembly did not permit exact evaluations due to the thermal delay of the hotplate after being switched on.

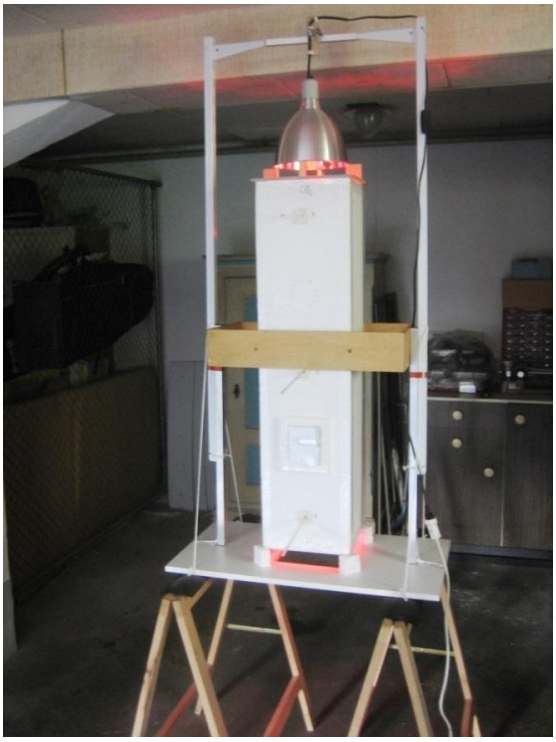

Fig. 3.11. Equipment with IR-lamp according to Allmendinger (2016)

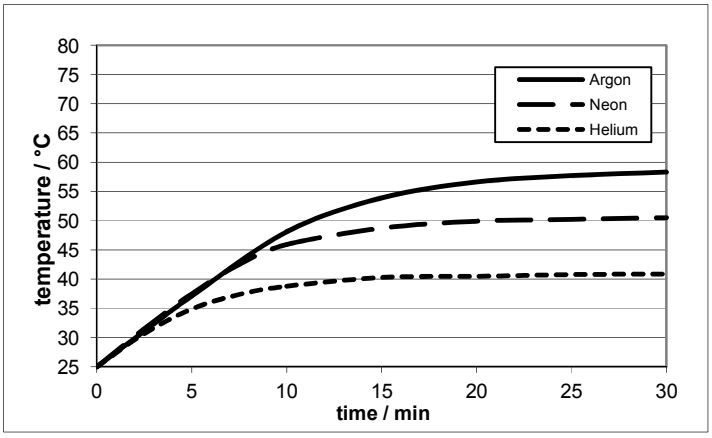

Fig. 3.12. Time-temperature curves of different noble gases
(150 W IR-spot, middle thermometer position) Allmendinger (2016b)

The *interpretation* of the results obtained with the IR-spot apparatus enabled the empirical determination of the heat absorbance coefficient of a gas, which turned out to be very low. So it is not surprising, that this effect has been overlooked so far. While a theoretical calculation of such an absorption coefficient was not feasible, at least a principal explanation may be given:

There is no good reason to assume that absorbed IR-radiation will be *entirely* transformed into heat. Instead, it is conceivable that a part of it is *re-emitted*, i.e. to say in all directions, before having induced a temperature enhancement. The absorption of infrared light by an atom or a molecule can be explained *quantum-mechanically* assuming excitations of electrons which are quantized. Vice versa, the radiation emission obeys the same quantum-mechanical regularities. According to the *de Broglie hypothesis,* such a quantisation is due to the occurrence of *standing electron waves* in the excited states. Obviously such phenomena are possible not only at molecules with *polar* bonds, as is the case at the absorption of medium-IR by CO_2 and H_2O - and as it is assumed as the only possible explanation for IR-absorption in the conventional theory -, but also with molecules exhibiting *nonpolar* bonds, and even at noble gases. So this is an *intra-molecular* phenomenon. On the other hand, heat is due to the kinetic energy content of the gas which correlates to the translational movement of whole molecules or atoms. So that is an *inter-molecular* phenomenon. That movement is *not* quantized and thus it cannot be described quantum-mechanically, but solely by means of the *kinetic gas theory*. The latter one is well-established, being satisfyingly applied for explaining simple heat-conduction in gases, but so far it has been completely disregarded in atmospheric physics.

Using the kinetic gas theory, it was feasible to explain the *ratio of the different limiting temperatures* as an implication of the radiative emission. The noble gases *argon*, *neon* and *helium* turned out to be optimal for comparison (Fig. 3.12) since their limiting temperatures differed enough to be interpreted, and since in any case one-atomic gases are involved. Assuming a direct correlation between the limiting temperature and the radiative emission power, a stringent dependency on the *product of the mean kinetic energy and the collision frequency* could be deduced, namely

$$\Phi_{emission} \sim a \cdot M^{0.5} \cdot T^{0.5} \cdot p \tag{3.11}$$

(a = cross sectional area, M = atomic mass, T = absolute temperature, p = pressure)

When the heating-up rates are equal, the comparison of two gases yields for the relevant absolute limiting temperatures T_1 and T_2 the relation

$$T_1/T_2 = M_1(r_2)^4 / M_2(r_1)^4 \tag{3.12}$$

where M_1 and M_2 indicate the atomic masses, and r_1 and r_2 the atomic radii of the compared gases. This relation could be empirically verified with the data of *helium*, *neon* and *argon*.

Moreover, a rough estimate of the *effective wavelength-range* was possible by comparing the absorbance rates at sunlight and at artificial light, delivering the value of approx. 1.9 µm. Finally, the calculation of the *radiative heat coefficient* yielded that the amount of radiative energy being transformed into kinetic heat energy is very small. Therefore, the empiric evidence was delivered that *any* gas is warmed up to a limiting temperature by near-infrared light as well as by sunlight.

As a consequence, it stands to reason that a *principal dependency* on the radiative emission intensity of a gas on the product of its mean kinetic energy and the collision frequency exists. This suggests a general application to *any* thermo-radiative emission process of gases – and thus likewise to atmospheric air -, delivering a hypothesis for the wanted term $f(p_{atm}, T_{atm})$ in relation (3.8). Since the cross sectional areas as well as the molecular masses of the main air components nitrogen and oxygen are similar, equation (3.11) can be simplified delivering the expression

$$\Phi_{emission} = A \cdot T^{0.5} \cdot p \tag{3.13}$$

whereby *A* represents a constant which has to be empirically determined. It may be called «atmospheric emission constant». Hence the modified Stefan-Boltzmann relation would be written

$$\Phi \cdot \beta_s = \sigma \cdot T_{SOB,\lim}^4 - A \cdot T_{atm}^{0.5} \cdot p_{atm} \tag{3.14a}$$

or rearranged $$\sigma \cdot T_{SOB,\lim}^4 = \Phi \cdot \beta_s + A \cdot T_{atm}^{0.5} \cdot p_{atm} \tag{3.14b}$$

yielding the expression $$A = \frac{\sigma \cdot T_{SOB,\lim}^4 - \Phi \cdot \beta_s}{p_{atm} \cdot T_{atm}^{0.5}} \tag{3.15}$$

In order to verify this hypothetical relation and to determine the constant *A*, measurements were made at different altitudes for varying the atmospheric pressure applying the above mentioned method, but using thinner aluminium plates which allowed to directly determine the limiting temperatures.

3.5 Equipment and Locations for the Present Investigation

In order to verify the Stefan-Boltzmann relation as well as the own modelling method described in chap. 1.7 according to Allmendinger (2016a), the original equipment (Fig. 3.3 and Fig. 3.4) had to be modified using 8 mm thick aluminium plates instead of 20 mm thick ones. They enabled to reach the limiting temperature within a shorter time (approx. in 1½ hours, instead of more than three hours). However, the lower heat capacity of the thinner plates entailed the disadvantage of a higher thermal interference in the embedding Styrofoam modules, as well as of heat losses due to ambient air convection, particularly at high plate-temperatures. The plates were painted with the same colours which had been applied within the original experiments; however, solely four colour types were used, namely white, light blue, light green, and black. The intensity of the solar radiation (given in Wm^{-2}) was measured by an electronic KIMO® «Solarmeter» SL 100. For comparison, the results of the original measurements with 20 mm thick aluminium plates were quoted.

In order to verify the hypothetical formal approach (3.14, 3.15) by studying the influence of the atmospheric pressure, measurements were made at two different locations: in *Glattbrugg* (near Zürich, Switzerland), 430 m above sea level, and on the top of the *Furka-Pass* (Switzerland), 2430 m above sea level. The atmospheric pressure was not measured but checked by official data of the respective weather stations. However, it should be known that, from meteorological reasons, such data do not concern real pressure values but only normalized ones, being formally converted to the values at sea-level (zero). But since the meteorological pressure variations are negligibly low compared to the pressure variations due to significant altitude variations of locations, the here relevant pressure values have solely been calculated using the usual barometric height formula (3.15),

$$p = p_0 e^{-\frac{\rho_0 \cdot g \cdot h}{p_0}} \cong p_0 e^{-\frac{h}{8km}} \tag{3.16}$$

ρ_0 = density of the air, g = gravity constant, p_0 = pressure at sea level (1 bar), h = altitude delivering the values of 0.948 bar for Glattbrugg, and 0.738 bar for the top of the Furka-Pass. Between the 20th June and the 5th July 2017, altogether four useable measurements were made, two in Glattbrugg and two on the top of the Furka-Pass, letting suppose only minimal differences in the characteristics of the solar radiation. The comparative measurements with 20 mm thick aluminium plate had been made on 4 Sept 2013 in Glattbrugg, hence approx. two months later.

As already mentioned, atmospheric pressure and temperature as well as intensity of the solar irradiation are not independent of each other, so it is not possible to vary solely the atmospheric

pressure by relocating. However, the here proposed approach implies the different influences of the three parameters, in contrast to the Stefan-Boltzmann relation.

Since the measurements had to last till the limiting temperatures had been attained, it was unavoidable that the ambient air temperature increased during the exposure time of 1½ hours, due to permanent sunshine. So the ambient air temperature was not well defined. However, this was of much less consequence with respect to the numerical verification of the alternative approach (3.14) than with respect to the one of the Stefan-Boltzmann relation (3.5) since the exponential dimension of T_{am} is in the former case much lower, namely 0.5 instead of 4.

Fig. 3.13. Equipment with hotplate according to Allmendinger (2017b)

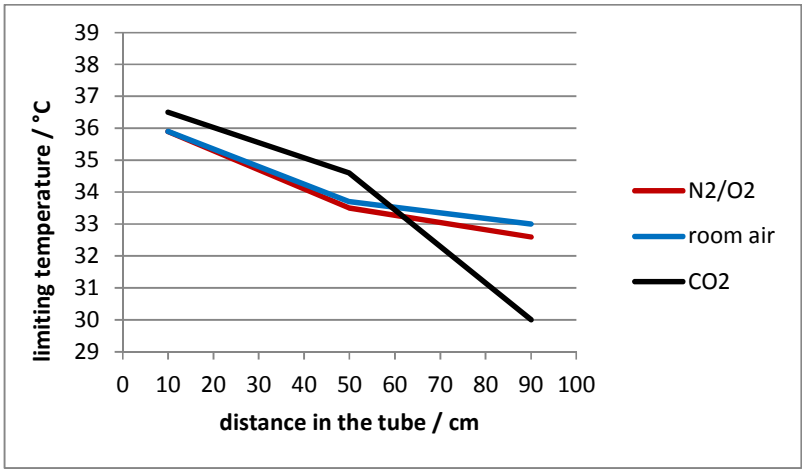

Fig. 3.14. Limiting temperatures for different gases at different thermometer positions, average values of two measurements, according to Allmendinger (2017b)
(heat power 37.1 W, initial temperature 23.5°, pressure ca. 0.948 bar, humidity 45-55%)

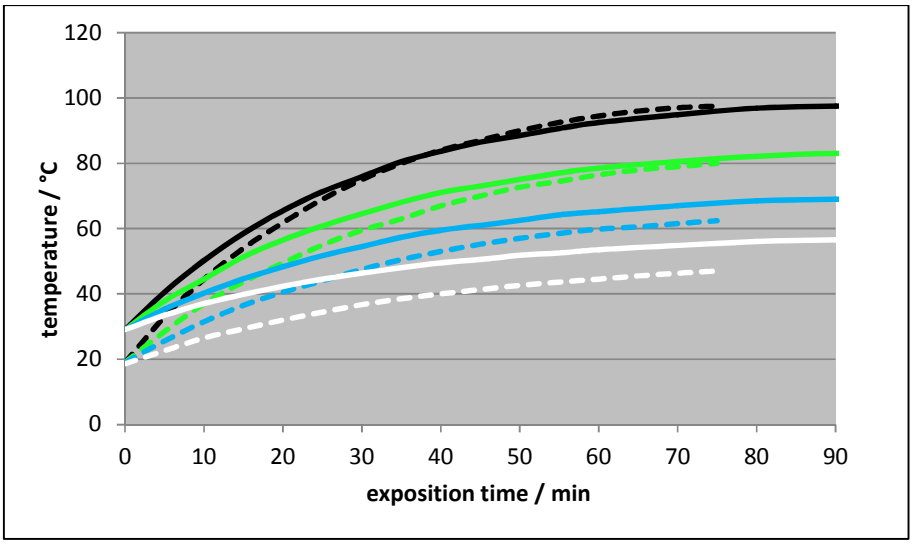

Fig. 3.15. Comparison of the temperature courses during the first two measurements
(continuous lines: Glattbrugg 1; dotted lines: Furka 1)

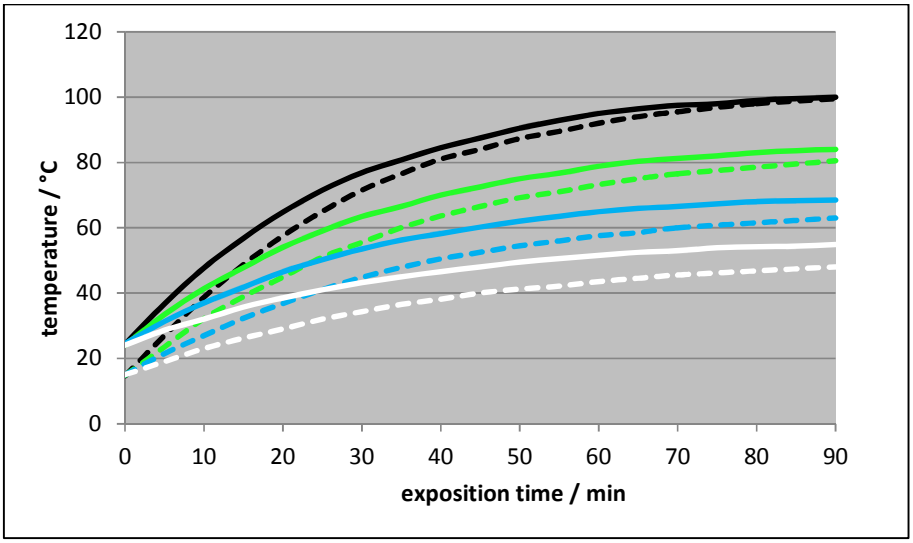

Fig. 3.16. Comparison of the temperature courses during the second two measurements
(continuous lines: Glattbrugg 2; dotted lines: Furka 2)

3.6 Results, Interpretation and Conclusions

As already mentioned, the measurements were made between the end of June and the beginning of July 2017, alternatingly in the low-lying Glattbrugg and on the high-lying Furka-Pass, and usually starting midday. During that whole summer the weather was windy and variable: even when the sky was clear it was often accompanied by small scattered clouds - perhaps as a result of climate change -, which made it difficult to find dates where the conditions were suited for measurements. Although the experiments were not perfect in every case, they delivered nevertheless satisfying results.

Obviously, the starting conditions for the two kinds of measurements were quite different: While in the low-lying Glattbrugg the starting temperature was considerably higher than on the high-lying Furka-Pass (on average 27°C, compared to 17°C), the solar radiation intensity was higher on the high-lying

Furka-Pass, due to the thinner atmosphere layer (on average 1210 Wm^{-2}, compared to 1075 Wm^{-2}). As is generally known, the portion of UV-light is larger in the mountains. Surprisingly, the limiting temperatures for the blackened plates were similar in both cases (cf. Figs. 3.15 and 3.16), which may be due to an UV-effect. Detailed information about the test conditions is given in the table below.

In Fig. 3.17 the actual results of the solar adsorption coefficients are compared with the results which have originally been obtained using 20 mm thick aluminium-plates (according to Allmendinger, 2016a; measuring date 4 Sept 2013, start 12:40 p.m., 1045 Wm^{-2}). In spite of some deviations, the value-patterns are quite similar. The tendency of getting higher values for the thicker plates may be explained by their higher heat capacity, allowing the expectation of smaller interferences in the module material. The larger deviations for darker colours, in particular for the black coloured plates, may be explained by the reduced insolation within the modules at higher temperatures. Moreover, the different times of year when the measurements were made may have a certain influence due to the different incident angle of the solar light effecting its spectral dispersion.

In Fig. 3.18 the measured limiting temperatures are displayed. Obviously, this pattern is very similar to the pattern of the respective solar adsorption coefficients displayed in Fig. 3.19. It empirically verifies the assertion of equation (3.10) that the limiting temperatures are proportional to the solar adsorption coefficients. Moreover, the reproducibility of the respective values is illustrated.

In Fig. 3.19 the measured limiting temperature values are compared with the computed values based on the Stefan-Boltzmann relation. This means that the real counter-radiation of the atmosphere is slightly weaker than the assumed one in the Stefan-Boltzmann relation. Therefore, according to these results, the Stefan-Boltzmann relation is fulfilled to a certain extent, but not precisely.

Finally, and above all, these results can be used for the verification in the alternative approach given by the formulas (3.13) - (3.15). In the following table the calculation results for the atmospheric emission constant *A* are listed, using formula (3.15). In view of the intricate measurement conditions, they coincide satisfyingly, in particular with respect to the results obtained with the colours light-blue and light-green, yielding an approximate average value of A = 22 $Wm^{-2}bar^{-1}K^{-0.5}$. As a consequence, the relation (3.13a, b) is verified as a general natural law, even if the value of the atmospheric emission constant *A* may slightly vary, also depending on the atmospheric conditions.

Table. Calculated A-values

Location Exp.-no.	Date (2017)	Start [h]	Start-temp. = t_{atm}	End-intensity [Wm^{-2}]	t_{lim} / A white	t_{lim} / A blue	t_{lim} / A green	t_{lim} / A black
G8 a	20 June	13:29	29.0°C	1095	56.5°C / 22.8	69.0°C / 22.5	83.0°C / 20.8	97.8°C / 17.2
G8 b	4 July	12:46	24.3°C	1065	54.9°C / 25.7	68.5°C / 20.7	84.0° / 23.6	100°C / 22.4
F8 a	26 June	13:01	18.9°C	1260	47.0°C / 26.4	62.4°C / 24.3	80.0°C / 22.1	99.5°C / 12.9
F8 b	5 July	12:42	14.8°C	1210	48.0°C / 25.9	63.0°C / 21.2	80.5°C / 20.0	97.5°C / 17.3

Explications:

- *First column: G = Glattbrugg, F = Furka-Pass; a or b means 'experiment-number'*
- *The A-values are listed in the last four columns, unit $Wm^{-2}bar^{-1}K^{-0.5}$*

This means that for the counter-radiation solely the *lowest layer of the atmosphere* – or the *boundary layer* of the Earth surface – is relevant, characterized by its temperature and – especially – by its pressure. Obviously, at lower atmospheric pressures the increase of solar irradiation, which is due to a reduced absorption within the atmosphere, is over-compensated by the decrease of counter-radiation due to the pressure loss. In the absence of solar irradiation, analogously to equation (3.7) the thermal emission power of the soil can be expressed by formula (3.17):

$$\Phi_{emission,soil} = \sigma \cdot T_{soil}^4 - A \cdot p_{atm} \cdot T_{atm}^{0.5} \tag{3.17}$$

When T_{atm} = T_{soil}, i.e. at a steady equilibrium state, T becomes 283.3 K = 10°C for p_{atm} = 1 bar. However, normally no radiative equilibrium exists at the Earth surface but rather a gradient. As a consequence, on mountains the cooling down of the Earth surface is accelerated, compared to the one on lowlands. This mainly explains the temperature decrease on mountains, even if additionally thermodynamic effects due to rising air and to horizontal wind-convection are relevant, besides the radiative heat transfer between the atmosphere and the Space.

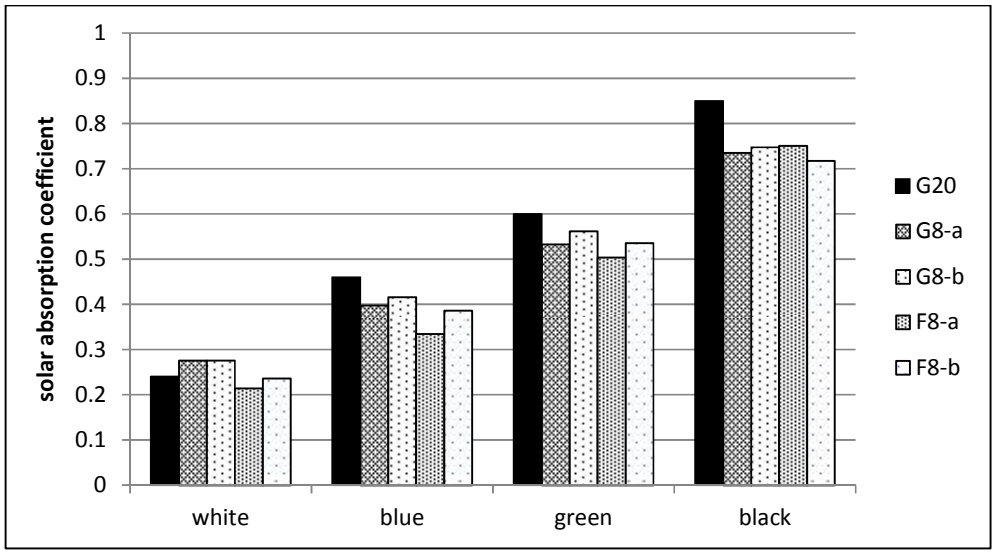

Fig. 3.17. Comparison of solar absorption coefficients determined by five different measurements

(Abbreviations: location/plate thickness in mm – experiment number; locations: G = Glattbrugg, F = Furka-Pass)

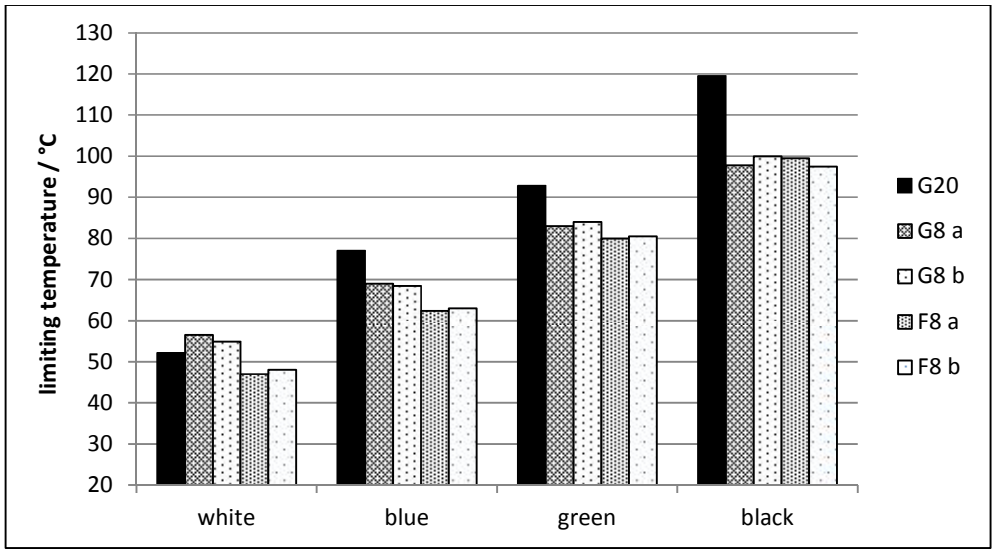

Fig. 3.18. Comparison of the limiting temperatures modelled (G20) and determined by four different measurements

(Abbreviations: location/plate thickness in mm – experiment number a or b; locations: G = Glattbrugg, F = Furka-Pass)

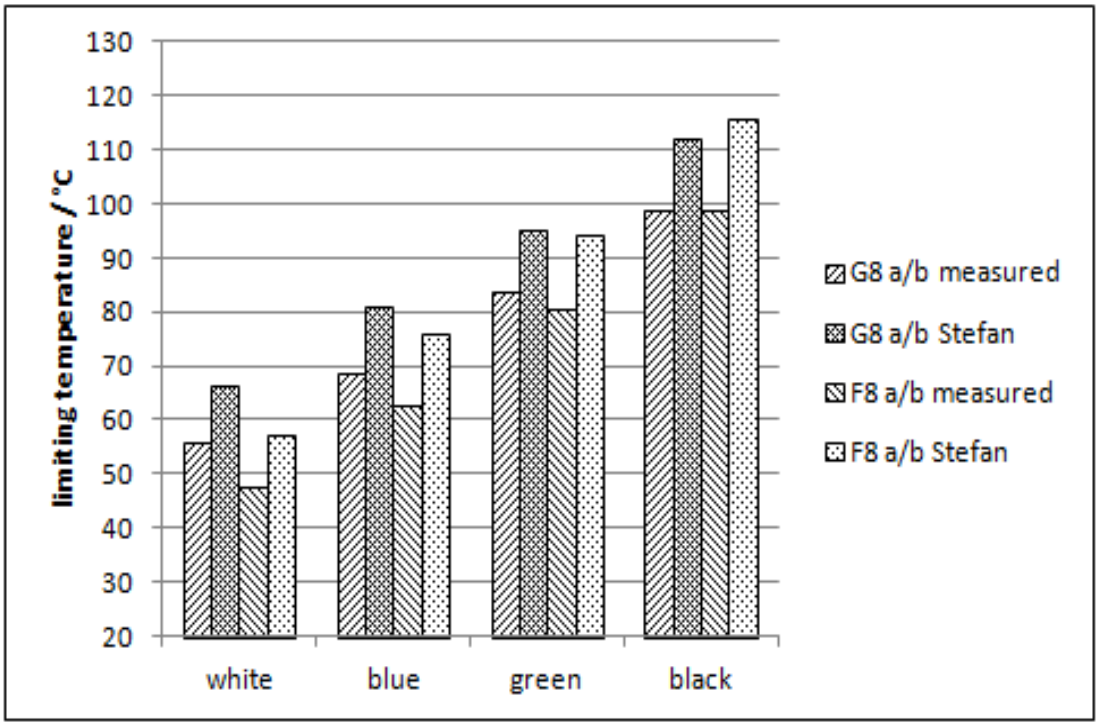

Fig. 3.19. Comparison of the mean limiting temperatures of 8 mm thick plates, measured and calculated according to Stefan for Glattbrugg (G8 a/b) and for Furka (F8 a/b)

This approach contradicts in many ways the conventional greenhouse theory: Firstly, the boundary processes at the Earth surface and at the lowest layer of the atmosphere are predominant, while the conventional greenhouse theory regards the whole atmosphere; and secondly – even more crucial – the radiation budged is solely determined by the air conditions of the atmosphere such as pressure and temperature while so-called 'greenhouse gases' such as carbon-dioxide do not have the slightest influence on the climate. Besides, the atmosphere cannot really be compared to a greenhouse, not least due to the absence of a glass-roof which absorbs IR-radiation, and which inhibits considerable air convection. Further objections are delivered in Allmendinger (2017c).

However, the atmosphere certainly plays a decisive part in enabling life on Earth. On the one hand it acts as insulation, absorbing hazardous radiation such as UV (by ozone), and on the other hand it keeps the heat of the Earth surface which is delivered by the sun. Presently, mankind fears that heat events become more frequent and severe. As a result of these considerations, brightening of the Earth surface - preferably roofs and buildings in cities (Allmendinger, 2017c) - is the only promising remedy for mitigating the climate and reducing the superficial pressure gradients which are responsible for storms, while the conventional greenhouse theory has definitively proved to be fallacious and should be abandoned.

ACKNOWLEDGEMENT

The present has been carried out independently but not without the critical support of Dr. Andreas Rüetschi and the translation assistance of Verena Ginobbi.

COMPETING INTERESTS

The author has declared that no competing interests exist.

REFERENCES

Allmendinger T. (2016a) The solar-reflective characterization of solid opaque materials. *International Journal of Science and Technology Educational Research 7(1)*, 1-17
Available: http://www.academicjournals.org/journal/IJSTER/article-full-text-pdf/E7435F759158

Allmendinger T (2016b): The thermal behaviour of gases under the influence of infrared-radiation. *International Journal of Physical Sciences 11(15)*, 183-205;
Available:http://academicjournals.org/journal/IJPS2016/article-full-text-pdf/E00ABBF60017

Allmendinger T (2017a): A novel investigation about the thermal behaviour of gases under the influence of IR-radiation: A further argument against the greenhouse thesis. *Journal of Earth Science & Climatic Change 8(3)*;
Available: https://www.omicsonline.org/open-access/a-novel-investigation-about-the-thermal-behaviour-of-gases-under-theinfluence-of-irradiation-a-further-argument-against-the-greenh-2157-7617-1000393.php?aid=87335

Allmendinger T (2017b): The refutation of the climate greenhouse theory and a proposal for a hopeful alternative. *Environment Pollution and Climate Change 1(2)*;
Available: https://www.omicsonline.org/open-access/the-refutation-of-the-climate-greenhouse-theory-and-a-proposal-for-ahopeful-alternative.php?aid=88698

Allmendinger T (2017c): Measures at buildings for mitigating the microclimate. *Environ. Pollut. Climate Change.1(3)*, 1-9.
Available: https://www.omicsonline.org/open-access/measures-at-buildings-for-mitigating-the-microclimate-2573-458X-1000128.php?aid=90625

Ångström K (1901): Ueber die Abhängigkeit der Absorption der Gase, besonders der Kohlensäure, von der Dichte. *Ann. Phys. 311/9*, 163-173

Arrhenius S (1896): On the influence of carbonic acid in the air upon the temperature of the ground. *Phil. Mag. 41/5*, 238-276

Beer A (1852): Bestimmung der Absorption des rothen Lichts in farbigen Flüssigkeiten. *Ann. Phys. Chem. 86*, 78-88

Boeker EG, van Grondelle RI (2011): Environmental Physics. John Wiley & Sons Ltd. Third Ed. 2011

Boltzmann L (1884): Ableitung des Stefan'schen Gesetzes betreffend die Abhängigkeit der Wärmestrahlung von der Temperatur aus der electromagnetischen Lichttheorie. *Annalen der Physik und Chemie 22*, 291-294

Dulong MM, Petit (1817): Des Recherches sur la Mesure des Températures et sur les Lois de la communication de la chaleur; *Annales de Chimie et de Physique, Ser. 2/7*, 225-264 ("Des Lois du Refroidissement"); 337-367 ("Du Refroidissement dans l'air et dans les gaz")

Kirchhoff G (1860): Ueber das Verhältnis zwischen dem Emissionsvermögen und dem Absorptionsvermögen der Körper für Wärme und Licht. *Ann. Phys. Chem. 109/2*, 275-301

Kirchhoff G (1861): On a New Proposition in the Theory of Heat. *Phil. Mag. Ser. 4, 21/140*, 241-247

Lummer O, Pringsheim E (1899): Die Verteilung der Energie im Spektrum des schwarzen Körpers. *Verh. Dt. Phys. Ges. 1*, 23-41

Meschede D (2002): Gerthsen Physik. Springer, 21. Auflage 2002

Planck M (1900a): Ueber irreversible Strahlungsvorgänge. *Ann. Phys. 306/1*, 69-116

Planck M (1900b): Entropie und Temperatur strahlender Wärme. *Ann. Phys. 306/4*, 719-737

Planck M (1900c): Zur Theorie des Gesetzes der Energieverteilung im Normalspectrum. Verhandlungen der Deutschen physikalischen Gesellschaft.2 (Nr. 17), 237-245

Stefan J (1879): Über die Beziehung zwischen der Wärmestrahlung und der Temperatur. *Sitzungsber. der mathemat.-naturwiss. Classe der kaiserlichen Akademie der Wissenschaften 79*, 391-428

Tyndall J (1861): On the absorption and radiation of heat by gases and vapours, and on the physical connexion of radiation, absorption, and conduction. *Phil. Mag. 22*, 169-94 and 273-85

Visconti G (2011): Fundamentals of physics and chemistry of the atmosphere. Springer 2001

Biography of the author

Thomas Allmendinger
Independent Scholar, ETH (Swiss Federal Institute of Technology), Zurich, Switzerland.

He was born 1947 in Zurich and went through the Swiss school and education system, followed by studies at the ETH (Swiss Federal Institute of Technology) and a Master degree (Diploma) in general and organic chemistry in 1971. His career started in a private environmental-lab, especially involved in research at sewage plants. It was followed by an interlude as a chemistry teacher at a private grammar school. Subsequently, the development of a time-/temperature-indicator for deep frozen foods was privately pursued which had been started at the environmental-lab by order of an industrial firm. Moreover, his interest for alternative energies was awakened, particularly with respect to electrochemical fuel cells. It finally led on to a R&D-project about an internal reforming methanol/air fuel cell, carried out at the ETH in cooperation with the PSI (Paul Scherrer Institute). Related to that, he finished his Ph.D. thesis in 1992. Afterwards, he ran his own private lab at the Technopark in Zurich, offering professional support for industrial firms with respect to electrochemical technology. Thereby, mainly recycling processes were treated (e.g. recycling of Ni/Cd-batteries and of nickel in galvanic baths). Moreover, he collaborated on a photovoltaic cell-project. This work was done in association with the AFIF (Arbeitsgemeinschaft für Industrielle Forschung / Consortium for Industrial Research). But since this institution was dissolved after just a short time, this independent activity could not be continued. Therefore, it was necessary to find permanent full-time employment in a company. This could be achieved by working for an electroplating firm (Collini AG), where he was engaged as a lab-head till his retirement in 2012. Thereby, also several characterization methods for galvanic layers were developed and published. Subsequently, he tackled climate physics as a novel research field within a private occupation, delivering considerable results. Besides, quantum mechanics arouse his interest since it delivers the foundations of physics.

DISCLAIMER
This monograph is an extended version of the following articles published by the same author in the following journals.
1) International Journal of Science and Technology Educational Research, 7(1): 1-17, June 2016.
2) International Journal of Physical Sciences, 11(15): 183-205, 16 August 2016.
3) Atmospheric and Climate Sciences, 8: 212-234, 2018.

London Tarakeswar

Registered offices
India: Guest House Road, Street no - 1/6, Hooghly, West Bengal, PIN-712410, India, Corp. Firm Registration Number: L77527, Tele: +91 8617752708, Email: contact@sciencedomain.org, (Headquarters)
UK: Third Floor, 207 Regent Street, London, W1B 3HH, UK
Fax: +44 20-3031-1429 Email: contact@sciencedomain.org, (Branch office)